Biomechanical sensors from the macro to the nanoscale - the way forward

Liviu Nicu

Habilitation à Diriger des Recherches

Préparée au Laboratoire d'Analyse et d'Architecture des Systèmes du CNRS

En vue de l'obtention du Diplôme de l'Université Paul Sabatier de Toulouse

Par **Liviu NICU**
Docteur de l'Université Paul Sabatier de Toulouse

Biomechanical sensors from the macro-to the nanoscale – the way forward

Remerciements

Bien sûr, il est très difficile d'écrire cette partie. Je ne sais pas si c'est la même chose pour tout le monde mais en ce qui me concerne, la crainte de ne pas être suffisamment exhaustif me tétanise.

Avant toute chose, je voudrais remercier vivement les membres de mon jury qui ont bien voulu dégager un peu de leur temps précieux pour venir juger l'ensemble du travail accompli par mon équipe et moi-même depuis quelques années. **Prof. Juergen Brugger** de l'EPFL, **Dr. Harry Heinzelmann** Vice-Président du CSEM Neuchatel, **Prof. Karsten Haupt** de l'Université de Compiègne, **Dr. Jean-Paul Leonetti** du Centre d'études d'agents Pathogènes et Biotechnologies pour la Santé de Montpellier, **Dr. Francesc Perez-Murano** du CNM Barcelone, **Prof. Robert Plana** du LAAS, **Prof. Olivier Bonnaud** de l'Université de Rennes, **Dr. Lionel Buchaillot** de l'IEMN Lille et **Dr. Christian Bergaud**, mon Directeur de Travaux.

Par qui continuer ? Je viens de faire un tableau avec deux colonnes, celle intitulée « qui ? » et celle « pourquoi ? ». La « qui ? », remplie naturellement, sans réfléchir, sans buter sur les noms aurait dû me débloquer sur le « pourquoi ? ». C'est là où j'ai eu le sentiment de refaire le même exercice d'écriture de remerciements qu'après ma thèse. Sept ans après… grâce à qui, grâce à quoi je crois aujourd'hui encore en ce que je fais ? Et si c'était celui-là mon fil conducteur dans l'écriture des remerciements ?

Grâce à qui ?

Tout d'abord, grâce à mes partenaires de travail de tous les jours : les séparer en « doctorants », « permanents », « amis » ça rimerait à quoi, exactement ? Je ne suis certainement pas tenu à refaire l'organigramme du LAAS « vu sous un angle personnel », enfin, je l'espère. Je me dois surtout de penser à tous ceux avec qui j'ai fait ce bout de chemin.

D'abord, sans compter, sans ordonner, venus entre une inspiration et une expiration, instinctivement : Thierry, Christian, Cédric, Laurent, Thomas, Fabrice, Jean-Bernard, Daisuke. Qui est qui, qui est quoi ? Mais quelle importance ça a ? Ils sont mes anges gardiens, ils l'ont été à un moment ou à un autre, parfois en se rendant compte, parfois en passant sans se douter de l'importance qu'ils ont à mes yeux. Avec certains j'ai construit, avec d'autres j'ai rêvé, avec tous j'ai avancé, jour après jour ; ils m'ont chacun appris quelque chose.

Thierry la rigueur et l'excellence issues d'une terrible exigence envers soi,
Christian la ténacité et le sacrifice de tout au nom d'idées et idéaux partagés,
Cédric l'ambition en distillant persévérance et doutes,
Laurent le jeu des miroirs, où âme et cérébralité peuvent en faire un,
Thomas le pilier qui roule et compresse avec fausse naïveté,
Fabrice la droiture et l'honnêteté d'un caractère en acier trempé par des vies vécues en une seule vie (au moins, on est deux à l'avoir éprouvé et ça lie, forcément !),
Jean-Bernard l'esprit des valeurs, des savoirs et de la présence inconditionnelle qui rassure,
Daisuke l'efficacité absolue de la discrétion.

Nous avons toujours été libres de faire, refaire ou ne pas faire s'il n'y avait pas lieu de faire. Cette liberté sans prix, avec son goût parfois salé par la peur de l'inconnu (appelant la

nécessité d'assumer ses responsabilités), parfois alcoolisé par l'ivresse d'instants d'égarement de l'égo, cette liberté là je la dois à Christophe, dont la direction de groupe a été assumée avec autant de tact que de fermeté. Je la dois également aux binômes directoriaux successifs, Mrs Laprie-Martinez, Ghallab-Garcia(Munoz), Chatila-Sanchez qui ont œuvré au fonctionnement irréprochable du LAAS. Eux seuls sachant l'ingratitude de la tâche, ça vaut la peine de l'écrire au moins une fois et rendre ainsi le ressenti au niveau périphérique.

Cependant, comment faire autre chose que rêver de faire sans ce pas du rêve à la réalité rendu possible par les services du LAAS ? Oh oui, pour les sceptiques, je pèse mes mots. Je n'ai jamais eu la prétention de pouvoir m'en sortir tout seul et de toute façon, quelle douceur que celle du confort d'une prise en charge là où les idées doivent prendre contours et formes ? TEAM, 2I, Doc, Logistique, Gestion… pas d'organigramme, mais pas le droit à l'oubli, juste le droit de dire Merci !, et la mention du rayon de lumière à odeur d'encre pour Christian B. (il se reconnaîtra, bien qu'ils soient 2 à partager les mêmes initiales, l'autre ayant la mention du cœur mais il le sait).

Une autre manière de « penser et c'est fait », dans un tout autre registre, celui de la gestion de l'imprévu, la où le moindre détail peut prendre des proportions insensées, porte tout naturellement ma reconnaissance envers l'efficacité et la gentillesse de Nicole, notre secrétaire.

A mon collègue de bureau (Fuccio, le sicilien) avec qui je partage le quotidien (à en rendre folles de jalousie nos épouses) en toutes les langues (ou presque, car l'italien l'emporte), je dois également un clin d'œil affectif. J'ai également une pensée toute particulière pour Childerick qui force mon admiration tant il est tenace et dont la force de travail n'a d'égal que la contenance de son cœur.

Il paraît que les temps changent, il paraît que nuages se montrent de plus en plus menaçants sur un univers professionnel qui m'a toujours été source de satisfactions… et si mon port d'attache, mon phare dans la tempête était mon autre univers, ma famille ? Qui de ceux qui prétendent me connaître sera étonné de le lire encore une fois ? Ma force, mon moteur, mon jour après la nuit, mes enfants et mon épouse. A eux, je dois TOUT !

Table of Contents

PREAMBLE

Life is made of opportunities that have to be seized. So was my life so far.

I realize that the meaning of the words above could make the reader think that the author is someone born in the first half of the past century. Those who know me are aware of the fact that this is not exactly the case (even if sometimes I do feel like it is).

I will try to illustrate the different opportunities that occurred in my (professional) life, the private one being beyond the scope of this manuscript. In 1994, I chose to give up my entire Romanian-native life and start a completely new one in France, my adult-life I would say. Even if it happened for personal reasons, this was not without significant consequences on my future professional life. Indeed, this life change occurred when I was about to finish my Electrical Engineering Graduate Studies at the Politechnica University of Bucharest. I chose not to finish my studies there but to continue to Paul Sabatier University of Toulouse (UPS), in 1995. Let me call it "the First Opportunity".

In 1997, while I was finishing a Master of Materials Sciences at UPS, I was recruited by the former Deputy Director of the Laboratory of Analysis and Architecture of Systems in Toulouse (Augustin Martinez) as PhD student in one of the laboratory's research groups that at that time was named Silicon Microstructures and Microsystems (M2I). My PhD thesis started under the responsibility of a young researcher (Christian Bergaud) who was just arriving from Japan bringing the silicon cantilevers technology at LAAS after 2 years of post-doc. This was the Second Opportunity of my career: the PhD Director and the subject.

In 2001, I failed to be admitted either as a CNRS[1] researcher or an Assistant Professor at the National Institute of Applied Sciences in Toulouse and this was the Third Opportunity in my career. For those who are not familiar with the French system, to get a permanent position in the academic research, the candidates have to successfully succeed annually organized national competitions and I brilliantly failed in my two attempts. This was an opportunity though, as I immediately applied for an R&D Engineer position at Thales Avionics in Valence (France). I was hired at the Inertial Department in charge of the scientific part of the European Project Gyrosil that was just starting. I learnt a lot during my (almost) two years of industrial life. It was a short but extremely intense experience. The project was very ambitious and quite strategic at that time (June 2001) for the company: we had in charge the demonstration of a silicon-based microgyrometer prototype satisfying both military and civil specifications. Unfortunately, September 11 arrived with its significant economic impacts on the world markets, leading specifically to a nearly 20% cutback in air travel capacity, and severely exacerbating financial problems in the struggling world-wide airline industry. The effects of this event were felt with a certain inertia (word play is not intentional here!) in our Department as we have had enough time to submit 3 patents on a new gyrometer design. However, in the end, even if the first prototypes were successfully demonstrated, the project was placed on "stand-by" position after 18 months of hard work. I so realized how the market laws could impact on the life of a project, no matter how "strategic" it could be. I also realized that this would be a source of frustrations in my future life and I decided to knock again at the CNRS' door.

In January 2003, I received my Researcher position in the Nanobiotechnology group, at LAAS. It thus became the Fourth Opportunity as I was back in my lab after a rich experience in the industrial world. The research project that I defended dealt with Microsystems for Biological Applications. Starting with that point, the opportunities took the form of projects (the European Project NaPa[2]) and of meeting extraordinary people (the European partners inside NaPa, the biologists from Montpellier,

[1] CNRS stands for the National Center of Scientific Research in France
[2] NaPa stands for Emerging Nanopatterning Methods (Integrated Project in the 6th Framework Programme)

the chemists from Compiègne, my colleagues from LAAS and my team of PhD students and post-docs).

Almost 5 years after my reintegration at LAAS, I can say that I kept the same research direction that I have initially defended during the CNRS competition in 2002. The present manuscript retraces all the research work carried during those 5 years and shows how such a huge subject was divided in several complementary sub-projects with a common target that was the demonstration of resonant silicon-based MEMS sensors for biological applications taking into considerations all the bioMEMS-related aspects, from the surface functionalization (either global or localized), through the transduction (from the biological recognition event to the physically measurable signal) to the fluidics issues related to biological sensors.

Before digging into the manuscript, I would like to mention the last opportunity that I recently had. A few days before starting to write this dissertation I read by chance an article issued in the weekly *Chemical and Engineering News* (March 26, 2007, p.13) written by Prof. George M. Whitesides, an address that he presented at the American Chemical Society 233rd National Meeting in Chicago (March 25-29, 2007), where he received the 2007 Priestley Medal for lifetime achievements and service to chemistry. In his article, Prof. Whitesides shares his point of view about the revolutions to arise in chemistry under the cover of Thomas Kuhn's theories about the scientific revolutions. Without this article in mind, I would certainly never have written this manuscript in the "awareness state" in which I am today. Reading Prof. Whitesides' article allowed me learning about Thomas Kuhn's "The Structure of Scientific Revolutions" book that shed a new lucid light on my past scientific activities and on my future strategy. I finally understood what kind of science I was doing and this manuscript will be the basis of an introspective analysis based on several Kuhn's assumptions.

However, the manuscript's structure is somehow "conventional"; it is divided in three chapters. In the first chapter, a state-of-the-art discussion upon the biosensors' structure and classification highlights the main elements to be considered in any basic biosensor issue, i.e. the biological receptors topic, the biomolecules' immobilization onto a substrate and the transduction techniques. To conclude this first chapter, a brief overview of the main nanodevices applied to the biology is given.

The second chapter contains the main results of my past 5 years research work dealing with silicon-based bio-microsensors. It is divided in three parts: the first one deals with microtools for local bio-functionalization of solid surfaces at the microscale (the so-called Bioplume system), the second part describes the microsensors developed for biological applications (from the mechanical structure to the biological application) and the third part presents promising applications yielded from the successful coupling between the Bioplume system and the microsensors described beforehand.

The final chapter is a more prospective one, from the biosensors field point-of-view (the limits of biosensing at the nanoscale is pointed out) and from a personal career point-of-view where a new research axis towards smart nano-electromechanical systems is proposed.

1. FROM BIOSENSORS TO BIOM(N)EMS – THE WAY FORWARD

Introduction

Before presenting an overview of biosensors, it is worth taking a closer look at Prof. Whitesides' article[3] cited previously. This will allow starting the discussion from a more general level.

Two theories of scientific revolutions are pointed out by the author. One is defended by Thomas Kuhn in its "The structure of Scientific Revolutions" book and it argues that scientific paradigm shifts occur when there is no way out, i.e. invention of new theories are brought about by the awareness of anomalies in existing ones. The transition between the worldview of Newtonian physics and the Einsteinian Relativistic worldview is an example. Moreover, Kuhn offers a dual vision of the science: the **normal scientific research** that is directed to "force nature into preformed and relatively inflexible boxes that paradigms are supplying" and discovery (or **scientific revolution**) that remains the basis of fundamental changes in thinking. *On this first basis, it will turn out that all the scientific work in the present manuscript can be hopefully qualified as "normal science"*.

The second theory, supported by Peter Galison (Professor in History of Science and Physics at Harvard University), states that new experimental techniques enable scientific revolutions (in Kuhn's sense of the word). Redefining this in Prof. Whitesides' terms would lead to "**new keys open new doors**". One example is the role of scanning tunneling microscope in nanosciences; another one is the surface plasmon resonance-based system that allows determining the affinity of two ligands meaning the measurement of their binding constants. With this second theory in mind, *it will be shown that the tools described within the next chapter of this manuscript can contribute to gain further insight into the biosensing issues*.

Finally, Prof. Whitesides gives a series of examples of problems (or potential scientific revolutions) that would concern the scientific community many years from now. Among them ("The Cell and the Nature of Life", "Energy, the Environment and Global Stewardship", "The Molecular Basis of Sentience"), **the molecular recognition in water and the design of drugs** seems to be of primary importance. In the author's opinion, the binding of a small molecule –a drug, ligand, substrate or transition state – to a protein is arguably the most fundamental molecular process in biology. Answers to fundamental questions in this area can without any doubt be conveniently brought by state-of-the-art biosensors, similar to those described in the following sections of this chapter.

Definition of the biosensor

There are numerous definitions of what a biosensor is, two of them will be given here: a *history-related* and a *general definition*, for the sake of exhaustiveness.

In its brief but remarkable review of the biosensors field, Peter T. Kissinger[4] goes back to the early days of the biosensing (the 1960s and the 1970s) to pinpoint that a *sensor seemed to always be a probe of some sort because of systematic association to pH, ion selectivity or oxygen electrodes*. Following the old literature, biosensors are found as being called bioelectrodes or enzyme electrodes, or biocatalytic membrane electrodes[5].

[3] G. M . Whitesides, *C&EN* March 26, 13 (2007)
[4] P. T. Kissinger, *Biosens. Bioelectron.* 20, 2512 (2005)
[5] M. A. Arnold, M. E. Meyerhoff, *Anal. Chem.*56, 20R (1984)

More generally, according to International Union of Pure and Applied Chemistry (IUPAC) recommendations in 1999, *a biosensor is a self-contained integrated receptor-transducer device, which is capable of providing selective quantitative of semi-quantitative analytical information using a biological recognition element* (Fig.1.1).

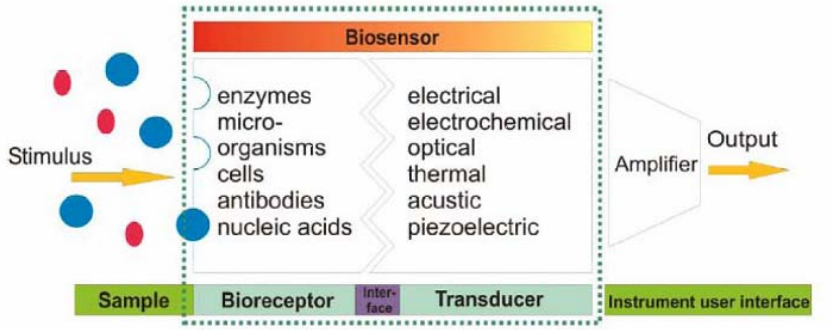

Figure 1.1: Schematic view of the general definition of a biosensor

The critical feature of the biosensor relates to the selectivity for the specific target analyte; this feature directly impacts on the specificity or how to maintain the selectivity in the presence of other, potentially interfering, species. The combination of these quality criteria with **miniaturization, low cost and essentially real-time measurements** in various fields has generated intense commercial interest.

The last twenty years have witnessed an extraordinary growth in research on sensors in general and on biosensors in particular. As underlined by Collings and Caruso in their excellent review on biosensors advances[6], "an intensively competitive research area is the result of the combined pressure from the traditional well-springs of research and development – science push and market pull"[7]. A measure of the rate of growth of interest in biosensors is quantified in Figure 1.2:

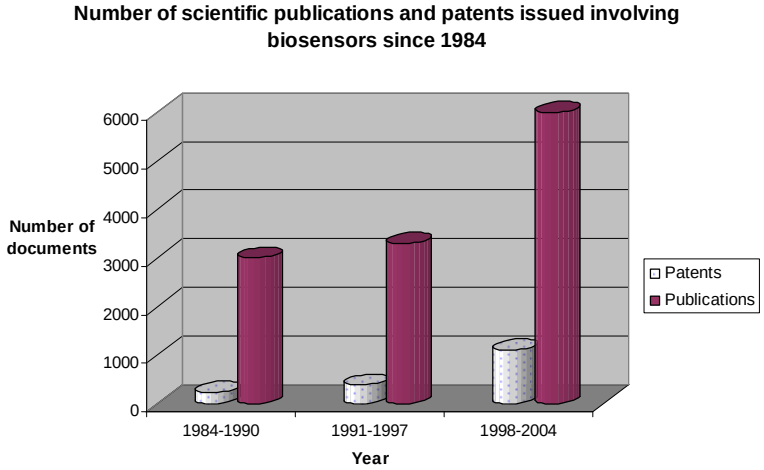

Figure 1.2: Overview of the rate of growth of activity involving biosensors since 1984[6,9]

[6] A. F. Collings and F. Caruso, *Rep. Prog. Phys.* 60, 1397 (1997)
[7] P. T. Kissinger (in Ref [4]) gives a « more provocative » vision of what motivates the biosensors interest, i. e. the triangle of "peer-review of science, funding agencies and politics".
[9] Fuji-Keizai USA, Inc., *U.S. & Worldwide: Biosensor market, R&D, applications and commercial implication* (2004), New York

In spite of all this, there is only one truly commercially successful biosensor and that is the blood glucose monitor. It is important to note that the glucose biosensor uses technology that was developed by Clark and Lyons well over 40 years ago and only recently has the world managed to grasp the true benefits of biosensors. Will commercial enterprises reap the benefits of the next generation of biosensors? In fact, it is suggested that between 80-90% of R&D activity in this area rarely results in a commercial product[9]. However, the observed growth in biosensor research increases the probability of witnessing another success story in the next couple of decades. The future R&D outlook for biosensors looks positive despite very little market growth / progress over the past several years[9].

As stated before, a biosensor is comprised of three essential components: the detector, which recognizes the biological stimulus; the transducer, which converts the stimulus to a useful, measurable, output; and the output system itself, which involves amplification, display etc. in an appropriate format. Because the biological detector or receptor is of primary importance (as it confers to the biosensor its specificity), receptors will be discussed in the next section of this chapter. The final component of the biosensor, the output system, is application or product-dependent, and while worthy of considerable effort as far as a finished product is concerned, is also beyond the scope of the first chapter.

It is the transduction process that completely falls into the physicist's domain. Since the physics aspect is largely concerned with the transducer and the transducer-receptor interface, this will constitute the main focus of this chapter.

Classification of biosensors

Biosensors can be classified according to three schemes: (a) *the receptor type*, e.g. an immunosensor, (b) *the physics of the transduction process*, e. g. an amperometric sensor, or (c) *the application*, e.g. a medical biosensor.

The biological recognition element or bioreceptor is the most crucial component of the biosensor device. The bioreceptor is the key to specificity, and can be classified according to several different groups as shown in Figure 1.3. Generally, there are three principal classes of biosensors. The three groups are distinguished from one another by the nature of the process and in terms of their biochemical or biological component, e.g. *biocatalytic* (i.e., enzyme), *immunological* (i.e., antibody) and *nucleic acid* (i.e., DNA). It is important to note that some biosensors have been developed on the basis of biomimetic or cell bioreceptors[10]. However, these bioreceptors will not be discussed here.

[10] T. Vo-Dinh and B. Cullum, *Fresenius J. Anal. Chem.* 366, 540 (2000)

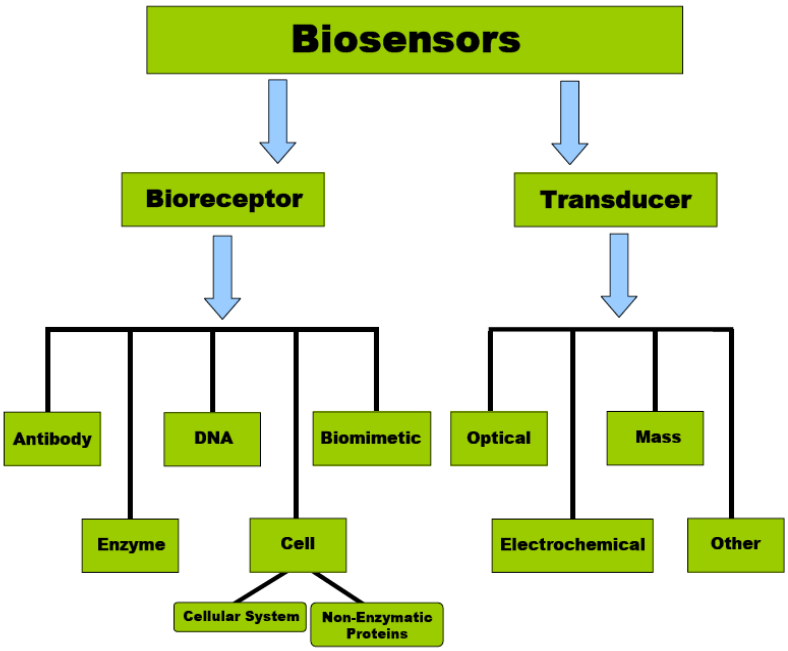

Figure 1.3: Biosensors' classification with respect to categories of bioreceptors and transduction principles

Though the bioreceptors immobilisation techniques onto solid surfaces will be discussed apart in this chapter, this topic is encompassed by the biological recognition element issue and, in practical cases, both are of equal concern.

The transducer is another component of the biosensor, which plays an important role in the detection process. A wide variety of transducer methods have been developed in the past decade; however, a recent literature review has shown that the most popular and common methods presently available are: a) electrochemical; b) optical; c) piezoelectric; d) thermal or calorimetric[6, 11-13]. To produce a manuscript that is consistent with the main authors' background (micromechanics), the focus will be narrowed to biosensors involving mainly piezoelectric transducers. For completeness sake, electrochemical and optical transduction principles in biosensing will be briefly reviewed across the first chapter when needed.

It is also important to note that these groups can be further divided into general categories: nonlabeled or label-free types, which are based on the direct measurement of a phenomena occurring during the biochemical reactions on a transducer surface; and labeled, which relies on the detection of a specific label. Research into 'label-free' biosensors continues to grow[14]; however "labelled" ones are more common and are extremely successful in a multitude of platforms.

From **the application** point of view, even if medical and clinical applications are the most lucrative and important avenues for biosensors, other areas like the environment, the industrial process monitoring and control or the defence require specific biosensing systems. Moreover, commercial biosensors can be divided into two categories on the basis of whether they are laboratory or portable/field devices. As no more market considerations will be highlighted in this chapter, a selection of the most significant commercial biosensors is made hereafter.

[11-13] E. A. H. Hall, *Biosensors* (1990), Open University Press ; [12]D. G. Buerk, *Biosensors: Theory and Applications* (1993), Technomic Publishing Company; [13]E. Gizeli and C. R. Lowe, *Biomolecular Sensors* (2002), Taylor&Francis
[14] M. A. Cooper, *Anal. Bioanal. Chem.* 377, 834 (2003)

As pointed out before, the most successful handheld biosensor to date is the blood glucose monitor for people with diabetes, which is based on electrochemical transduction technology[15]. Commercial blood-glucose meters are produced by many companies[16]. However, in terms of laboratory-based instrumentation an optical detection system appears to be more commercially viable. Companies such as Affymetrix and Agilent have developed various commercial microarray optical detectors and scanners for genomic and proteomic analysis. Optical sensors that employ surface plasmon resonance (SPR) detection have also been successfully used in many laboratories and universities[17]. Hence, commercially available optical bench-size immunosensor systems such as BIAcore™ (Biacore AB, Uppsala, Sweden) and IAsys (Affinity Sensors, Cambridge, UK) have found their market in research laboratories for the detection and evaluation of biomolecular interactions, noting that these technologies are based on the principles of surface plasmon resonance.

The development of disposable sensors in conjunction with handheld devices for point of care measurements has featured prominently. Microfabrication technology has played an important part in achieving miniaturised biosensors. Such technology has provided cheap mass-producible and easy-to-use / disposable sensor strips. Similarly, electrochemical methods have played a pivotal role in detecting the changes that occur during a biorecognition event, and the merging of microfabrication with electrochemical detection has enabled various handheld biosensor devices to be developed. In fact, i-STAT has developed the world's first hand-held device for point-of-care clinical assay of blood (see Figure 1.4), noting that this biosensor array employs several electrochemical-based transduction methods (i.e., potentiometric, amperometric, conductometric).

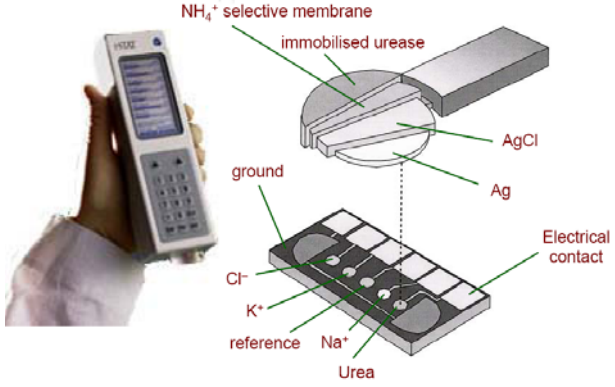

Figure 1.4: The i-STAT multisensor for monitoring various blood electrolytes, gases and metabolites[18]

The i-STAT Portable Clinical Analyser™ is a hand-held silicon-based multiple-analyte sensor array[18], which is used to monitor various blood electrolytes (i.e., sodium, potassium, chloride, calcium, pH), gases (i.e., carbon dioxide, oxygen) and molecules (i.e., urea, glucose, hematocrit). Oxford Biosensors has also developed a portable hand-held device (Multisense™) for cholesterol detection[19]. The biosensor consists of disposable test strips (microelectrodes) and uses the electrochemical detection strategy.

Receptors

Identified beforehand as the most crucial component of a biosensor, the biological receptor is responsible for the selective recognition of the analyte to be detected thus generating the signal issued from the transducer and, ultimately, the sensitivity of the device. Three categories of biological

[15] P. D'Orazio, *Clin. Chim. Acta* 334, 41 (2003)
[16] A. P. T. Turner *et al., Clin. Chem.* 45, 1596 (1999)
[17] R. L. Rich and D. G. Myszka, *J. Mol. Recogn.* 16, 351 (2003)
[18] http://www.i-stat.com
[19] http://www.oxford-biosensors.com

receptors can be precisely pointed out, catalytic (as typified by enzymes), affinitive (of which the antibodies are the best-known example), and DNA-based detection.

Even if non-biological, the molecular imprinted polymers (MIPs) have to be highlighted here as an alternative to biological receptors. A specific section dedicated to MIPs will be included further in this section.

1.4.1 Catalytic receptors and related biosensing techniques

Enzymes are protein molecules, long chains of 20 different amino acids which are so structured as to confer a remarkable ability for catalysing specific reactions. This same structure also limits their functional stability. Compared to non-biological catalysts, enzymes are 10^{18}-10^{13} more active and are capable of producing hundreds of thousands of molecules per second[20].

Enzymes have the longest tradition in the field of biosensors. Since 1997, there have been over 2000 articles published in the literature on enzyme-based biosensors. These biosensors primarily rely on two operational mechanisms. They can be used as a bioreceptor based on their specific binding capabilities or according to their catalytic transformation of a species into a detectable form[11,21]. In most reports in the literature they have been employed according to *their* catalytic activity[10,22]. Horseradish peroxidase (HRP), alkaline phosphatase (AP) and glucose oxidase (GOD) are three enzymes that have been employed in most biosensor studies[23,24].

The detection limit of these biosensors is mainly determined by the enzyme's activity, which can be described by the Michaelis-Menten equation[11]. However, the major limitation of enzyme-based biosensors is the stability of the enzyme, which depends on various conditions such as the temperature, pH, etc[22,23]. The ability to maintain enzyme activity for a long period of time still remains a major obstacle[23]. Another issue that governs the success of an enzyme-based sensor depends primarily on the contact between the enzyme and electrode surface[21]. Despite these pitfalls the enzyme-based sensor is still the most commonly used biosensor, and this is largely due to the need for monitoring glucose in blood[22]. Some recent studies have shown that enzyme-based biosensors can be used to detect very low levels (i.e., ~10−16 M) of pesticides[25].

1.4.2 Affinity receptors and related biosensing techniques

The affinity class of receptors is more specific in the nature of the binding than the enzymes, with binding constants of 10^{9}-10^{12} M^{-1}, but do not exhibit catalytic activity. This fact has consequences for sensing applications. Affinity receptors are more suited to "one-shot" detection rather than monitoring applications, since the binding is essentially irreversible. It is possible to break the binding complex, usually by changing the pH to acid values (1 to 2), but this tends to reduce the affinity and specificity of the receptor. The high binding constant also favours the selective detection of very small analyte quantities. Lowe *et al.*[26] suggest that affinity receptors are suited to analyte concentrations of 10^{-6}-10^{-9} M (note that concentrations as low as 10^{-15} M has recently been demonstrated, as it will be shown in the "nanodevices" further section), as compared with 10^{-3}-10^{-6} M for catalytic systems. These authors also point out that the nature of the binding process is different, the receptor sites for catalytic binding "turning over", whereas the binding sites of affinity receptors can be saturated.

[20] M. Madou and M. J. Tierney, *Appl. Biochem. Biotech.* 41, 109 (1993)
[21] J. Wang, *Analytical Electrochemistry*, 2nd ed. (2000), New York, Wiley-VCH
[22] I. E. Tothill, *Comp. Elec. Agr.* 30, 205 (2001)
[23,24] K. R. Rogers and M. Mascini, *Field Anal. Chem. Technol.* 2, 317 (1998); S. Laschi *et al., Electroanal.* 12, 1293 (2000)
[25] K. A. Law and S. P. J. Higson, *8th World Congress on Biosensors* (2004), Granada, Spain
[26] C. R. Lowe *et al.*, *J. Chromat.* 510, 347 (1990)

Of the affinity receptors concerned by biosensing applications (any proteins like transmembrane proteins, for instance), the immunoreceptors (antibody/antigen) are the dominant type. Antibodies are highly selective, chemical attractor molecules (*glycoproteins*) which are produced by mammalian immunological systems in response to the introduction of an antigen, a foreign molecule. An antigen is simply any substance (molecule, hormone, virus bacteria etc) which elicits antibody formation and reacts specifically with that antibody (*antigenic reactivity* or *antigenicity*). It should be noted that *immunogenicity* is not an intrinsic property of the antigen but a relational property that depends on the gene repertoire and regulatory mechanisms of the host being immunized and which has no meaning outside the context of the host[13]. For instance, human serum albumine (HSA) is an antigenic protein that is immunogenic in the mouse but not normally in human because of the regulatory mechanism known as immunological tolerance (the opposite being the starting point of autoimmune diseases).

Since the antibody-antigen reaction is so specific, each can be utilized as a specific chemical detector for the other. Antibodies are typically represented schematically as Y-shaped structures (Figure 1.5).

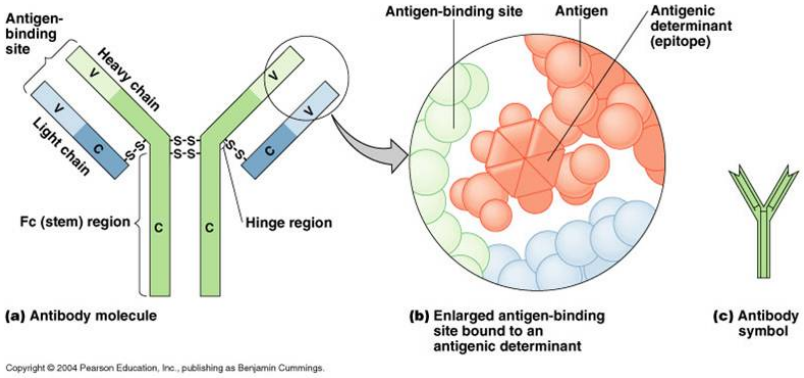

Figure 1.5: Structure of an antibody

The antibody consists of two identical ***Fab*** (fragment antibody) portions hinged to an ***Fc*** (fragment crystallizable) part. The variable regions of the Fab fragments are where the amino acids are organized to produce a binding site for the specific antigen, two binding sites per antibody. The ***Fc*** fragment of the antibody does not combine with the antigen but contains carboxyl terminated amino acids which allow linkage to solid substrates (like transducers). The protein chains are, of course, not straight as represented in Figure 1.5 but are highly folded as revealed by the three-dimensional model of proteins determined by X-ray crystallography studies.

Immunoassays have become a standard tool in clinical chemistry, as they are highly sophisticated automated instruments used to analyze a number of samples in a short time frame[27]. It is important to note that immunosensor technologies have been derived from the standard immunoassay approach[27,28]. A tracer either labels the occupied sites of the antibody or the free ones[28]. Immunosensors can incorporate either the antigen or the antibody onto the sensor surface, although the latter approach has been used most often[29]. Optical and electrochemical detection methods are most frequently used in immunosensors[29] though since the recent commercialization of the Quartz Crystal Microbalance-Dissipative (QCM-D) system by Q-Sense company (Gotteborg, Sweden), the piezoelectric detection becomes a promising immunoassay technique[30]. A number of papers have been recently published on various immunosensors, noting that these have employed either an

[27] M. C. Henion and D. Barcelo, *Anal. Chim. Acta* 362, 3 (1998)
[28] B. Hock, , *Anal. Chim. Acta* 347, 177 (1997)
[29] R. I. Stefan *et al.*, *Fresenius J. Anal. Chem.* 366, 659 (2000)
[30] C. Ayela *et al.*, *Biosens. Bioelectron.* In press, (2007)

electrochemical[31,32] or optical[33-36] transduction method. Detection by electrochemical immunosensors is generally achieved by using either electroactive labels or enzyme labelling[22]. A common challenge facing immunosensors is that they are not completely reversible, so that only a single immunoassay can be performed[12]. Subsequently, some research efforts have been directed towards the development of renewable antibody surfaces[37].

1.4.3 DNA-based receptors and related biosensing techniques

In DNA sensors, the recognition is based on the formation of stable hydrogen bonds between the two nucleic acid strands. The bonding between nucleic acids takes place at regular (nucleotide) intervals along the length of the nucleic acid duplex[38]. The specificity of nucleic acid probes relies on the ability of different nucleotides to form bonds only with an appropriate counterpart. An important property of DNA is that the nucleic acid ligands can be denatured to reverse binding and then regenerated by controlling buffer-ion concentrations[38]. It is important to note that some workers have employed peptide nucleic acid as the biorecognition element[10]. The peptide nucleic acid is an artificial oligo-amide that is capable of binding very strongly to complementary oligonucleotide sequences[10].

Traditional techniques for DNA sequencing are based on the coupling of electrophoretic separations and radio-isotopic (^{32}P) detection[39]. These methods are known to be labour intensive, time consuming, high cost, hazardous, have disposal problems associated with radioactive waste, and are not well suited for routine and rapid environmental analysis[38,39]. Subsequently, various promising alternative methods of DNA detection, which use a non-radioactive labelled probe, have been developed. The detection of specific DNA sequences provides the fundamental basis for detecting a wide variety of microbial and viral pathogens[40]. Several reviews have been published on the development and application of DNA sensors for the testing of virus infections[38-40], noting that viruses appear to be almost uniquely DNA or RNA-composed within an outer coat or capsid of protein[11]. In essence, the technology relies on the immobilisation of a short (20−40mer) synthetic oligomer [the single-stranded DNA (ssDNA)], whose sequence is complementary to the target of interest[39]. Exposure of the sensor to a sample containing the target results in the formation of the hybrid on the surface, and various transduction methods (i.e., optical, electrochemical and piezoelectric) have been used to detect duplex formation[39,41]. Gooding (2002) revealed that relatively few DNA biosensor studies have been carried out in real complex biological samples[42].

Well over 700 papers have appeared in the literature, since 1997, on the development of nucleic acid biosensors. Almost all papers that have dealt with the DNA biosensor have used relatively short synthetic oligonucleotides for detecting target DNAs of about the same length[43]. Most reports have immobilised DNA in the form of a self-assembled monolayer onto a gold surface using thiol chemistry[42-44]. However, in some cases binding of the oligonucleotide probe to the sensing surface is achieved by using the biotin / avidin interaction[45], immobilization technique that will be explain in Section 1.5.

[31,32] W. E. Lee *et al., Biosens. Bioelectron.* 14, 795 (2000); [32]S. Susmel *et al., Biosens. Bioelectron.* 18, 881 (2003)
[33-36] A. W. Kusterbeck *et al., Field Anal. Chem. Technol.* 2, 341 (1998); [34]M. J. Gomara *et al., J. Immunol. Meth.* 246, 13 (2000); [35]S. Koch *et al., Biosens. Bioelectron.* 14, 779 (2000); [36]V. Koubova *et al., Sens. Act. Chem. B* 74, 00 (2001)
[37] G. A. Ganziani *et al., Anal. Biochem.* 325, 301 (2004)
[38] D. Ivnitski *et al., Bioens. Bioelectron.* 14, 599 (1999)
[39] J. Wang *et al., Anal. Chim. Acta* 347, 1 (1997)
[40] M. Yang *et al., Anal. Chim. Acta* 346, 259 (1997)
[41] M. Campas and I. Katakis, *Trend. Anal. Chem.* 23, 49 (2004)
[42] J. J. Gooding, *Electroanal.* 14, 1147 (2002)
[43] E. Palecek, *Talanta* 56, 809 (2002)
[44] T. Peng *et al., Electroanal.* 14, 455 (2002)
[45] K. Kukanskis *et al., Anal. Biochem.* 274, 7 (1999)

1.4.4 Molecularly imprinted polymers and related biosensing techniques

Even if from the early works dealing with biosensors this concept was likely to revolutionise "point-of-sample" analysis, biosensors development pace has been slow and only a very small proportion of the perceived market has been filled. Many of the key issues are directly related to the biological stability of the biological macromolecule at the heart of the biosensor. Thus, problems such as unpredictable shelf-life and stability of biological receptors, poor inter-batch reproducibility and availability, difficulties in incorporating biomolecules into sensor platforms, environmental intolerance (e.g. pH, temperature, ionic strength, organic solvents) and poor engineering characteristics have to be effectively addressed by alternative solutions.

Molecular imprinting is a technology that can potentially address some of the key issues listed above. It deals with the design and synthesis of biomimetic receptors (artificial macromolecules) capable of binding a target molecule with similar affinities and specificities to their natural counterparts[46]. In this technique, a target molecule (acting as a molecular template) is used to direct the assembly of specific binders trapped in a polymer matrix formed by a polymerization step (Figure 1.6). Besides the simplicity in separating MIPs from the soluble template (that allows easily recovering and using them as artificial immobilized antibody, small molecules or enzyme mimic), it is a higher chemical and physical stability compared to biomacromolecules that make them very attractive for applications covering biochemical analysis, separation and catalysis.

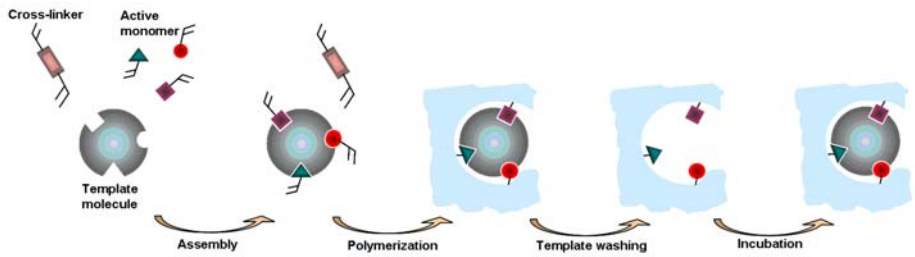

Figure 1.6: Schematics of the molecular imprinting principle

Since 1993, the ISI Web of Knowledge[47] Database registered more than 1100 publications dealing with MIPs, taking roots in a report by Mosbach's group on the development of a MIP-based immunoassay against theophylline and diapzepam[48]. Starting with that moment, MIPs have been used as substitutes for antibodies in radioimmunoassays (RIA) for drugs, showing strong binding to the target analytes (with dissociations constants from the nM to µM range) and cross-reactivity profiles similar to those of antibodies[49,50]. MIPs were later used to develop assay systems for other compounds as well, such as herbicides[51,52] (such as 2,4-dichlorophenoxyacetic acid, mostly known as 2,4-D, which detection by means of silicon-based micromachined sensor is addressed in the second chapter of this manuscript).

Another aspect in assay development is the MIPs potential use in automated systems for unattended monitoring. In a recent paper[53], Surugiu *et al.* described the design of a flow-injection ELISA-type MIP assay using polymer microspheres-coated (using polyvinyl alcohol as glue) glass capillary. A photomultiplier tube (PMT) was used for 2,4-D analyte detection and concentrations ranging from 0.5 ng/mL-50 µg/mL (2.25 nM-225 µM) were detected, making the system one of the most sensitive MIP-based assays reported so far.

---

[46] L. Ye and K. Haupt, *Anal. Bioanal. Chem.* 378, 1887 (2004)
[47] http://portal.isiknowledge.com/
[48] G. Vlatakis *et al., Nature* 361, 645 (1993)
[49,50] L. I. Andresson *et al., PNAS* 92, 4788 (1995) ; O. Ramström *et al., Chem. Biol.* 3, 471 (1996)
[51,52] M. T. Muldoon *et al., J. Agric. Food Chem.* 43, 1424 (1995) ; K. Haupt *et al., Anal. Chem.* 70, 628 (1998)
[53] I. Surugiu *et al., Anal. Chem.* 73, 4388 (2001)

Though non-exhaustive, the before listed successful demonstrations of the use of MIPs for assays, sensors and very recently for drug development[54], reveal the great potential of the technology and amply justify our choice to dedicate a substantial effort in structuring MIPs at the microscale as well as integrating them with acoustic microsensors, as further highlighted in the second chapter.

Immobilization techniques

One key factor in the biosensors design is the development of immobilization technologies for stabilizing biomolecules and tethering them to surfaces[6]. The aim is to create a molecular recognition interface that involves localisation and attachment of a molecular receptor (like those discussed in the previous section) near to or onto the transducer surface. Several approaches are available and the choice of the most adapted one to a particular application depends on various factors like the transduction principle, the nature of the biological receptor and the nature of the analyte to be detected. It will also depend on the way the biosensor will be used, and on its surface chemistry. The immobilization can be achieved in several ways:

- Adsorption of the biological receptor directly to the biosensor's surface;
- Physical entrapment near the biosensor's surface (e. g. in a polymer layer);
- Covalent coupling of the biological receptor directly to the biosensor's surface;
- Covalent coupling to a polymer layer on the biosensor's surface;
- Use of a chemical/biochemical "capture system".

Before entering into the details of each technique, one must note that the method chosen for immobilisation depends on the answers to several elementary issues to be addressed before adopting the final design of the biosensor:

- Will the sensor be regenerated and reused or just dedicated to "unique use" applications?
- What is the nature of the biological receptor (hydrophobic/hydrophilic, large/small)?
- Is it sensitive to handling and, as a main concern, what are the storing constraints? The biological receptors must be kept functional during immobilization and until the biological recognition takes place at the surface of the biosensor. Indeed, if a breakthrough could be achieved in immobilization technologies, in which the progressive loss of activity of the attached bioreceptors was eliminated, many of the present disadvantages of biosensors would be overcome.
- Is the development intended as a proof of principle or a research tool, or is it intended to be translated to commercial mass-production?

As stated by Andrew G. Mayes in Ref[6], "arriving at the correct compromise for any particular situation is a matter of knowledge, experience and careful consideration of the known parameters in relation to the types of issues outlined above".

1.5.1 Adsorption to the biosensor's surface

The following considerations will mostly concern the attachment of proteins onto a solid surface. This choice is deliberately made because the proteins attachment issue is so complex (due to the folded spatial structure of the proteins and to the tremendous arsenal of forces that a protein deploys while approaching and fixing to a solid surface) that the immobilization strategies in other receptor cases may be considered as a deviation of the protein-surface focus.

[54] A. L. Hillberg *et al., Adv. Drug Deliv. Rev.* 57, 1875 (2005)

In the tailoring issue of a surface for proteins attachment, the physico-chemical properties of that surface have first to be considered. In general, proteins adsorb natively to hydrophobic surfaces; this phenomenon is often followed by a thermodynamically-driven unfolding of the protein structure, in order to increase the amount of hydrophobic polypeptide[55] chain (usually from the protein interior) in contact with the surface[56]. Though this lead to denaturation (and deactivation) for most proteins, antibodies are rather resistant since they have a very rigid tertiary structure (see Section 1.4.2), which has evolved to stand the rigours of life in circulatory system.

The main concern regarding hydrophobic surfaces deals however with the non-specific binding issue. Indeed, strong adsorption means that any protein present in solution will tend to bind to the biosensor's surface thus leading to high background signals that cannot be differentiated from the intended specific binding. Not only hydrophobic but also charged surfaces may non-specifically bind proteins due to ion-pair interactions between immobilised charges and ionised surface groups on the protein. However, charged surfaces may benefit to DNA fixing on positively charged membranes or to create exclusion barriers to prevent undesirable analytes reaching a transducer surface (particularly with electrochemical devices).

To prevent non-specific binding and denaturation of proteins from happening, surfaces most closely mimicking an aqueous solution (i.e. *uncharged* – so it does not ionise under any physiological conditions, *rich in hydroxy groups* – thus minimising the possibility of hydrophobic effect, *environment*) have to be engineered. The best type of surface for (covalent) immobilization of a protein is probably one containing a mixture of OH and oligo(ethylene glycol) chains[57] – known for their repellent effect regarding proteins – and just enough of another type of functional group to achieve the required degree of surface derivatisation.

So far the term "biosensor's surface" has been used within a generic purpose; in the following sub-section several kinds of surfaces (gold, glass and similar, and polymers) will be described, though a very wide range of materials is used to fabricate transducers used in biosensors devices.

1.5.1.1 Gold

Gold is the most popular noble metal used in biosensors (either as an electrode material in electrochemical and acoustic sensors or as an integral part of most SPR sensor devices). Its main advantages yield from the properties listed below:

- Inert nature (it does not oxidise in air);
- Highly compatible with most semiconductor manufacturing processes;
- Quite hydrophilic when freshly evaporated, it rapidly becomes hydrophobic due to adsorption of various organic molecules;
- Suitable as a substrate for forming self-assembled monolayers (SAMs)[58].

Thiols (R – SH), sulphides (R – S – R) and disulphides (R – S – S – R) all self assemble on gold. They are adsorbed directly from solution, usually in an alcohol. The solution is typically a few mM and self-assembly takes several hours (much less at higher concentration) to form a dense layer. The gold surface is simply immersed in the solution and left for a period of time before being removed and thoroughly washed (if a collective functionalization is suited). Dip-pen lithography technique[59] may be used if nanoscale thiol-based features have to be "written" onto the gold surface (a specific section will be dedicated to the functionalization techniques further in this first chapter).

---

[55] representative fragments (several amino-acids) of proteins
[56] M. Wahlgren and T. Arnebrant, *Trend. Biotechnol.* 9, 201 (1991)
[57] Z. Yang and H. Yu, *Adv. Mater.* 9, 427 (1997)
[58] R. G. Nuzzo and D. L. Allara, *J. Am. Chem. Soc.* 105, 4481 (1983) – first publication reporting the phenomenon of self-assembly of thiols on gold
[59] M. Jaschke and H. J. Butt, *Langmuir* 11, 1061 (1995)

Thiols with long alkyl chains (n>10) assemble into dense monolayers with a 2D crystalline order. Maturation and reorganization to form this perfect self-assembled layer may take several hours (up to 24 hours) after the initial SAM deposition. Extensive characterizations have shown that the chains pack with a tilt angle of about 30° to the surface normal[60].

Thiols deprotonate upon adsorption to create strong gold thiolate bond:

$$R - SH + Au \rightarrow R - S - Au + e^- + H^+ \quad (1.1)$$

These bonds show little tendency to dissociate under normal conditions. Moreover, the adsorbed molecules tend to remain in place and do not migrate around the surface.

Many different thiols with different chain lengths and functionality are available. This is due to the widespread interest in SAM technology, the rate of development in this area is thus constantly increasing.

1.5.1.2 Glass and similar

The common point of many glass, silica and metal oxides relies on the same general types of surface bonds as they usually contain a mixture of oxygen-bridged metal (or semiconductor) atoms and hydroxy groups. The latter make such surfaces quite hydrophilic and also provide them an opportunity to be modified using organosilanes reagents.

It has been shown in Section 1.5.1.1 that SAMs on gold are simple to prepare. Even though thiols have greater uniformity than silane monolayers, gold is not always suited for biosensor applications. Indeed, in most optical transducers (except SPR sensors), absorbance or fluorescence measurements are performed and in this case transparency of the substrate is mandatory. For such applications, glass or silica is often used, in the forms of fibres or optical waveguides. Silicon dioxide is exclusively used for micro-fabricated structures such as field-effect transistors and tin oxide is also popular since it is transparent, electrically conducting and compatible with semiconductor manufacturing technology.

Various chemical reactions may be used to couple chloro- or alkoxysilanes to the hydroxy groups on metal oxide surfaces. Silane derivatives are available with different terminal functional groups such as amine, thiol, epoxy, etc. These groups may be subsequently coupled to proteins or other receptors to biosensor's surface.

The most common silanisation procedures involve exposing the thoroughly cleaned surface to the silane either in vapour phase or in an inert solvent such as toluene, although aqueuous methods are also available using water-soluble silanes such as 3-aminopropyl-triethoxysilane (APTES)[61,62].

1.5.1.3 Polymers

Natural and artificial polymers are likely to become increasingly important in biosensors due to their low cost, optical properties and possibilities of processing options such as injection moulding, extrusion and thermal micro-moulding. Using such techniques allows producing complex shapes and surface structures (such as diffraction gratings) paving the way towards low-cost integrated devices with, for instance, combined liquid handling and optical components. This trend represented a real

[60] H. O. Finklea, *Electroanalytical chemistry: A Series of Advances,* Vol. 19 (1996), A. J. Bard and I. Rubinstein (eds.), Marcel Dekker, New York
[61,62] I. Haller, *J. Am. Chem. Soc.* 100, 8050 (1978); D.G. Kurth and T. Blein, *Langmuir* 9, 2965 (1993)

paradigm shift in the analytical systems area with the apparition of micro-scale total analysis systems[63] (which may or may not contain sensing devices).

The most important natural polymers are carbohydrates, such as cellulose, agarose and dextran. These materials are very hydrophilic, due to the dominance of hydroxy groups which make them "protein friendly" non-denaturing materials. This means that there is very little adsorption (favourable to minimize non-specific binding) but needs the proteins be covalently coupled.

The properties of polymer surfaces intrinsically range from very hydrophobic to very hydrophilic. The strong adsorption of proteins to hydrophobic polystyrene surfaces was used in the development of radio-immunoassay and enzyme-linked immunoassay[64]. Many other polymers also adsorb strongly such as poly(L-lysine), used as intermediary layer in one of the biosensing applications described in the second chapter.

The large size and additive interactions of such molecules lead to almost irreversible binding under relatively mild aqueous conditions. Adsorption thus provides a convenient way to introduce functional groups such as amines onto polystyrene surfaces for subsequent covalent coupling[65]. Similar approaches can also be used with many other polymers.

1.5.2 Entrapment methods

Physical or chemical entrapment of bioreceptors within semi-permeables membranes or polymers has attractive features as it deals with very simple and applicable system for a wide range of macromolecules, the using conditions being very mild, generally requiring no chemicals or procedures liable to cause denaturation or loss of viability. The main entrapment methods (physical entrapment behind membranes, entrapment in hydrogels, and entrapment within conducting polymers) will be briefly discussed in the followings.

1.5.2.1 Physical entrapment behind membranes

Physical entrapment deals with semi-permeable membranes, such as cellulose dialysis tubing, used to retain a solution containing the receptor molecules in a compartment adjacent to the transducer. Small molecules (in terms of molecular weight) are free to diffuse in and out of this compartment while the high molecular component is held insight. The first demonstration of a biosensor device based on an oxygen electrode[66] used the physical entrapment approach, thus representing an important breakthrough in the history of biosensors' development. The technique is still quite used and is particularly suitable for cells and organelles although it can also be used for enzymes and antibodies.

For large bio-molecules such as enzymes and antibodies, dialysis tubing is often used as the semi-permeable membrane. The molecular weight cut-off (determined by the pores' size) of such a membrane is typically around 5 – 10 kDa[13] for globular molecules and thus completely retains typical proteins while allowing relatively unhindered diffusion for small molecules. Many other types of membranes are also available, made from other materials and with different porosities, like polycarbonate and nylon.

A key limitation is the difficulty of transferring this approach to mass production, due to problems of sealing wet membranes over devices; thus while it remains a useful approach for laboratory demonstrations, it is unlikely to find its way into mass –produced sensors.

---

[63] D. R. Reyes *et al., Anal. Chem.* 74, 2623 (2002)
[64] R. C. Zangar *et al., Exp. Rev. Prot.* 3, 37 (2006)
[65] I. V. Kalashnikova *et al.*, *J. Chromat. A* 1144, 40 (2007)
[66] L. C. Clark and C. Lyons, *Ann. N. Y. Acad. Sci.* 102, 29 (1962)

1.5.2.2 Entrapment in hydrogels

Enzymes and antibodies can be physically entrapped within the volume of a polymer hydrogel[67], rather than behind a membrane, while retaining substantial activity. In this technique polymers that can be dissolved in warm or hot water (while taking a "gel" form on cooling, due to hydrogen-bond formation) are used. The most used polymer is agarose, a polysaccharide obtained from marine algae. Due to its quite high porosity, agarose is most suitable for whole micro-organisms or organelles, rather than isolated proteins, since these would leach out from the gel's structure.

Poly(vinyl alcohol) is an alternative used in case of proteins' physical entrapment[68]. These can be mixed with the polymer solution and deposited on surfaces by printing, droplet deposition, etc. The film is then dried, entrapping the protein. When subsequently rehydrated, the polymer swells rapidly and the protein becomes biologically functional, but cannot diffuse out of the polymer.

In order to reduce the amount of proteins that can leach out of an entrapping hydrogel, it may be desirable to covalently link the protein to the growing polymer chains. In order to do so, it is often necessary to derivatise the protein so that it contains polymerisable functional groups that can be covalently incorporated into the growing polymer chains. The most common way to obtain this is to form acrylamide groups on a protein surface by reacting the protein with N-hydroxysuccinimide (NHS) reagent[13].

1.5.2.3 Entrapment within conducting polymers

In some cases of biosensors based on electrochemical transduction principle, an electrically conducting polymer is used in the entrapment procedure. The conducting properties of the polymer may either be used as part of the transduction mechanism or to perform active grafting of biomolecules on metallic surfaces with a real-time control[69]. The most widely approach is by using pyrrole which can be electropolymerised under relatively mild aqueous conditions at a potential that does not damage functional bioreceptors. This method has been used with a variety of enzymes, antibodies and DNA[70,71] and ensures proper orientation and packing of biological receptors onto solid surfaces. With regard to the fabrication of biochips, controlling the surface arrangement is mandatory since the sensitivity of the detection is dictated either by the amount of receptors immobilized or by their accessibility.

1.5.3 Covalent coupling

An alternative approach to the attachment of biomolecules to sensor surfaces is through covalent binding, where biomolecules have been immobilized on solid surfaces through the formation of defined linkages[72,73]. Covalent binding of biomolecules to the surface is a favoured method and procedures resulting in minimal loss of biomolecule activity have been employed[74-79].

Biomolecules such as enzymes and proteins have many functional groups present for covalent immobilization onto surfaces; these include *amino-acid* side chains (e.g. amino groups of lysine), *carboxyl groups* (aspartate and glutamate), *sulfhydryl* groups (cysteine), *phenolic*, *thiol* and *imidazole*

---

[67] K. F. O'Driscol, In *Immobilised Enzymes* Vol. XXXIV (1976), K. Mosbach (ed.), Academic Press, New York
[68] M. T. Reetz, *Adv. Mat.* 9, 943 (1997)
[69] T. Livache *et al., Biosens. Bioelectron.* 13, 629 (1998)
[70,71] J. N. Barisci *et al., Trends. Pol. Sci.* 4, 307 (1997) ; T. Livache *et al.*, *Synth. Met.* 121, 1443 (2001)
[72,73] J. N. Lin *et al., IEEE Trans. Biomed. Eng.* 35, 466 (1988) ; J. I. Peterson and G. G. Vurek, *Science* 224, 123 (1984)
[74-79] H. Muramatsu *et al., Anal. Chim. Acta* 188, 257 (1986) ; [75] M. Thompson *et al., Anal. Chem.* 58, 1206 (1986) ; [76] M. Thompson *et al.,IEEE Trans. Ultrason. Ferroelec. Freq. Contr.* UFFC-34, 127 (1987) ; [77] H. Muramatsu *et al., Anal. Chem.* 59, 2760 (1987) ; [78] E. Prusak-Sochaczewski and J. H. T. Loung, *Anal. Lett.* 23, 401 (1990); [79] G. J. Legget *et al.*, *Langmuir* 9, 2356 (1993)

groups. This method has been employed to improve uniformity, density and distribution of the bound proteins, as well as reproducibility of the surfaces. Problems associated with instability, diffusion and aggregation, or inactivation of proteins which are common when biomolecules are trapped on sensor surfaces by polymer matrices, can also be overcome by using covalent immobilization. Moreover, covalent binding has the advantage that the biomolecule is generally strongly immobilized on the surface and therefore unlikely to detach from the surface during use. Reagents such as gluteraldehyde, carbodiimide, succinimide esters, maleinimides and periodate are extensively used for covalent immobilization, as it will be outlined in this section.

1.5.3.1 Coupling to carboxylic acids

Carboxylic acids on surfaces can be readily produced via SAMs, by oxidation through surface hydrolysis of olymers and via polymer grafting. As pointed out before, in most cases the soluble biomacromolecule to be detected has an available amine group; for instance, if an antibody is used, the majority of linkages will be made to surface amine groups (part of lysine amino-acid), even if a few surface tyrosine, cysteine or histidine residues are present (since the latter are usually much less abundant).

The most used immobilisation technique involving carboxylic acids is probably amide bond formation using carbodiimide reagents. This reaction has been studied extensively due to its importance in organic chemistry in general and in solid-phase peptide synthesis in particular[80]. the reaction involves two stages; activation by the carbodiimide reagent to form an O-acyl isourea intermediate and nucleophilic displacement of the intermediate by the amine to form the final amide bond. This can be done either in organic solvents or under aqueous conditions. If in the former case the carboxylic acid is simply mixed with the amine in the presence of a mole equivalent amount of a suitable carbodiimide, things are a little more complex in the latter case where water soluble carbodiimides must be used (such as 1-ethyl-3-(3-dimethylaminopropyl)carbodiimide, mostly known as EDC). In order to increase the efficiency of the reaction, other reagents such as N-hydroxy succinimide (NHS) are used.

The EDC/NHS procedure has been popularised and extensively optimised by Biacore, since it is the most common method of coupling proteins to carboxymethyl-dextran SPR chips[81] (typical conditions being use of about 0.1 M EDC and NHS in a mild buffer[82] at around pH 5-6).

Other immobilisation techniques by means of modification of carboxylic groups are available such as displacement of active esthers and mixed anhydride formation but their detailed description is far beyond the scope of this dissertation. For more details, readers are invited to refer to Ref [74-79].

1.5.3.2 Reactions involving thiols

Thiols groups are important in antibody coupling, due to the possibility of producing Fab fragments with free thiols[82]. They are generally coupled either y disulphide formation or by creating thioethers. Disulphides are relatively easily formed and have the unique property that, while stable under normal conditions, they can be readily cleaved and reformed via thiol-disulphide exchange. This offers the possibility of regenerating the biosensor's surface by mild chemical stripping followed by reactivation and recoupling.

---

[80] J. C. Sheehan and G. P. Hess, *J. Am. Chem. Soc.* 77, 1067 (1955)
[81] B. Johnson and S. Löfas, *Anal. Biochem.* 198, 268 (1991)
[82] Note that the nature of the buffer is important as it must not contain any traces of carboxylic acid that might interfere with the reaction.
[82] A. Johnston and R. Thorpe, *Immunochemistry in practice* (1987), Blackwell Scientific Instrumentation Publications, Oxford

To remove a coupled protein, the surface is treated with a thiol containing reducing agent such as dithiothreitol (DTT). This removes the protein, leaving free thiol groups on the surface again, so that the cycle can be repeated. DTT is the reagent of choice for this step since it "excises" itself from the surface by an internal thiol-disulphide exchange leading to a cyclic disulphide and a free surface-bound thiol[13].

1.5.3.3 Reactions involving amines

Coupling of proteins and other ligands to amine surfaces has already been covered in the previous Sub-section 1.5.3.1 as the reactive groups are simply reversed in this case but the same chemistry and conditions can be used. It has to be noted that for coupling of proteins it is generally better to have a carboxylic acid surface, since the activation and coupling can be separated to avoid aggregation which cannot be achieved with an amine surface. However, for some small ligand such as biotin, coupling to amine surface is very convenient as the carboxylic acid entering in its structure can be directly coupled using NHS/EDC chemistry thus avoiding the need for expensive biotin derivatives.

Two other reactions available for coupling to amine surfaces, by means of isothiocyanates and sulphonil chlorides, are extensively used for quantitating amines by formations of fluorescent derivatives; they can be used in a similar way on surfaces to confirm that amine-containing surfaces have been produced. However, as far as protein coupling is concerned, these reactions have little use.

Though many other covalent immobilisation procedures have been developed (that involve hydroxy groups or aldehydes, for instance), they will not be further described; interested readers may find related details in the affinity chromatography literature.

1.5.4 Other capture systems

The use of a chemical or a biochemical capture system often offers the possibility of creating generic surfaces where specificity can be switched even if non-specific binding to components of capture system has to be carefully considered, as it will be outlined in the following paragraphs. This technique is compatible with various options for regeneration while giving some control over the biomacromolecules' orientation.

1.5.4.1 Use of antibody-binding proteins

The most obvious class of proteins capable of binding to antibodies are antibodies themselves. Species and class selective antibodies, such as goat anti-human immunoglobulins (IgG) can be used to capture the antibody of interest. This type of approach is extensively used in ELISA technology.

There are a number of proteins, isolated from bacteria, that have the ability to bind to the Fc region of IgGs. The best known examples are Protein A (from *Staphylococcus aureus*) and Protein G (from *Streptococcus* strain G148)[83]. When immobilised, Protein A and Protein G, can be used as capture systems; since they bind the Fc region, the captured antibodies have the correct orientation to maximise access to the binding sites. The drawback of this method is that in case of random immobilisation of Proteins A and G, they may not all be able to bind antibodies. Hence, although the captured antibody will function efficiently, it may be present at lower densities than if it had been immobilised directly.

The most important property of using Protein A of Protein G capture systems is not so much the orientation effect but the ability to remove the active antibody layer and replace it with a different one under relatively mild conditions (usually by treatment with acidic buffers such as 20mM citrate pH3.5[13]). These surfaces thus act as generic immunosensors platforms.

[83] F. Breitling and S. Duebel, *Recombinant Antibodies* (1999), John Wiley and Sons Inc., New York.

1.5.4.2 Avidin/streptavidin capture systems

Because of the extremely high affinity of avidin/biotin (or streptavidin/biotin) interaction (which is essentially non-reversible under normal assay conditions), the use of this capture technique is widespread in assay and labelling methodology. The various uses of avidin/biotin technology have been reviewed extensively in the litterature[84] and will not be commented here. Although streptavidin and avidin are interchangeable, the former is usually preferred (despite its higher cost) due to its lower non-specific binding characteristics.

A variety of methods for immobilising avidin have been used including general covalent strategies and the capture of the avidin using covalently-immobilised biotin (see Sub-section 1.5.3.3). Avidin is ideal for forming two-dimensional crystalline arrays on suitable surfaces[85,86] due to its "block-shaped" protein structure, with four biotin-binding sites. The binding sites are distributed with two on each of nearly parallel faces of the molecule. If an appropriate surface is prepared with immobilised biotin molecules, avidin can bind to this surface to form a tightly-anchored array, with a high density for biotin binding[87]. This is an ideal surface for biotinylated antibodies (obtained by use of NHS/EDC chemistry which couples biotin molecules at random onto the antibody).

Other chemical/biochemical systems like generation of specifically-located thiols groups or use of tags with engineered antibody fragments[13] have to be cited though details specific to these techniques will not be given here.

1.5.5 Spatial control of surface immobilization

As biosensors are getting smaller, coating their surface with bioactive layers is becoming challenging. In many cases, commonly used immersion is not appropriate because selective functionalisation of active areas can be difficult to achieve. Application areas include medicine (e.g. auto-immune diseases diagnosis purpose), environmental monitoring (e.g. monitoring herbicides on cultivated soils), customs and sports (e.g. detection of drugs or doping illicit substances) and military uses (e.g. detecting biological warfare agents).

In some cases, arrays of sensors are constructed from a number of separate components, which are subsequently combined together. In other cases, it is more appropriate to make a single device with different elements of the array defined by their geometric location and specific functionalisation. Such systems would be appropriate for subsequent analysis either using *extrinsic* means like SPR or mass spectrometry or *intrinsic* means like fully integrated bio(micro electromechanical systems) – or bioMEMS – that will be discussed further in this chapter.

In order to create such arrays, spatial control of biofunctionalisation is mandatory. A number of different approaches are available, including replication of patterns, photochemical methods, the use of photo-deprotection strategies and control of biomacromolecules' deposition by physical placement.

As an important part of the research work described in this manuscript deals with the development of liquid patterning tools at the micron scale, the state-of-the-art in this field is of key significance. An exhaustive, remarkable review of these patterning techniques has recently been done by T. Leïchlé in his PhD thesis[88], a summary of which will be given in the followings.

[84] M. Wilchek and A. E. Bayer, *Anal. Chem.* 171, 1 (1988)
[85,86] W. Mueller *et al., Science* 262, 1706 (1993) ; J. Spinke *et al., Langmuir* 9, 1821 (1993)
[87] M. Morgan and D. M. Taylor, *Biosens. Bioelectron.* 7, 405 (1992)
[88] T. Leïchlé, *PhD thesis* (2007) Université Paul Sabatier, Toulouse

1.5.5.1 Replication of patterns

The use of positive and negative photoresist procedures has been developed into a highly reproducible and high-resolution (sub-micrometre) technique by the semiconductor industry[89]. such approaches can also be used to protect certain areas of a substrate while others are derivatised by an appropriate surface-modification procedure. This method can work well only if a few different types of surface functionality are required for subsequent attachment of biological molecules. Hydrophilic/hydrophobic patterns have been produced in this way for directing the growth of neuronal cell cultures onto surfaces[90].

The main drawback with photoresist methodology is that the current types of available photoresists are not compatible with aqueous conditions. The organic solvents as well as high temperatures and high radiation intensities used to pattern the photoresists would denature proteins if they were attached to the substrate; therefore, the patterning must be completed before the biomolecules are introduced. Nevertheless, lithography was adapted in the late 1990's for the manufacture of DNA chips[91]. In this method, repetition of lithographic steps with different chemical reagents and appropriate masking enable the construction of oligonucleotide chains with different DNA bases in desired sequences, though it remains suited only when a small number of sequences is involved.

An alternative technique to conventional lithography to be used for biofunctionalisation purposes has been developed during the last decade called "micro-contact printing"[92]. This is a very simple and rapid technique, particularly suitable for patterning gold surfaces although it also can be combined with other types of chemistry. The basic procedure deals with making a flexible silicone rubber stamp containing the required pattern; the stamp is coated with a suitable thiol compound and used to contact print the thiol onto the required areas of the gold substrates where it spontaneously self-assembles. Untreated areas can subsequently be coated with another thiol by immersion in a solution of the thiol.

The micro-contact printing method has been used to define the surface chemistry of substrates used, for example, to control the growth of cell cultures in particular patterns[93] or to induce controlled chemical gradients[94]. It can also be used in many other ways to perform deposition of lipid layers, proteins and DNA[95-96]. Apart from its simplicity (relevant results may be achieved in laboratory without the need for complex equipment and clean-room facilities), micro-contact printing has another advantage over conventional lithography; it can be used with curved surfaces and other three-dimensional surfaces, providing there is access for a shaped rubber stamp. This considerably increases the impact of this technique.

1.5.5.2 Light direct immobilisation and patterning

In this Sub-section, the use of direct photochemical immobilisation methods will be outlined: the direct photocoupling reactions and the photo-deprotection reactions.

It is well known that a number of chemical functional groups such as aryl azides, aryl diazirines and benzophenones, transform into highly reactive intermediates when activated by light[13].

---

[89] A. Reiser, *Photoreactive Polymers: the Science and Technology of Resists* (1989), John Wiley and Sons, New York.
[90] P. Clark *et al., J. Cell. Sci.* 105, 203 (1993)
[91] M. Schena *et al., Tibtech* 16, 301 (1998)
[92] M. Mrksich and G. M. Whitesides, *Tibtech* 13, 228 (1995)
[93] R. Singhvi *et al., Science* 264, 696 (1994)
[94] T. Kraus *et al., Langmuir* 21, 7796 (2005)
[95-96] A. Bernard *et al., Adv. Mat.* 12, 1067 (2000) ; S. A. Lange *et al., Anal. Chem.* 76, 1641 (2004)

Simple aryl azides were the first photo-crosslinkers to be used in bioconjugate chemistry[97] and a number of different substituted aryl azides have subsequently been introduced. These compounds absorb a photon usually in the UV range around 330-370nm to generate a nitrene, with loss of nitrogen. The nitrene is highly reactive and will take out a proton from a C-H bond which is particularly abundant in proteins.

Aryl diazirines are relatively unstable compounds and undergo UV induced photo-decomposition to generate highly reactive carbene species[98]. The carbenes can insert into a wide range of bonds, particularly acidic species such as R-NH and R-OH bonds. The carbenes thus react favourably with proteins and many other types of biomacromolecules, but also with water, which somewhat reduces the coupling efficiency.

Benzophenone derivatives also absorb photons in the UV range around 360nm to generate a O-radical[99] which in turns will abstract a proton preferentially from a C-H group belonging, for instance, to a specific protein. These compounds are very stable in storage and under ambient light conditions.

The general procedure for using any of the above reagents would be to immobilise the reagent on the surface via any suitable coupling method. A variety of amino and thio reactive derivatives with aryl azide or benzophenone groups are commercially available, as are simple compounds such as benzoylbenzoic acid[100] that can be easily coupled to a amine surface by carbodiimide coupling (see Sub-section 1.5.3.1). The surface is covered with a solution of the biomolecule to be coupled and with a mask which defines the areas the areas that will be radiated. The structure is then exposed to UV light for a few minutes to achieve coupling[101-105]. By repeating the coupling cycle with different biomolecules and masks, an array of different immobilised molecules can be realized.

The alternative to direct photo-activation and coupling is to use a photo-deprotection strategy to "unmask" a functional group and make it available for a conventional covalent coupling reaction. This method is extensively used in light-directed combinatorial synthesis to make arrays of molecules such as peptides at a surface[106]. Methods for photo-deprotecting amine groups are thus particularly well developed and the amines can subsequently be used in a wide range of covalent coupling methods (see Sub-section 1.5.3.3). The same strategy was used in the development of a photo-activatable polyacrylamide gel containing protected amino groups that could be photo-exposed and used for coupling of antibodies and antigens[107].

1.5.5.3 Control of deposition by physical placement

Various methods exist for spatial delivery of liquid samples, the most appropriate one depending on the scale of the array to be produced and the throughput required. Two different classes of methods are generally used: the non-contact and the contact method. While the former consists in projecting liquid drops on the surface form a droplet ejector, the latter allows transferring droplets thanks to the liquid meniscus formed between the depositing tool (usually, a tip) and the contacting surface.

---

[97] G. W. J. Fleet *et al., Biochem. J.* 128, 499 (1972)
[98] T. Yamaguchi *et al., Nucl. Acid Res.* 25, 2352 (1997)
[99] T. Kanamori *et al., PNAS* 94, 485 (1997)
[100] P. B. Jones *et al., J. Org. Chem.* 61, 9455 (1996)
[101-105] D. J. Pritchard *et al., Angew. Chem. Int. Ed. Engl.* 34, 91 (1995) ; [102]N. Barie *et al., Biosens. Bioelectron.*13, 855 (1998) ; [103]L. F. Rozsnay *et al., Angew. Chem. Int. Ed.Engl.* 31, 759 (1992) ; [104]H. Gao *et al., Biotech. Appl. Biochem.* 20, 251 (1994); [105E]. Delamarche *et al., Langmuir* 12, 1997 (1996)
[106] J. W. Jacobs and S. P. A. Fodor, *Tibtech* 12, 19 (1994)
[107] M. S. Sanford *et al., Chem. Matter.* 10, 1510 (1998)

Non-contact methods include ultrasonic micropipette technique[108-109], electrospray[110-111], capillary-free jetting mechanism[112] and, the most popular, ink-jet printing[113,114]. As indicated before, a complete review of these tools may be found in Ref[88]. As the depositing tool developed in the research work described within this manuscript belongs to the contact method, a short overview of the contact liquid delivery tools will be provided in the followings, together with the introduction of their foreseen applications and comparison of their performances.

In contact methods, a solid tip or the extremity of a capillary touches the surface to pattern, allowing species to be transferred or liquid drops to be deposited, respectively. The advantage of having a direct contact between the patterning tool and the surface are numerous. First of all, because the transfer occurs thanks to capillary forces acting on the liquid, the contact method is a passive delivering technique. Thus there is no need for liquid actuation means and tools are greatly simplified. Sensors can be incorporated to the tool itself to have a direct control of the deposition process and direct information on the tool position. However, this method depends greatly on the physical and chemical states of the surface to pattern.

a) Micro- and nanopipettes

A very interesting patterning solution relying on the use of a double-barrel nanopipette, fabricated from a glass capillary, has been recently presented[115]. The main strength of this method is the ability to deliver independently two different species from each barrel of a single tip. The use of electrodes placed inside each barrel enables the selection of the depositing barrel and the voltage control of deposition parameters such as the distance between the tip and the surface and the volume of liquid delivered. Moreover, it has been demonstrated that volumes could simply be added to an existing droplet with this tool.

Microfabricated tools that mimic the capillary pipettes have been also lately introduced[116]. They consist in silicon or polymer tubes arranged on a surface. Liquid is provided on one side of the device, and flows into the tubes to reach the depositing surface. These tools have several advantages over conventional pipettes. The tube inner and outer diameters, which control the size of the deposited drop, can be fabricated with high precision and can exhibit very small dimensions. Moreover, the microfabrication approach easily allows the parallelization of the technique deposition, as several tubes can be fabricated on the same device. However, these tubes are usually not flexible and cannot undergo large stresses and strains, thus microfabricated pipette arrays have to be very carefully operated. Alignment with pre-fabricated patterns can also be an issue.

b) Scanning probe lithography-based liquid delivery systems

Scanning probe techniques are based on atomic force microscopy, for which silicon cantilevers with sharp tips are scanned across a surface to create an image of the surface topography with nanometric precision. The original idea of the scanning probe lithography (SPL) technique is to use the cantilever tip to deposit chemical and biological materials. The interesting feature of SPL is that the same tip can be used to write patterns and to image them. SPL methods take advantage of the high resolution of AFMs resulting so far in the minimum features sizes patterned by add-on processes

---

[108-109] D. B. Hager and N. J. Dovichi, *Anal. Chem.* 66, 1593 (1994); C. H. Lee and A. Lal, *IEEE Trans. Ultrason. Ferroelec. Freq. Contr.* 51, 1514 (2004)
[110-111] J. Zeleny, *Phys. Rev.* 3, 69 (1914) ; M. Yamashita and J. B. Fenn, *J. Phys. Chem.* 88, 4451 (1984)
[112] J. A. Barron *et al., Proteomics* 5, 4138 (2005)
[113,114] T. Goldman and J. S. Gonzalez, *J. Biochem. Biophys. Meth.* 42, 105 (2000); T. R. Hughes *et al., Nat. Biotechnol.* 19, 342 (2001)
[115] K. T. Rodolfa *et al., Angew. Chem. Int. Ed.* 44, 6854 (2005)
[116] O. T. Guenat *et al., J. Micromech. Microeng.* 15, 2372 (2005)

(sub-100 nm). This high resolution is balanced by the long writing times necessary to pattern microareas. There are three approaches in SPL techniques, detailed hereafter.

Dip-pen nanolithography (DPN) principle was first demonstrated by Butt et al. with the use of a scanning force microscope (SFM) tip to deposit organic material[59]. In their experiments, a SFM tip was covered with octadecanethiol (ODT), by dipping it into liquid ODT, and then brought into contact with a mica surface. Upon contact with the surface, ODT was transferred from the tip onto the surface. This technique has been further developed and popularized by Chad Mirkin's group[117]. In this technique, the ink loaded onto the AFM tip is delivered to the substrate via a water meniscus that forms between the tip and the surface. This meniscus serves as a medium for ink transport with nanometric precision and is thus fundamental for the success of ink-delivery. This requires working in a suitable humid environment with enough water vapor to allow proper condensation on the tip. Importance to control the humidity level is necessary for reproducible patterning results[118]. DPN has been initially used to pattern alkylthiols (e.g. MHA and ODT) onto gold films with an overwriting capability and a 15 nm resolution[119,120]. Its writing potential has rapidly been extended to numerous SAMs and surfaces (e.g. HMDS on semiconductor surfaces[121]), allowing the indirect patterning of bigger entities. The indirect method consists in firstly patterning the surface with functional chemistry via DPN to generate a template for the subsidiary grafting of colloids, DNA strands or proteins. Because only the template fabrication is carried out locally (unlike the immobilization procedure), it is difficult to produce patterns of different compounds on the same surface. For this purpose, the direct patterning of large molecules has been demonstrated. DNA and proteins, adsorbed on tips, have been deposited without altering their biofunctionality[122-124]. Thanks to the rising attention paid by the scientific community to DPN and the increasing research work focusing on that subject, the direct patterning of a lot of other materials have been investigated: nanoparticles, metal-salts, sol-based inks, colored inks and polymers have been successfully used targeting various applications.

In **scanning probe contact printing** (SPCP), the cantilever tip is made of an elastomeric material. It is used to print chemicals onto surface analogously to a microcontact stamp. The tip is usually made of PDMS and the dimensions of the tip can be controlled during the fabrication of the cantilever. The initial fabrication process of these tips was proposed by the Mirkin group[125], and a simpler fabrication approach, developed by NanoInk Inc., consists in dip-coating the tip of a regular AFM cantilever with PDMS[126]. In SPCP, a chemical ink is firstly absorbed into the PDMS tip. Each contact of the tip on the surface leads to the transfer of molecules onto the surface and creates a pixel print. Arbitrary patterns can thus be formed in dot-matrix manner. Unlike DPN, SPCP can be operated at ambient conditions and features are inherently larger. Thus it can be considered as a brick bridging the gap between: i) the lower resolution but massively parallel μCP method and ii) the higher resolution but lower throughput DPN process.

Because both DPN and SPCP techniques rely on the use of AFM probes, they can all be integrated on the same chip, including printing and imaging capabilities. Wang et al. have demonstrated the fabrication of such an integrated device, with probes being able to perform a dedicated function[127]. To take advantage of the combination of different tools, thermal electric actuators have been integrated to each cantilever, allowing an individual addressing. This multifunctional probe array is therefore capable of performing a rich variety of operations with minimal chemical crosstalk and high registration accuracy. It is extremely well-suited for the

[117] D. S. Ginger *et al., Angew. Chem. Int. Ed.* 43, 30 (2004)
[118] M. Su et al., *Langmuir* 21, 10902 (2005)
[119,120] R. D. Piner et al., *Science* 283, 661 (1999) ; S. Hong *et al.*, *Science* 286, 523 (1999)
[121] A. Ivanisevic, and C. A. Mirkin, *J. Am. Chem. Soc.* 123, 7887 (2001)
[122-124] J.-H. Lim *et al., Ang. Chem. Int. Ed.* 42, 2309 (2003); [123]S.-W. Chung et al., *Small* 1, 64 (2005); [124]K.-B. Lee *et al.*, *J. Am. Chem. Soc.* 125, 5588 (2003).

[125] X. Wang *et al., Langmuir* 19, 8951 (2003)
[126] H. Zhang *et al., NanoLett.* 4, 1649 (2004)
[127] X. Wang, and C. Liu, *NanoLett.* 5, 1867 (2005)

fabrication of nanometer scale patterns with high resolution and in-situ characterization means. However, inherently to the dip-pen and SPCP principle of operation, only small areas can be patterned in a time consuming process. Moreover, because of the tiny amount of ink material that a probe can carry, writing steps must often be alternated with necessary reloading procedures.

Lewis et al. have proposed a **nanofountain pen** system based on the use of cantilevered quartz micropipettes mounted onto the probe of an AFM[128] The deposition of different materials has been carried out with this system: local delivery of chromium etchant for mask repair applications, local printing of proteins, and formation of polymer droplets for microlenses fabrication[129,130]. However, despite its interesting capability, this system is not suited for parallelization and integration. Lately, a very promising approach has been proposed within the NaPa framework by Meister et al. to overcome these drawbacks. The key feature of their nanodispensing system (NADIS) is the deposition of liquids through apertured scanning force microscopy probe tips. The first probes were fabricated using a dedicated process allowing the creation of an open reservoir on top of the cantilever with a nanochannel at the apex and an alternative fabrication method relying on the modification of commercial AFM tips by FIB milling has also been proposed[131,132]. Nanodrops of 20 nm polystyrene particles were deposited with this system. The open reservoir on top of the cantilever raises two important issues. The loading of the cantilever is very delicate, and giving the small volume of the drop reservoir, only liquids with a low evaporation rate can be used as solvent mediums. Hence, Deladi et al. have recently fabricated a cantilever with a close channel allowing a continuous liquid supply to the cantilever tip[133]. However, this closed-channel configuration can experience clogging, thus leading to a failure to write. Besides, simple cleaning procedures are difficult to foresee.

c) In-plane microcantilevers for liquid delivery

Recently, direct liquid delivery techniques inspired from the stainless steel pins currently used to fabricate biochips have been proposed. Systems based on commercial quills and pins allow printing spots with 60 µm diameters[134]. The needles are machined in a serial fashion and are usually very expensive. Besides, because the pins are made of stainless steel and the deposition occurs by a direct contact of the pin tip with the surface, the tips are easily damaged, causing inconsistent drop sizes. Finally, parallelization can only be obtained by manually placing several needles on the same support.

The idea of using silicon microcantilevers as printing pins has emerged from Bergaud and its team at LAAS[135] quickly followed by other research groups in the U.S.A.[136,137], leading to very similar devices. This idea offers several advantages: thanks to the microfabrication techniques, arrays of cantilevers can be realized on the same chip resulting in cheap and disposable devices. Due to the micrometric precision of photolithography, these cantilevers can be made very small, enabling the deposition of smaller droplets, typically with diameters of several tens of micrometers. Unlike the dip-pen technique, the tip used for liquid transfer is in the plane of the cantilever, and can directly be fed by a fluidic system placed on top or in the cantilever. Usually the fluidic system consists in an open channel etched in the cantilever, thus solving any clogging issue (however this usually requires one to work with low evaporation rate solvents). The size of the channel is usually large enough to allow printing hundreds of spots without reloading the cantilever that can be thus loaded with an external chip. However, a liquid reservoir can also be incorporated on the chip bearing the cantilevers. Similarly to DPN, droplet size is controlled by the contact time between the tip and the surface, but deposited volumes are much bigger. Because the targeted application of these devices is the

---

[128] A. Lewis *et al., Appl. Phys. Lett.* 75, 2689 (1999)
[129,130] H. Taha *et al., Appl. Phys. Lett.* 83, 1041 (2003) ; M. Sokuler and L. A. Gheber, *NanoLett.* 6, 848 (2006)
[131,132] A. Meister *et al., Microelectron. Eng.* 67-68, 644 (2003); Meister *et al., Appl. Phys. Lett.* 85, 6260 (2004)
[133] S. Deladi *et al., Appl. Phys. Lett.* 85, 5361 (2004)
[134] http://www.arrayit.com/
[135] P. Belaubre *et al., Appl. Phys. Lett.* 82, 3122 (2003)
[136,137] J. Gin Fai Tsai *et al.,* P*roc. 16th Ann. Int. Conf. on MEMS* (MEMS'03), (2003) 19-23 Jan, Kyoto, Japan, 295; J. Xu *et al., Biomed. Microdev.* 6, 117 (2004)

fabrication of biochips, they have only been so far used to print DNA or proteins. These cantilever pins are very attractive for the delivery of picoliter droplets because of their simplicity and low-cost, however, the deposition of other materials needs to be carried out to prove their versatility.

1.5.6 Conclusion to immobilisation techniques issues

Despite the intense research into biomolecules' immobilisation techniques, no generic method has yet been identified and proposed. The Table 1.1 below summarizes the advantages and drawbacks of the different immobilisation strategies discussed so far.

Immobilisation technique		**Pros**	**Cons**
Adsorption		Simple, low-cost; Single-use applications adapted	Non-specific binding; Relatively unstable; Highly dependent upon pH, solvent, temperature, surface and biomolecule nature
Entrapment	***Behind membranes***	Simple universal approach for macromolecules; Mild conditions; Long working life	Difficult to mass-produce; Diffusion barrier slows response time
	In hydrogels	Mass production potential	Protein denaturation by free radicals
	Within conducting polymers	May participate to the transduction mechanism; Proper orientation and packing of active bioreceptors	Necessitates in-situ electrochemical activation means
Covalent coupling		Stable; Intimate contact with transducer; Low diffusion barrier – rapid response	Complexity and cost of derivatisation steps; Limited sites for attachment
Capture systems		Generic surfaces where specificity can be switched; Many options for regeneration; Opportunities for antibody orientation	High-cost, complex multi-step derivatisation procedures; Multi-layer structure may reduce signal; Non-specific binding to components of capture system

Table 1.1: Advantages and drawbacks of different immobilisation techniques (based upon Ref[13])

Although the variety and number of techniques previously reviewed might seem puzzling, by focussing on the surface properties of the biosensor and the available functional groups on the material to be immobilized, the choices will be greatly reduced. Moreover, considerations of the mechanism of transduction being employed, which will be the topic of the following section, will further limit the options. At this point, the best way forward is to test out a few procedures to see which one gives the best compromise between speed, cost and performance for the particular system under development. What is to be kept in mind is that in every specific application requiring biomolecules immobilisation onto a solid surface, a pragmatic approach is the only option.

Transduction techniques

As previously discussed (in Section 1.3), biosensors can also be classified upon the transduction methods they employ. Transduction may be accomplished via a great variety of methods. As most form of biosensing-related transduction can be categorized in one of the following three main classes: i) ***optical detection***, ii) ***electro(chemical) detection***, and iii) ***mechanical detection***, the discussion that follows will be articulated around these key methods. However, it has to be noted that each of these three classes contain many different subclasses, creating an infinite number of possible combinations. That is why, only the main detection methods within each class will be highlighted (i.e. the SPR system for optical transduction) and emphasis will be placed more on the progressive miniaturisation of the biosensors. As these miniaturised biosensors (or Biological Micro-Electro-Mechanical Systems, bioMEMS) will be the common denominator of the present section, they will be briefly introduced before entering the main topic. Finally, the discussion will rapidly narrow to mechanical biosensors as they represent the major part of the author's research work.

1.6.1 Definition of BioMEMS

Biological Micro-Electro-Mechanical Systems ca be defined as electro-mechanical devices or systems fabricated using micro/nano-scale technologies and dedicated to manipulation, analysis or assembly of biological and chemical entities. Areas of research and applications of BioMEMS range from diagnostics, micro-fluidics, tissue engineering, surface modification, microsystems for drug delivery, implantable systems, etc., as witnessed by the amount of review articles dealing with MEMS for biology and medicine[138-141]. The word is now used so broadly that devices which do not have any electro-mechanical components (such as DNA and protein arrays) are also sometimes improperly categorized under BioMEMS.

Three classes of materials are generally used to fabricate bioMEMS: (i) microelectronics related materials, such as silicon, glass, etc., (ii) plastic and polymeric materials such as poly(dimethylsiloxane) or PDMS, and (iii) biological materials and entities such as tissues, cells and proteins. The first class has been extensively reported on, both from research and implementation point of view, and has traditionally been used in MEMS and devices[139-141]. The second class has been exclusively promoted by microfluidics applications and was shown to be very attractive due to increased biocompatibility, ease of prototyping[142], low cost and ability to integrate functional hydrogel materials[143]. The work encompassing the third class remains relatively unexplored though representing new and exciting possibilities at the frontier between bioMEMS and bio-nanotechnology, for example, in the application of micro- and nano-technology inspired cell and tissue engineering[144].

In the following paragraphs dealing with the main transduction methods in the biosensing field, few examples of BioMEMS generally based on the use of the first class of materials (microelectronics-related) will be introduced.

1.6.2 Optical techniques

Optical transducers offer the largest number of possible subcategories of all three of the transducer classes cited before[10-13]. This is due to one of the major advantages of optical sensors that is their ability to probe surfaces and films in a non-destructive manner. Moreover, they offer advantages

---

[138-141] G. T. A. Kovacs, *Micromachined Transducers Sourcebook,* (1998) WCB/McGraw-Hill, Boston, MA; [139] D. L. Polla *et al., Ann. Rev. Biomed. Eng.* 2, 551 (2000); [140] R. Bashir, *Adv. Drug. Deliv. Rev.* 56, 1565 (2004); [141] R. Bashir, S. Wereley, *Biomolecular Sensing, Processing, and Analysis in BioMEMS and Biomedical Nanotechnology*, (2006) Springer, Berlin

[142] Y. Xia and G. M. Whitesides, *Ann. Rev. Mater. Sci.*28, 153 (1998)

[143] N. A. Peppas, *Hydrogels in Medicine and Pharmacy,* (1986) CRC, Boca Raton, FL

[144] S. N. Bhatia and C. S. Chen, *Biomed. Microdev.* 2, 131 (1999)

in speed, safety, sensitivity and robustness, as well as permitting *in situ* sensing and real-time measurements. The various types of optical transducers exploit properties such as light absorption, fluorescence/phosphorescence, bio/chemoluminescence, reflectance, Raman scattering and refractive index.

It is largely beyond the scope of this section to give an exhaustive review of the optical transducers, that is why the emphasis will be particularly placed on optical immunosensors, more specifically on Surface Plasmon Resonance (SPR). Briefly, SPR is an optical reflectance procedure which is sensitive to changes in the optical properties of the medium close to a metal surface[145,146]. A surface plasmon is an electromagnetic field charge-density oscillation that can exist at a metal-dielectric interface. Upon excitation of the surface plasmons, an electromagnetic field is formed which decays exponentially with the distance from the metal film surface into the interfacing medium. When resonance occurs, the reflected light intensity from the metal surface goes through a minimum at a defined angle of incidence, known as the plasmon resonance angle.

Since 1977 when Pockrand *et al.*[147] were one of the first groups to apply SPR as a sensing technique to thin organic assemblies of cadmium arachidate deposited onto silver surfaces), this technique was widely used for sensing applications either in gas[148] or liquid media. Despite numerous studies using SPR to examine the interactions between antigens and antibodies for biosensing applications, only more than twenty years after the first description of the phenomenon has a real-time immunosensor become commercially available (BIAcore™, Pharmacia Biosensor AB, Uppsala, Sweden). The biosensor group from Uppsala in Sweden has described the use of SPR for the detection of various proteins on a sensor chip consisting on a thin gold film deposited on a glass prism and covered with a carboxymethyl-dextran hydrogel matrix[149-151]. The hydrogel matrix provides (as explained in Sub-section 1.5.2.2) covalent linkage sites for antibody binding and also protects the metal film from non-specific adsorption. Additionally, this polymer matrix increases the amount of antibody loading compared to that on a flat surface. BIAcore system uses a flow injection cell, which permits kinetic measurements over a wide dynamic range, and significantly reduces the ncubation time required for interaction analyses compared with static solid-liquid interface systems.

The sensitivity of a SPR-based biosensor could be very high[152] with nanomolar concentrations of proteins of molecular weight larger than 10^4 Da[153] being detected. The sensitivity of the SPR system depends on the molecular weight of the analyte since it is the physical amount of bound material which generates the signal. Thus, the SPR technique has the advantage of not requiring labelled molecules. The major drawback with SPR sensing at present is that the commercially available instrumentation is extremely expensive, and since the sensitivity depends on the optical thickness of the adsorbed layer, small molecules cannot be measured in low concentrations.

Maybe the best way to find a transition towards optical bioMEMS at this point is through the portability of the SPR instruments. For instance, the most recent commercialized BIAcore instrument (BIAcore X100) weighs around 47 kg, it is thus difficult to imagine that the same system could be easily moved from one point-of-care to another. Though attempts have been made to miniaturize SPR instruments (thus rendering them portable[154], even potentially drone-carried[155]!), the integration levels proper to optical bioMEMS is still difficult to achieve.

[145,146] A. Otto, *Z. Phys.* 216, 398 (1968) ; E. Kretschmann and H. Raether, *Z. Naturforsch.* A23, 2135 (1968)
[147] I. Pockrand *et al., Surf. Sci.* 74, 237 (1977)
[148] C. Nylander *et al., Sens. Act.* 3, 79 (1982)
[149-151] S. Löfas and B. Johnsson, *J. Chem. Soc.* 21, 1526 (1990); B. Johnsson *et al., Biotech.* 11, 620 (1991); B. Johnsson *et al., Anal. Biochem.* 198, 268 (1991)
[152] B. Liedberg *et al., Sens. Act.* 4, 299 (1983)
[153] 1 Da = 1 g/mol
[154] T. M. Chinowski *et al., Biosens. Bioelectron.* 22, 2268 (2007)
[155] A. N. Naimushin *et al., Sens. Act. B.* 104, 237 (2005)

One representative example of optical bioMEMS is the biosensor developed by the recent joint work of Centro Nacional de Microelectronica and Ikerlan institutes in Spain[156]. This optical biosensor is based on integrated Mach–Zehnder interferometers, which have been designed to have high surface sensitivity and monomode behaviour. As a biosensing application of the devices, the real-time detection of the covalent immobilization and hybridization of DNA strands without labeling is demonstrated. In order to achieve a lab-on-a-chip portable microsystem, the integration of the sensor with a CMOS compatible microfluidic system using SU-8 photolithography patterned layers is successfully proven.

1.6.3 Electro(chemical) transduction

Bioassays with electrochemical detection have gained growing attention since the 1990's[157-160] because it is possible to measure current precisely even in coloured and turbid samples (which is practically not achievable using optical transduction). Electrochemical biosensors include three basic types as follows:

(i) amperometric biosensors, which involves the electric current associated with the electrons involved in redox processes (fairly sensitive, currents as low as 10^{-10} A can be recorded with commercial devices);
(ii) potentiometric biosensors, which measure a change in potential at electrodes due to ions or chemical reactions at an electrode;
(iii) counductometric biosensors, which measure conductance changes associated with changes in the overall ionic medium between two electrodes.

Under optimum conditions – with high enzyme loading under fast mass transport in thin layers and efficient external mass transfer[13] – an enzyme electrode can measure substrates down to 10μM with acceptable precision. To further increase the sensitivity (down to nM range), the enzymatic substrate regeneration technique makes use of continuous regeneration of the analyte in cyclic reactions.

A ***potentiometric*** biosensor for protein and amino acid estimation was reported by Sarkar and Turner[161]. A screen-printed biosensor based on a rhodinized carbon paste working electrode was used in the three electrode configuration (reference, working electrode, counter-electrode) for a two-step detection method. Electrolysis of an acidic potassium bromide electrolyte at the working electrode produced bromine which was consumed by the proteins and amino-acids involved in the assay. The bromine production occurred at one potential while monitoring of the bromine consumption was performed using a lower potential. The method proved to be very sensitive to almost all of the amino-acids, as well as some common proteins in fruit juice, milk and urine, consuming approximately 10μL of sample for direct detection.

Electrochemical flow-through enzyme-based biosensors for the detection of glucose and lactate have been developed by Rudel *et al.*[162]. In this application, glucose oxidase and lactase oxidase were immobilized in conducting polymers generated from pyrrole, N-methylpyrrole, aniline and o-phenylenediamine on platinum surfaces. There various sensor matrices were compared based on ***amperometric*** measurements of glucose and lactate and it was found that the o-phenylenediamine was the most sensitive polymer. This polymer matrix was then deposited on a piece of graphite felt and used as an enzyme reactor as well as a working electrode in an electrochemical detection system. Using this system, a linear dynamic range of 500μM-10mM glucose was determined with a limit of

[156] B. Sepulveda *et al.,J.Opt. A: Pure Appl. Opt.* 8, 561 (2006)
[157-160] M. J. Green *et al., Principles and Practice of Immunoassay* (1991), Macmillan, London; [158] W. O. Ho *et al., Biosens. Bioelectron.* 10, 683 (1995); [159] O. Niwa, *Electroanal.*7, 606 (1995); [160] F. F. Bier *et al., Fresenius J. Anal. Chem.* 354, 861 (1996)
[161] P. Sarkar and A. P. F. Turner, *Fresenius J. Anal. Chem.* 364, 154 (1999)
[162] U. Rudel *et al., Electroanal.* 8, 1135 (1996)

detection <500µM. For lactate, the dynamic range covered concentrations from 50µM-1mM with a detection limit <50µM.

Electrical or electrochemical detection techniques can be amenable to portability (through miniaturisation) as witnessed by several potentiometric and conductimetric sensors which have been transposed to the micro- and even nano-scale. Thus, the most common form of potentiometric microsensors are the ion-sensitive field effect transistors (ISFETs) or chemical field effect transistors (ChemFETs). These devices are available commercially as pH sensors and many examples have been reported in the literature[163]. For instance, potentiometric sensors with ion-selective ionophores in modified poly(vinyl chloride) have been used to detect analytes from human sera[164]. Cellular respiration and acidification due to the activity of colon adenocarcionoma cell lines have been measured with CMOS ISFET[165]. Potentiometric sensors have been downscaled to nano-meter dimension through the use of silicon nanowires[166] and carbon nanotubes[167] as field effect sensors; nano-scale biosensors' issue will be further detailed in the last section of this chapter.

Micro-fabricated conductimetric sensors were also fabricated and used to measure for instance extracellular neuronal activity for a long time[168,169]; the micro-electrodes and the area of neuro-electric interface would worth a review in itself. As conductance techniques are attractive due to their simplicity and ease of use (since a specialized reference electrode is not needed), they have been used to detect a wide variety of entities such as agents of biothreat[170], biochemicals[171] and nucleic acids[172]. Moreover, conductimetric sensors provide information on the ionic strength in electrolytes and can provide convenient selectivity if coupled with enzyme membranes, as in the case of the detection of glucose[173] and urea[174], for instance.

To summarise, it has to be noted that a few years ago, more than half of the biosensors reported in the literature are based on electrochemical transducers[175]. This may not be surprising considering that electrochemical transduction possesses the advantages highlighted in the previously discussed applications: low cost, high sensitivity, independence from solution turbidity, easily miniaturised / well suited to microfabrication, low power requirements and relatively simple instrumentation. These characteristics make electrochemical transduction methods highly compatible for implantable and/or portable hand-held devices.

1.6.4 Mechanical detection

Most of time, mechanical bio(chemical)sensors are referred to as "mass sensitive" due to gravity or thickness measurements of thin rigid films in vacuum or gaseous environment for which they were employed first. Although the mass effect is only one of several contributions to the sensor response in liquids, particularly in the case of non rigid biological layers, this terminology will be used throughout this section to stress the mechanical basis of the acoustic transduction compared to the other transduction methods previously discussed.

---

[163] U. Schnakenberg *et al., Sens. Act. Chem. B*34, 476 (1996)
[164] R. Hintsche *et al., Sens. Act. Chem. B*27, 471 (1995)
[165] M. Lehmann *et al., Biosens. Bioelectron.* 16, 195 (2001)
[166] Y. Cui *et al., Science* 293, 1289 (2001)
[167] K. Besteman *et al., NanoLett.* 3, 727 (2003)
[168,169] G. W. Cross *et al., Neurosci. Lett.* 6, 101 (1977) ; D. A. Borkholder *et al., J. Neurosci. Methods* 77, 61 (1997)
[170] T. Z. Muhammad and E. C. Alocilja, *Biosens. Bioelectron* 18, 813 (2003)
[171] H. Suzuki *et al., Biosens. Bioelectron.* 16, 725 (2001)
[172] T. G. Drummond *et al., Nat. Biotechnol.* 21, 1192 (2003)
[173] A. A. Shul'gas *et al., Biosens. Bioelectron.* 9, 217 (1994)
[174] A. Steinschaden *et al., Sens. Act. Chem. B*44, 365 (1997)
[175] D. Meadows, *Adv. Drug Deliv. Rev.* 21, 179 (1996)

Acoustic wave devices give information on two physical quantities, the acoustic energy storage and the energy dissipation which can be respectively measured by the frequency[176] shift and the damping of the acoustic oscillation. Therefore, more than one signal can be obtained from a single sensor (it has to be kept in mind that acoustic resonators exhibit infinity of resonant modes of vibration, each characterized by specific resonant frequency and damping factor). This paves the way towards multicomponent signal analysis with a small number of different sensors.

In the last few years the interest in using acoustic wave devices as biosensors increased for studying kinetic and thermodynamic parameters of many biochemical or biological systems as well as in the field of understanding the acoustic transduction mechanisms in terms of mechanical interfacial processes. The present section will be structured as follows: first, physics of piezoelectric excited acoustic waves in solids will be briefly discussed, then a general classification of piezoelectric mass-sensing devices will be given. An in-depth discussion of each kind of acoustic sensor would dramatically unbalance the general bisensors' overview performed so far; that is why the focus will narrow to two specific classes of sensors the author is most familiar with, i.e. the thickness shear mode resonators and the general acoustic microsensors. To conclude, a specific application to the detection of bacterial infection will be briefly introduced.

1.6.4.1 Piezoelectric excited acoustic waves in solids

Piezoelectricity (or direct piezoelectric effect) as first reported in 1880 by the Curie brothers describes the generation of electrical charges on the surface of a solid caused by pulling, pressure or torsion. In contrast, the occurrence of a mechanical deformation arising from an external field is called the converse piezoelectric effect. Figure 1.7 shows schematically the general relationships between mechanical and electrical variables[177].

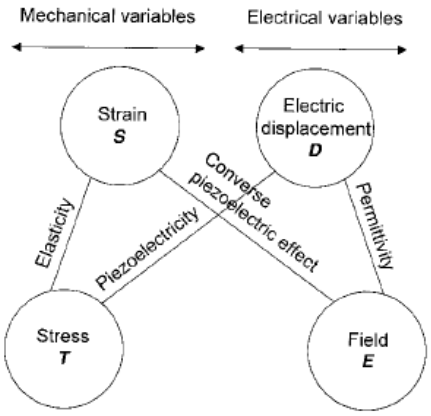

Figure 1.7: Relationship between mechanical and electrical variables. The direct piezoelectric effect is the production of electric displacement by applying a mechanical stress. The converse piezoelectric effect results in a strain in the crystal when an electrical field is applied. The relation between stress and strain is determined by the elasticity of the solid[177] (*courtesy of Angewandte Chemie editorial board*)

For piezoelectric effect to potentially occur in a crystalline material, it has not to exhibit a centre of symmetry. Of the thirty-two crystal classes, twenty-one are non-centrosymmetric, and of these, twenty exhibit direct piezoelectricity. Although a large number of crystals show piezoelectricity, only quartz provides the unique combination of mechanical, electrical, chemical, and thermal properties which has lead to its commercial success, as it will be further shown in Sub-section 1.6.4.3.

[176] Frequency is an analog value but can easily be converted into a digital signal, e.g. by counting the number of cycles in a defined period of time
[177] A. Janshoff *et al., Angew. Chem. Int. Ed.* 39, 4004 (2000)

1.6.4.2 Classification of acoustic piezoelectric resonators

Usually, as stated above, piezoelectric devices consist of quartz; other piezoelectric materials are lithium niobate or tantalate, oriented zinc oxide (ZnO), aluminium nitride (AlN) or lead zirconate titanate (PZT). Substrate material, crystal cut (if any) and electrode geometry determine the type of acoustic wave and device, respectively. Moreover, acoustic waves are discriminated by the particle displacement direction either relative to the propagation direction of the wave (longitudinal, transverse) or relative to the surface (horizontal, vertical). Bulk waves travel unguided through the volume of the material, surface waves are guided along a device surface, and plate waves are guided by reflection from multiple surfaces. In longitudinal waves, particle displacement and wave propagation direction are parallel (compressional waves) whereas in transverse waves they are perpendicular to each other (shear waves). To characterize surface and plate shear waves, one can also distinguish vertical waves with a particle displacement normal to the surface and horizontal waves in which the displacement is parallel to the surface.

Because of the severe damping of acoustic waves in liquid, only devices based on oscillations with particle displacement parallel to the surface can be used for liquid sensing. Surface acoustic wave devices (SAW) employ Rayleigh waves with both horizontal and vertical components and are therefore not able to be driven in liquids. An exception from the above stated rule are flexural plate wave devices (FPW) because the velocity of the antisymetric Lamb wave is too small for coupling to compressional waves in liquids[177]. ***For a more in depth review and comparison of acoustic sensors in terms of sensitivity and temperature stability, Ref.[177] is highly recommended***.

All surface and plate wave devices mostly use interdigitated electrodes (IDE) as transmitter and receiver of the acoustic waves. In contrast, the most frequently used device, the transverse shear mode resonator (TSMR), often named quartz crystal microbalance (QCM), consist of quartz plate with metal electrodes on each side which generate bulk waves travelling perpendicular to the sensor surface. A typical recently successful commercialized QCM set-up is described in the followings.

1.6.4.3 The quartz crystal microbalance with dissipation monitoring (QCM-D)

The use of piezoelectric transducers in biosensors was foreshadowed in the work of Sauerbrey[178] who not only pioneered the use of the QCM but thoroughly analysed the physics of the device. He thus demonstrated that there is proportionality between mass added to the QCM sensor and the shift in its resonant frequency.

The major advantage of the QCM sensor derives from the extremely high precision with which the resonance frequency can be measured. Under ideal conditions (temperature and pressure control), the mass sensitivity is down to tens of picograms per cm^2. The mass sensitivity can be expressed as the so-called Sauerbrey equation:

$$\Delta m = \rho_f \delta_f = -\frac{t_q \rho_q}{f} \Delta f = \frac{C}{n} \Delta f \qquad (1.2)$$

where ρ_f and δ_f are the density and the thickness of the added film, ρ_q and t_q are the density and thickness of the quartz plate respectively, f is the operation frequency of the sensor, n the overtone number and C is the so-called mass sensitivity (depending on the rate propagation of the elastic transverse wave in, and the density of, quartz) of the QCM.

[178] G. Z. Sauerbrey, *Z. Phys.* 155, 206 (1959)

The first application of the QCM was a film thickness monitor for film deposition in vacuum systems or as an oxidation rate sensor[179-181]. Other early applications were in the direction of gas sensing in air[182]. In 1985, Kanazawa opened the door to a whole new set of applications by demonstrating that the QCM can be operated in a stable and reproducible manner in a liquid[183]. The by far most important application of this liquid phase QCM has until the late 1990's been the electrochemical QCM or EQCM[184].

In spite of many applications of the QCM, it also became successively more evident that a single parameter measurement, i.e. frequency measurements only, had some severe limitations, especially when non-rigid films were studied. This last point rapidly led to a reconsideration of the Sauerbrey model. Indeed, a condition for Sauerbrey model to be valid is that the added film perfectly couple to the shear oscillation of the sensor (as, for example, in case of metals or ceramic films deposited onto the active face of the QCM). However, when the QCM started to be used for studying soft films (as biofilms) a regime was entered where the Sauerbrey relation often failed which led to confusion and misinterpretation of data.

A qualitative interpretation of why the Sauerbrey relation loses applicability when the applied films are soft was given in Ref[13]: under such circumstances, the film does not follow the sensor's mechanical oscillation as a "dead mass", but is deformed in the shear direction, such as "a jelly lying on a plate". The frequency shift caused by the jelly-like soft film will not correspond to its static mass but to a dynamic value that depends in a complex manner on its viscous and elastic components. This is the case for soft polymer or biomolecules films that can therefore not be treated as rigid films obeying the Sauerbrey equation implying that the energy dissipation[185] of the QCM may be affected.

Fredrik Höök demonstrated in the frame of his PhD thesis[186] how the simultaneous measurement of both *f* and *D* helps in the interpretation of the frequency shift in terms of mass uptake and, for the first time, he shown that information about the conformational state of adsorbed protein molecules onto a specifically functionalized QCM sensor can be achieved (Figure 1.8).

[179-181] B. Kasemo and E. Törnquist, *Surf. Sci.* 77, 209 (1978); [180] B. Kasemo and E. Törnquist, *Phys. Rev. Lett.* 44, 1555 (1980); [181] W. H. King Jr., *Anal. Chem.* 36, 1735 (1964)

[182] G. G. Guibault, *Int. J. Env. Anal. Chem.* 10, 89 (1981)

[183] K. K. Kanazawa, *Electrochem. Soc. Ext. Abst.* 85, 652 (1985)

[184] K. Takada *et al., J. Am. Chem. Soc.* 119, 10763 (1997)

[185] The dissipation factor *D* is the inverse of the more known *Q* factor related to *D* as: $D = \frac{1}{Q} = \frac{E_d}{2\pi E_s}$, where E_d is the energy dissipated during one period of QCM's oscillation and E_s is the energy stored in the oscillating system.

[186] F. Höök, *Development of a novel QCM technique for protein adsorption studies* (1997), PhD thesis, Chalmers University of Technology, Göteborg, Sweden.

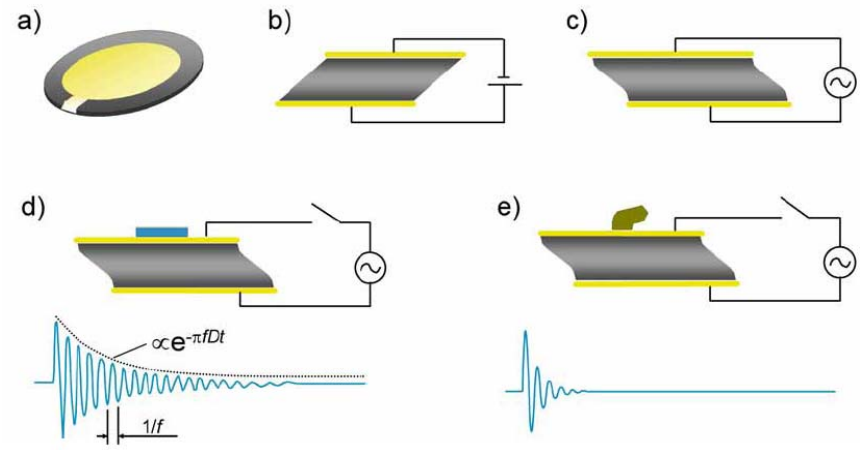

Figure 1.8: Schematic presentation of the QCM-D working principle. The piezoelectric quartz crystal is sandwiched between two gold electrodes (a). The application of an electric field across the crystal results in shear motion of the crystal (b). Resonance in the shear motion can be excited with an oscillating field of appropriate frequency (c). After cutting the driving circuit, the freely decaying oscillation of the crystal is monitored (d, e). The temporal change in the crystal's movement, $A(t)$, can be fitted by $A(t) = A \exp(-\pi f D t)\sin(2\pi f t + \varphi)$ 0 in order to extract the resonance frequency, f, and the dissipation, D (D is the reverse of the well known Q-factor). Attachment of a rigid mass (d) to the crystal's surface will only lead to a decreases in f, while a soft (viscoelastic) mass (e) will also affect D. Monitoring changes in f and D allows thus to follow interfacial processes in real time[186-bis]. (*Ralph Richter's courtesy*)

This work, in turn, opened up the possibility to extract information about the viscous and elastic components of a soft film added onto a QCM sensor thus paving the way towards a new technique (called QCM-D, where D stands for dissipation). Systems using the QCM-D technique are now successfully commercialized by Q-Sense[187] (Goteborg, Sweden), F. Höök being one of the company's founding members.

T**he adsorption of hemoglobin (Hb)** was chosen as a first model in order to illustrate the performance of the QCM-D principle[188,189] (i.e. simultaneous measurement of both Δf and ΔD as a function of time). The resonant frequency and the dissipation factor variations are shown in Figure 1.9 for the adsorption of Hb at a concentration of 1.3µM on a hydrophobic, methyl terminated thiol covered gold surface in a 10mM Hepes solution at pH 6.5 and pH 7.5[188].

[186-bis] Ralph Richter, *The Formation of Solid-Supported Lipid Membranes and Two-Dimensional Assembly of Proteins. A Study Combining Atomic Force Microscopy and Quartz Crystal Microbalance with Dissipation Monitoring* (2004), PhD Thesis, Université Bordeaux I, France.
[187] www.q-sense.com
[188,189] F. Höök *et al., Langmuir* 14, 729 (1998) ; F. Höök *et al., PNAS USA* 95, 12271 (1998)

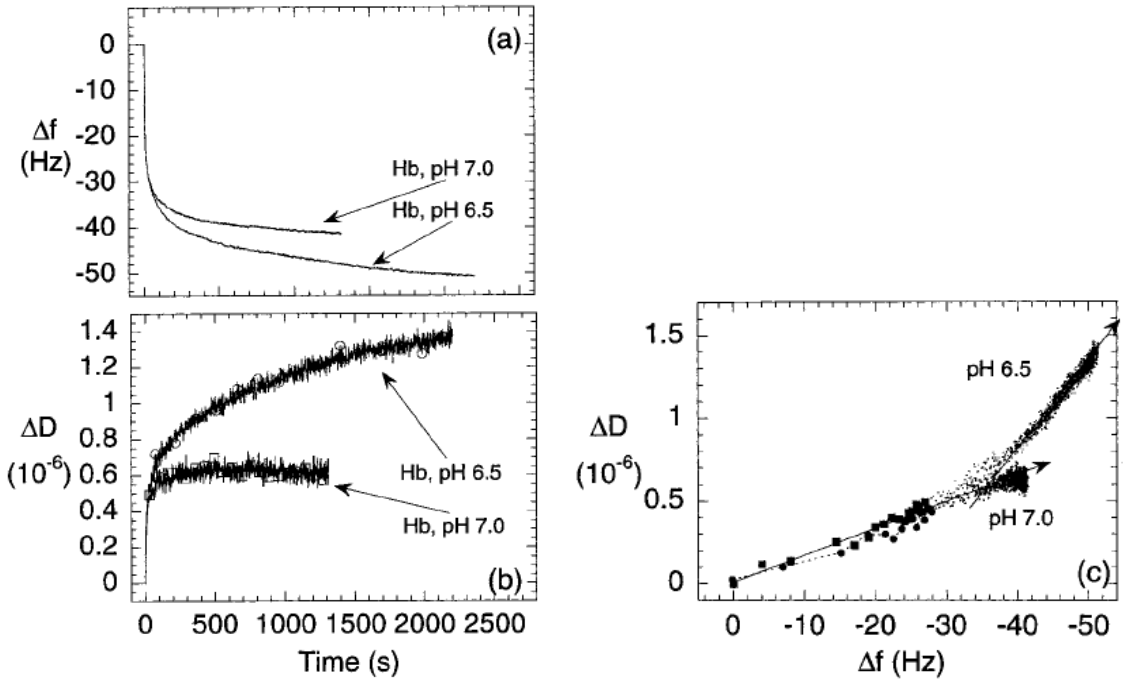

Figure 1.9: (a, b) Δf vs t and ΔD vs t for the adsorption of Hb on the hydrophobic surface at pH 6.5 and 7.0. The influence of pH on the Hb adsorption kinetics is also illustrated by the D-f plot (c). The simple linear behavior at pH7.0 is replaced by a two-phase behavior at pH6.5, where also the total mass uptake and final dissipation shift are larger. (●) pH7.0 and (■) pH6.5.

It can be noted that the adsorption causes an initial rapid frequency decrease (equivalent to a mass uptake) at both pH values, followed by a slower frequency decrease as the surface coverage saturates. Additionally, the D-shifts are positive (meaning increase of dissipative effects), and display kinetics similar to the f-shifts. A useful illustrative way to display the D- and f- data is to plot ΔD vs. Δf that eliminates time as an explicit parameter. It is interesting to note in Figure 1.9.(c) that the fast and slow phases of the Hb adsorption cause different slope values (relative dissipation per unit frequency shift) meaning that Δf and ΔD measure different properties of the adsorption kinetics. This illustrates that one single type of protein can form adlayers with different viscoelastic properties depending on their interaction with the surface and/or with each other.

1.6.4.4 Acoustic micro(bio)sensors

Although friendly-to-use, ruggedized, performant in terms of measurement resolution, the QCM-D technique still suffers from its lack of multiplexing capabilities (recently taken into account in the E4 system configuration from Q-Sense) and integration. Moreover, improvement of sensitivity remains the driving force in biosensors development. Sticking again with the mass sensitivity argument, mass sensitivity of resonant sensors is basically governed by the ratio of mass change to the overall vibrating mass. As a rule of thumb, the lighter the resonator the larger the relative mass increase.

Silicon technology can lead to new possibilities – the capability to detect even smaller mass, but also the capability to fabricate arrays with a much number of elements per unit area[190], the capability of monolithically integrated electronic circuitry and mass production at low cost.

[190] Quartz resonators have also been fabricated as arrays, see J. R. Vig *et al., IEEE Int. Freq. Contr. Symp. Proc.* 852, (1995); B. Zimmermann *et al., Sens. Act. Chem. B*76, 47 (2001) ; J. Rabe *et al., IEEE Sensors J.* 3, 361 (2003)

Nowadays commercial cantilevers are usually used, typically made of silicon, silicon nitride or silicon dioxide. One of the main advantages of the cantilever sensors is the ability to detect interacting compounds without the need of introducing an optically detectable label on the binding entities. In the recent years, very exciting and significant advances in biochemical detection have been made using this microdevice. Direct, label-free detection of DNA and proteins have been demonstrated using silicon cantilevers[191] through stress-sensing mode (i.e. the real-time monitoring of cantilevers' bending that traduces a change in surface free energy induced by adsorption of biomolecules on one of its specifically functionalised sides[192]).These sensors can also be used to detect proteins and cancer markers such prostate specific antigen, which have also been detected at 0.2 ng/mL in background of human sera in clinically relevant conditions[193]. Recently, challenging experiments have been proposed aiming to monitor conformational changes of proteins (either bacteriorhodopsin[193.a] or human oestrogen receptors[193.b]) fixed onto microcantilevers.

The resonant principle can also be used, keeping in mind that it needs active driving of the cantilever and feedback for frequency measurements. Piezoelectric thin films (see 1.6.4.3) are often used for that purpose though magnetic actuation[194] has also been applied. Cantilevered AT-cut quartz-crystal resonators have also been fabricated by deep reactive ion etching[195]. One major challenging issue is to improve the quality factor of the resonator. *Q*-factors of approximately 10^3 in the upper kHz frequency range in air enable a mass resolution in the picogram range[196]. Magnetic actuation and a closed feedback loop can substantially enhance the quality factor[197]. Another method for mass sensitivity to be improved is the use of higher modes[198] (as they exhibit higher resonant frequency and *Q* factor values).

However, in a liquid environment, especially in biosensing applications, the out-of-plane vibration of a microstructure is strongly damped and results in an essentially reduced *Q* factor (of a few units for cantilevered microstructures[199]). One solution would consist in intentionally trapping air bubbles in the fluidic cell[200], as it will be detailed in the second chapter of this manuscript. Another approach allows avoiding the out-of-plane vibration through the use of disc-shaped microstructures operated in rotational in-plane mode thus exhibiting *Q*-factors as high as 5800 in air and 100 in liquid[201]. A real paradigm shift has been proposed recently by S. Manalis' group consisting in the integration of the fluids' circulation through channels buried in the sensors[202]; in this case, the resonator bears the fluidic cell which is the contrary of the by far way of thinking. In this application, though requiring multiple steps of microfabrication, the sensor (a cantilevered structure) still vibrates in air; the mass change occurs within the buried channels because of adsorption of the molecules of interest on the channel walls. The sensor's signal is actually based on density differences between the attached molecule and the buffer.

---

[191] J. Fritz *et al., Science* 288, 316 (2000)
[192] Stress-sensing and mass-sensing methods at the microscale were reviewed in detail by C. Bergaud, *Habilitation à diriger les recherches thesis*, Université Paul Sabatier (2005), Toulouse, France
[193] G. Wu *et al., PNAS USA* 98, 1560 (2001)
[193.a] T. Braun *et al., Biophys. J.* 90, 2970 (2006)
[193.b] R. Mukhopadhyay *et al., NanoLett.* 5, 2385 (2005)
[194] C. Vancura *et al., Anal. Chem.* 77, 2690 (2005)
[195] Y. C. Lin *et al., 13th Int. Conf. Solid-State Sens. Act. Micvrosyst. (Transducers '05) Proc.* 593 (2005)
[196] R. Lucklum and P. Hauptmann, *Anal. Bioanal. Chem.* 384, 667 (2006)
[197] A. Vidic *et al., Ultramicroscopy* 97, 407 (2003)
[198] D. Saya *et al., Rev. Sci. Instrum.* 75, 3010 (2004)
[199] C. Bergaud and L. Nicu, *Rev. Sci. Instrum.* 71, 2487 (2000)
[200] C. Ayela and L. Nicu, *Sens. Act. Chem. B*123, 860 (2007)
[201] J. H. Ho and O. Brand, *13th Int. Conf. Solid-State Sens. Act. Micvrosyst. (Transducers '05) Proc.* 247 (2005)
[202] T. Burg *et al., Nature* 446, 1066 (2007)

1.6.4.5 One specific application: acoustic microsensors for pathogen agents detection

After the world-wide shockwave provoked in 2001 by the inability to prevent and face a terrorist strike against an overprotected country such as the United States, an attack using a biological pathogen agent (BPA) became a conceivable event. Evidence of the destructiveness of such attacks, and the associated fear they create, have already been proven through episodes such as the Sarin gas and anthrax attacks by the Aum Shinrikyo cult in Tokyo in 1995, the use of *Salmonella* in Oregon restaurants in 1984 by the Rajneeshee cult and the anthrax letter attacks soon after September 11th. One of the problems with biological attacks is actually determining whether an attack has occurred. The difficulty arises because often the initial symptoms after infection from BPAs are difficult to distinguish from symptoms from infections from more benign biological agents. The solution to this detection problem is to employ biosensing techniques, which can identify chemical markers from known biological agents.

These agents are now well known and classified as category A agents by the Center for Disease Control and Detection (CDC) in the USA[203], including anthrax, tularemia, botulinum toxin, plague (aerosol version only), smallpox and hemorrhagic fever. They cover the main types of biological agents from **Gram-positive bacteria**, which form **spores** (*Bacillus anthracis*, Anthrax; *Yersinia pestis*, Pneumonic plague), **gram-negative** (*Francisella tularensis*, tularemia), **toxins** derived from bacterial species (botulinum toxin from *Clostridium botulinum*) and **viruses** (Smallpox).

To develop biosensors for these analytes, the important considerations are the matrix in which **the analyte** will be found (for example, air, water, food, person), **the form** the analyte will be in (spore, bacteria, virus, toxin) and **the possible features of the analyte**, which could be recognised with an appropriate biorecognition molecule. Identification of such features requires some knowledge of the biological species and the forms in which they are found. Other considerations further concern the kind of measurement the biosensor has to perform, i.e. **early identification** of an infection ("detect-to-treat" systems) or **provide a warning** that a site is contaminated by BPAs to prevent infection ("detect-to-prevent" systems). The criteria for such biosensors are quite different. A detect-to-treat system must be able to identify a BPA, from a biological sample, within a few hours of infection. Hence detect-to-treat biosensors are compatible with an analytical laboratory using personnel trained to perform the analysis. A detect-to-protect system must be able to provide a warning within a couple of minutes from, most frequently, an airborne sample without user intervention. Portability, reliability, fast response in real-time, low detection limit, ruggedized packaging are critical requirements that correspond to the latter class of systems and which could be compatible with micromachined acoustic sensors.

Though no commercial "detect-to-protect" microsystems were developed so far, the very last years' literature abounds of papers where acoustic microsensors are fabricated and tested aiming to the detection of BPAs or simulants. A representative list of affinity biosensing concepts that are motivated towards studying detect-to-protect micromechanical devices are listed in Table 1.2 with some of their attributes.

[203] L. A. Broussard, *Mol. Diagn.* 6, 323 (2001)

Analytes	Detection limit	Assay time	Reagent free	Real samples	Comment
Bacillus subtilis spores	NA	40 min.	Yes	Yes	Array of 8 cantilevers (4 are used for the detection, the remaining being the control) measuring in static mode[204]
Escherichia Coli	50 cells/mL	2h – 6h	Yes	Yes	Piezoelectric-excited millimeter-sized cantilever measuring in resonant mode, in flow[205]
Bacillus anthracis	300 spores/mL	1h	Yes	Yes	Piezoelectric-excited millimeter-sized cantilever measuring in resonant mode, in flow[206]
B. Anthracis	333 spores/mL	30 min.	Yes	Yes	Piezoelectric-excited millimeter-sized cantilever measuring in resonant mode, in flow. The targeted spores are mixed with other bacterial strains[207]
B. Anthracis	NA	Few hours	Yes	Yes	Microcantilevers driven by thermally induced oscillations, detection of resonant frequency shift in air and in water using a laser Doppler vibrometer[208]
Group A Strepotococus	700 cells/mL	Few minutes	Yes	No	Piezoelectric-excited millimeter-sized cantilever measuring in resonant mode[209] in flow.
E. Coli	100 cells/mL	Few minutes	Yes	Yes	Piezoelectric-excited millimeter-sized cantilever measuring in resonant mode, in flow, sequential injection of the different materials[210]
Salmonella enterica	10^6 cfu[211]/mL	Few minutes	Yes	Yes	Atomic Force Microscope set-up, measurements performed in static mode, no circulating flow[212]
Vaccinia virus	2 mg/mL	Several hours	Yes	Yes	Piezoresistive cantilevers in static mode, measurements performed either in aerosol or liquid samples[213]

Table 1.2: A representative list of affinity biosensing concepts implemented on detect-to-protect micromechanical devices

Of course, none of the microsensors cited above went out from the laboratory, let alone satisfying the most important requirement, i.e. a detect-to-protect biosensor which could be worn by a soldier or a civilian in an environment where the possibility of exposure to BPAs is prevalent. There are still a number of impediments to the development of such a biosensor including (1) transferring an airborne sample to an aqueous environment where the biosensor can operate, (2) reducing the detection limit, and (3) obtaining more rapid responses. If the first criterion is quite specific to BPAs-related biosensors, the two others are generic and must be satisfied for other biosensing applications going from pathologies diagnosis to fundamental biophysics.

[204] B. Dhayal *et al., J. Am. Chem. Soc.* 128, 3716 (2006)
[205] G. A. Campbell *et al., Biosens. Bioelectron.* 22, 1296 (2007)

[206] G. A. Campbell and R. Mutharasan, *Biosens. Bioelectron.* 22, 78 (2006)
[207] G. A. Campbell and R. Mutharasan, *Anal. Chem.* 79, 1145 (2007)
[208] A. P. Davila *et al., Biosens. Bioelectron.* 22, 3028 (2007)
[209] G. A. Campbell and R. Mutharasan, *Biosens. Bioelectron.* 22, 35 (2006)
[210] D. Maraldo *et al.*, *Anal. Chem.* 79, 2762 (2007)
[211] cfu = colony forming units
[212] B. L. Weeks *et al., Scanning* 25, 297 (2003)
[213] R. L. Gunter *et al., Sens. Act. Phys. A*107, 219 (2003)

A major challenge yields from the decreasing the response time issue coupled to ultimate detection limit, which relates to detecting single particles or a few particles. How long must one wait for a measurable output signal shift? Expressed in another way, is the absence of a positive signal evidence that there is no biological agent or is it a false negative due to the fact that the biological agent did not cross the nano-dimensional space occupied by the biosensor? An array of the nanoscale biosensors could reduce this problem but still presents a related problem, which can be referred to as 'the needle in a haystack problem'[214]. When a biosensor is in a defined location in space, on a surface, even if the analyte is present it must still diffuse to the sensing surface for recognition to occur. Even in a small volume this could represent diffusing a long distance on the molecular scale. Hence the analyte may never be found by the biosensor in a reasonable time in a similar manner to a needle in a haystack never being found.

Before going more into detail regarding the course to miniaturisation debate in the biosensing field (which will be emphasised in the concluding chapter of this manuscript), a specific focus on biosensors at the nanoscale will be provided in the following section.

Nano(bio)sensors: the future?

Nanoscale biosensors may overcome many of the roadblocks that prevent widescale use of affinity biosensors without any of their major drawbacks. One can draw such a concluding remark from a recent paper from the Lieber group on silicon-nanowire-based- field-effect transistors[215], and examples that follow in the next paragraphs show that it just may be right. Indeed, nanostructures such as nanowires and carbon nanotubes[216] as well as nanoparticles[217,218] offer new and sometimes unique opportunities for detection and quantification of biological and chemical species. Such inorganic nanostructures exhibit unique electrical, optical and magnetic properties that can be exploited for sensing and imaging. For instance, iron oxide nanocrystals with superparamagnetic properties and semiconductor nanocrystals with size-tunable emissive properties are being developed as specific contrast agents in magnetic resonance and optical imaging, respectively, being able of wide-ranging applications, including the imaging of cancer tumors in live animal models[219-221].

Moreover, reproducible and tunable conducting properties of conducting nanowires combined with surface binding properties have recently opened the doors of new approach to nanomedecine. Coupling the ability of direct, label-free electrical read-out and the integration levels that can be reached, together with ultrahigh sensitivity and resolution, nanowire-based devices have been positioned as potential, powerful challengers to the state-of-the-art actual biosensors applied to diagnosis and monitoring of disease treatment but also to the discovery and screening of new drug molecules, as illustrated by several applications discussed further.

The most popular by far nanowire-based sensors is the field-effect nanowire transistor (nanowire-based FET) which, like its "big brother" conventional FET of the microelectronics industry, uses the field effect to modulate the charges quantity (switching it "on" and "off") in a silicon channel through which a current is injected and collected, respectively, by means of two metal electrodes (source and drain). The FET transposed to the nanoscale makes use of Si-nanowire channels that can be prepared as single-crystal structures with diameters as small as 2-3 nm[222,223] and has been shown to exhibit reproducible performance characteristics comparable to or better than the best achieved in the

[214] J. J. Gooding, *Anal. Chim. Acta* 559, 137 (2006)
[215] G. F. Zheng *et al., Nat. Biotechnol.* 23, 1294 (2005)
[216] R. J. Chen *et al., PNAS USA* 100, 4984 (2003)
[217,218] S. Tyagi and F. R. Kramer, *Nat. Biotechnol.* 14, 303 (1996); T. A. Taton *et al., J. Am. Chem. Soc.* 123, 5164 (2001)
[219-221] A. Saleh *et al., Brain* 127, 1670 (2004) ; [220] V. Dousset *et al., Am. J. Neuroradiol.* 20, 223 (1999) ; [221] J. M. Perez *et al., Chem. Bio. Chem.* 5, 261 (2004)
[222,223] A. M. Morales and C. M. Lieber, *Science* 279, 208 (1998); J. Hu *et al., Acc. Chem. Res.* 32, 435 (1999)

microelectronic industry[224-226]. Thus, a generic biosensing device has been proposed from the high-performance, field-effect nanowire transistor concept, where specific sensing is achieved by linking a recognition group to the surface of the nanowire. Si nanowires with their natural oxide coating make this receptor linkage straightforward since extensive data exists for the chemical modification of silicon oxide or glass surfaces from planar chemical and biological sensors, as previously shown in Sub-section 1.5.1.2. When the sensor device with surface receptor is exposed to a solution containing a macromolecule like a protein that has e.g. a net positive charge in aqueous solution, specific binding will lead to an increase in the surface positive charge and a decrease in conductance for a *p-type*[227] nanowire device (Figure 1.10).

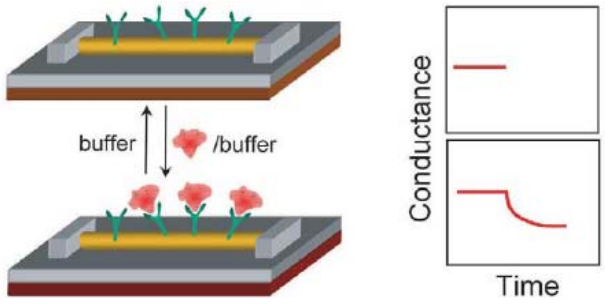

Figure 1.10: Schematic of a Si nanowire-based FET device configured as a sensor with antibody receptors (*Y-shaped*), where binding of a protein with net positive charge yields a decrease in the conductance (upon Patolsky and Lieber[228])

The first reported nanowire-based chemFET operating in a liquid solution to detect hydrogen ion concentration (**pH sensing**) dates from 2001[166]. A *p-type* Si nanowire device was converted into such a sensor by modifying the silicon oxide surface with APTES[61,62], which yielded amino groups at the nanowire surface, and thus exhibited increases in conductance as the pH of the solution (delivered through a microfluidic device) was increased stepwise from 2 to 9.

More recently, Si nanowire FET have been investigated as sensors for the **detection of single – stranded DNA**, where the binding of this negatively charged polyanionic macromolecule to *p-type* nanowire surfaces leads to an increase in conductance[227,229]. Studies of *p-type* Si nanowire devices modified with a peptide nucleic acid (PNA) receptor designed to recognize wild type versus the DF508 mutation site in the cystic fibrosis transmembrane receptor gene show that the conductance increases following addition of a **60 fM** wild-type DNA sample solution.

Even more spectacular, one single viral particle has been detected using the same concept. The starting idea was that when a virus particle binds to an antibody receptor on a nanowire device, the conductance of that device will change from the baseline value, and when the virus unbinds again, the conductance will return to the baseline value. Significantly, delivery of highly dilute influenza A virus solutions, on the order of 80 aM (10-18 M) or 50 viruses/µl, to p-type Si nanowire devices modified with monoclonal antibody for influenza A produces well-defined, discrete conductance changes (Figure 1.11) that are characteristic of binding and unbinding of single negatively charged influenza viruses[230]. Definitive proof that the discrete conductance changes observed in these studies are the

[224-226] M. C. McAlpine *et al., Nano. Lett.* 3, 1531 (2003); [225]S. Jin *et al., Nano Lett.* 4, 915 (2004); [226]A. B. Greytak *et al., Appl. Phys. Lett.* 84, 4176 (2004)

[227] In the case of *p-Si* (where the material is "doped" with minute quantities of impurity atoms allowing controlled change in its electrical properties), applying a positive gate voltage depletes carriers and reduces the conductance, while applying a negative gate voltage leads to an accumulation of carriers and an increase in conductance. Reverse phenomena occur in case of *n-type* Si.

[228] F. Patolsky and C. M. Lieber, *Mat. Today* 20 (Apr. 2005)

[229] J. Hahm and C. M. Lieber, *Nano Lett.* 4, 51 (2004)

[230] F. Patolsky *et al., PNAS USA* 101, 14017 (2004)

result of the detection of single virus binding/unbinding was obtained from simultaneous optical and electrical measurements using fluorescently labeled influenza viruses.

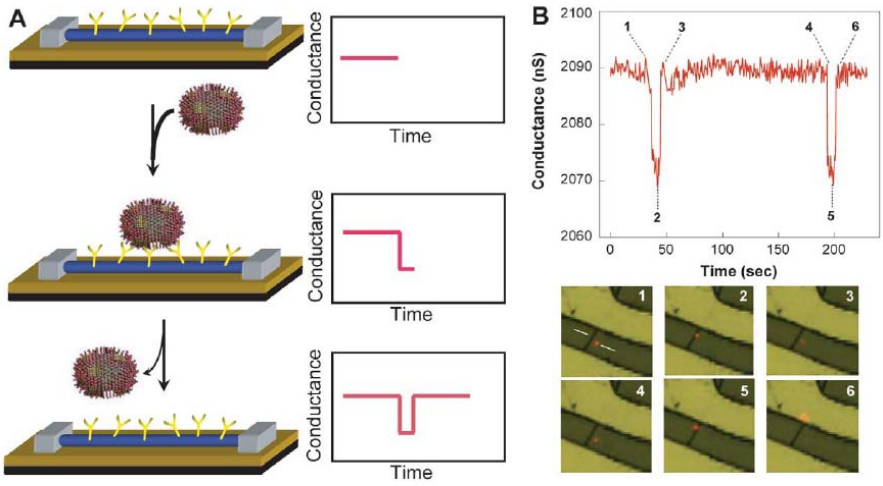

Figure 1.11: *(A)* Schematic of a single virus binding and unbinding to the surface of a Si nanowire device modified with antibody receptors and the corresponding time-dependent change in conductance. *(B)* Simultaneous conductance and optical data recorded for a Si nanowire device after the introduction of influenza A solution. The images correspond to the two binding/unbinding events highlighted by time points 1-3 and 4-6 in the conductance data, with the virus appearing as a red dot in the images (upon Patolsky and Lieber[228])

Ultimately, Lieber's group has recently reported strategies that enable parallel and scalable integration of nanowire FET devices over large areas without the need to register individual nanowire-electrode interconnects[231,232]. Electrically addressable arrays are fabricated by a process that uses fluid-based assembly, such as microfluidic[231] or Langmuir-Blodgett methods[232,233], to align and set the average spacing of nanowires over large areas, and then photolithography to define interconnects. An example of a state-of-the-art sensor fabricated in this way is the hybrid structure consisting of arrays of nanowire field-effect transistors integrated with the individual axons and dendrites of live mammalian neurons, where each nanoscale junction can be used for spatially resolved, highly sensitive detection, stimulation, and/or inhibition of neuronal signal propagation[234]. Arrays of nanowire-neuron junctions enable simultaneous measurement of the rate, amplitude, and shape of signals propagating along individual axons and dendrites (Figure 1.12). This outstanding configuration of nanowire-axon junctions in arrays, as both inputs and outputs, makes possible controlled studies of partial to complete inhibition of signal propagation by both local electrical and chemical stimuli. In addition, nanowire-axon junction arrays were integrated and tested at a level of at least 50 ''artificial synapses'' per neuron.

[231,232] Y. Huang *et al., Science* 291, 630 (2001) ; D. Whang *et al., Nano Lett.* 3, 1255 (2003)
[233] D. Whang *et al., Jpn. J. Appl. Phys.* 43, 4465 (2004)
[234] F. Patolsky *et al., Science* 313, 1100 (2006)

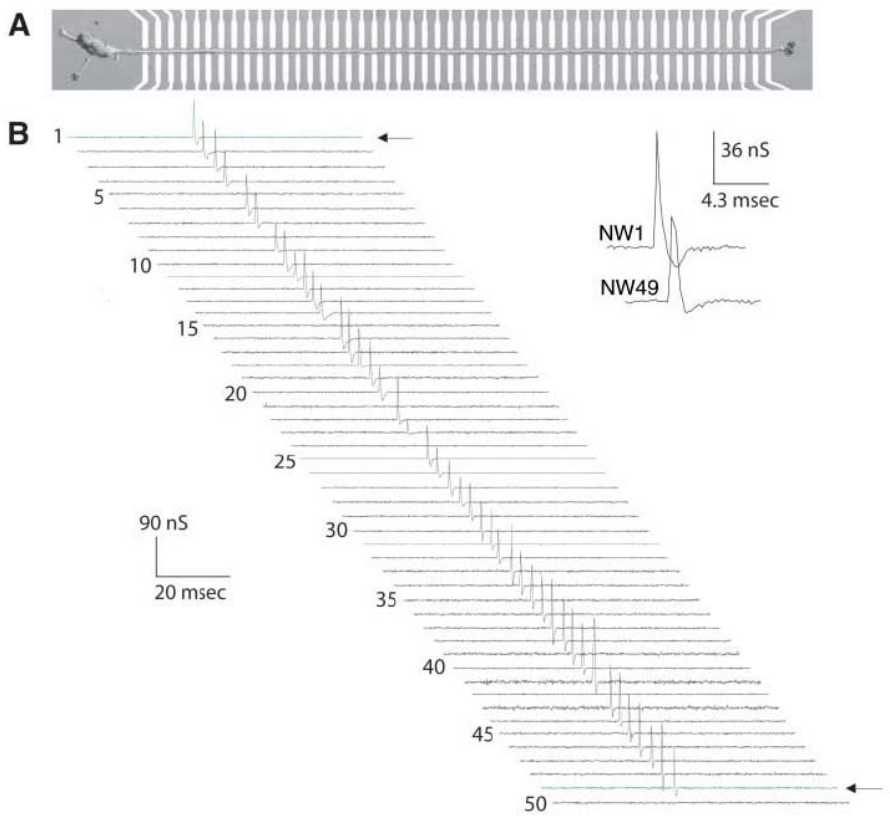

Figure 1.12: Highly integrated NW-neuron devices. (*A*) Optical image of aligned axon crossing an array
of 50 NW devices with a 10-mm interdevice spacing. (*B*) Electrical data from the 50-device array shown above. The yield of functional devices is 86%. The peak latency from NW1 (*top arrow*) to NW49 (*bottom arrow*) was 1060 ms (courtesy from Ref.[234], © 2006 Science)

Without any doubt, nanowire-based FET (and nanoscale devices, in general) modified with specific surface receptors present a powerful detection platform for a broad range of biological and chemical species. Let alone a number of key features illustrated in the previous examples like direct, label-free and real-time electrical signal transduction, it becomes obvious that the ultrahigh sensitivity and the potential for integration of addressable arrays on a massive scale set them apart from other sensor technologies available today. Nonetheless, intrinsic limits related to detection schemes based on static of conventional microfluidic delivery of analyte to nanoscale sensing zones were recently pointed out[235] and will be part of the concluding discussion in the last chapter of this manuscript.

The crusade for ultimate performance – a snapshot of the present time and perspective

The word may seem too strong, yet the first author's intention was to use "battle" or "race" instead of "crusade". It was the figurative meaning of the latter, given as "an enterprise undertaken with zeal and enthusiasm" that made the final choice. Indeed, while following the mainstream of the biosensors' development as provided in the present chapter, one can easily figure out that the winning configuration would be the **most sensitive, most integrated, highest-throughput, fastest response, less expensive**,… that has more the flavour of a race than of a quasi-linear, smoothly evolving scientific and technological field. It is only when considering the "zeal and enthusiasm" factor of the research teams involved in the biosensing challenging area that things become clear, the "race" becomes "crusade" and the lands to be conquered become " better understanding living organisms", "early stage diagnosis", "protect against bioterrorism".

[235] P. E. Sheehan and L. J. Whitman, *Nano Lett.* 5, 803 (2005)

What does this competitive area look like nowadays? Let us take six representative examples of "ultimate performance" found in the literature:

A. Craighead's group from Cornell University recently demonstrated the enumeration of DNA molecules bound to a nanomechanical oscillator[236]. Resonant nanoelectromechanical systems (NEMS) were used to detect the binding of individual DNA molecules through resonant frequency shifts resulting from the added mass of bound analyte and allowing to **detect a single 1587 base pair long DNA molecule** (equivalent estimated mass of several 10^{-18} grams) in a 0.03 ng/μL concentrated solution.

B. J. B. H. Tok *et al.* from Lawrence Livermore National Laboratory shown that nano-barcode[237] technique would allow immunoassays for the **detection of ricin or botulinum toxin with a limit of detection estimated at 5 ng/mL**, the assay time being of 3 to 4 hours.

C. C. Mirkin's and C. Liu's groups (from Northwestern University and University of Illinois, respectively) demonstrated bio-barcode on-chip assay with **attomolar-sensitivity protein detection** (prostate specific antigen - PSA) representing only 300 copies of protein analytes in 1 μL total sample volume, that is four orders of magnitude higher sensitivity compared to commercially available ELISA-based PSA tests[238].

D. S. Bencic-Nagale *et al.* from Tufts University developed a polymer microbeads-based assay that, after coating with fluoresceinamine and poly(2-vinylpyridine), have **sub-second response time when exposed to 13 ppm vapors** of diethyl clorophosphate (DCP) nerve agent vapors[239].

E. Joint work of C. Mirkin's and C. Liu's groups (again) developed a **massively parallel dip-pen nanolithography system with 55 000-pen two-dimensional array** allowing to pattern gold susbtrates with sub-100-nm resolution over square centimetre areas that reveals astonishing perspectives in high-throughput microarray technologies (provided the corresponding read-out systems are available)[240].

F. Whitesides' group demonstrated that **patterning paper to create well-defined, millimetre-sized channels could result into platforms for inexpensive, low-volume, portable bio-assays** applied to the simultaneous detection of glucose (2.5 mM) and proteins (0.38 mM of bovin serum albumin – BSA) in 5μL of urine[241]. These platforms could be easy to implement in remote regions such as those found in less-industrialized countries, in emergency situations, or in home-health care settings.

While a direct comparison is hard to make, the previous examples unveil the present key issues in the biosensing area and form a snapshot that would be interesting to take a look back on in a few years. It is straightforward to imagine that applications like examples B, C, D and F could find short-time commercial counterparts as they simultaneously address major requirements like cost, time-of-response, reliability related to societal concerns like health of security, while the remaining ones (A and E) would find more long-term echoes as more biophysics-related tools.

[236] B. Ilic *et al., Nano Lett.* 5, 925 (2005)
[237] J. B. H. Tok *et al., Angew. Chem. Int. Ed.* 45, 1 (2006)
[238] E. D. Goluch *et al., Lab Chip* 6, 1293 (2006)
[239] S. Bencic-Nagale *et al.*, *J. Am. Chem. Soc.* 128, 5041 (2006)
[240] K. Salaita *et al., Angew. Chem. Int. Ed.* 45, 7220 (2006)
[241] A. W. Martinez *et al., Angew. Chem. Int. Ed.* 46, 1318 (2007)

Comparing biosensors – impossible mission?

The biosensors' review provided in the previous pages, though non-exhaustive, allows raising a major issue: what are the comparison criteria for all those systems? Their classification gives some clues for a first answer: one can choose either technical considerations or biological considerations to make a comparison.

If commercial systems had to be compared based on technical considerations, one would think that this is a "lucky" situation. Indeed, datasets are provided when a commercial system is acquired; these deal generally with specifications concerning the analyte flow profile and rates ranges, the typical sample volume, the working temperature, the temperature stability, the sensitivity, the resolution of measurement, etc. Yet these data are complete and precise enough, they are most of time difficult to compare as they are related to different modes of transduction, different species to be detected (proteins, small molecules, cells,…), different ways of functionalizing the active areas of the core sensors, etc, let alone the non-commercial systems which are often incompletely qualified.

What about the biological considerations? This criterion means that different biosensing systems should be compared in a specific detection case, for one given analyte (i.e. one antibody kind). It seems that this second configuration meets if not all the requirements at least the most important ones in order to have a better idea concerning the origin of the differences in performance of various systems. A relevant example of comparing known biosensing systems is provided by T. R. Glass *et al.*[242]; the authors compare the least detectable concentration (LDC) and dynamic range (DR) of three immunoassay systems using for distinct antibodies (all specific for the same analyte, the estradiol, but with different affinities) on each system. The systems evaluated include the industry standard, ELISA, and two biosensors, surface plasmon resonance and kinetic exclusion. In all cases, the measurements of inhibition curves (response vs estradiol concentration) were contracted to outside experts (the biosensor manufacturers themselves in the case of the biosensors), each of whom was supplied with the same blind samples. Each biosensor manufacturer also reported an estimate of the equilibrium dissociation constant (*K*d) for each of the antibodies. The LDC and DR observed for the kinetic exclusion biosensor are consistent with an interpretation of *K*d limited detection while that from the other biosensor and ELISA show limits of detection somewhat above those expected for *K*d limited performance. The determined LDC and DR of each biosensor is self-consistent in the sense that none of the inhibition data contradicts theoretical limits associated with the *K*d as measured on that system; however, some contradictions are apparent across platforms. The use of multiple antibodies of differing *K*d improves confidence that the observed differences in performance are associated with the immunoassay system rather than the particular analyte.

Another example encompassed by the "biological considerations" criterion is the EILATox-Oregon Biomonitoring Workshop organised in 2004[243] that allowed the gathering of a diverse set of technologies for environmental toxicant detection that challenged the notion that bioassay approaches cannot be used reliably within the safe confines of one's own laboratory. The blind samples that were provided to each of the participating groups consisted of a diverse array of toxicants at toxic concentrations. Blind agent samples in 25-ml aliquots were prepared by dissolving the chemicals in synthetic water. A list of the toxic agents was previously available to the participants, but the toxicant identities of the blind samples were unknown until the end of the workshop. Both commercially available kits as well as prototype assays were included in the workshop. Several noteworthy observations emerged from the workshop findings: even though it was problematic to compare directly the sensitivity of the biomonitoring technologies (for two reasons: some groups could only process a limited number of samples during the workshop due to time, material or travel constraints; and there was not complete uniformity with respect to the dilution levels of toxicant samples across the different technologies), no false positives were reported across any of the technologies, regardless of the stage of maturity.

[242] T. R. Glass *et al., Anal. Chem.* 79, 1954 (2007)
[243] J. J. Pancrazio *et al.*, *J. Appl. Tox.* 24, 317 (2004)

These examples allow emphasising several complications when attempting to compare systems based on published or manufacturer–supplied accounts of the i.e. LDC and DR of individual systems. First, if different antibodies are used, then comparisons may reflect the antibody's contribution to the LDC rather than the immunoassay system. Second, even if the antibody is the same, the system noise will usually contain a component reflecting the skill of the practitioner, and the comparison may represent differences in the experimental skill. Third, different practitioners may use different nonequivalent methods or assumptions in calculating the LDC and DR, resulting in invalid comparisons.

To conclude, the golden path towards getting the right biosensor for a given application still requires access to platforms gathering various types of biosensing systems in order to perform the targeted bioassay (if possible) by the same practitioner using similar biological models to interpret data.

Finally, is it the fact that having a so tremendous choice of systems would sometimes complicate the choice itself? This is another question that remains to be answered…

2. RESEARCH ACTIVITIES SINCE 2003

Introduction

Before going into the details of my research activities since 2003, it is worth taking a closer look to understand the motivation that stands behind the overall work. As mentioned in the very beginning of the first chapter, I had to leave the LAAS a few months after having completed my PhD thesis. I was frustrated in leaving Christian Bergaud's team because a new exciting research theme was about to be initiated dealing with the emergence of microtechnologies applied to the biology and I could not be part of it. The frustration was all the more acute because of the excellent relationships we had inside the team.

At that time, the fields of activities where I was, say, "experienced" mostly addressed microfabrication and micromechanics. The Thales years that followed and the micro inertial R&D activities I managed there (far away from the biology) allowed me gaining knowledge in the microsensors and, more generally, in the microsystems area. I thus better realized the real meaning of MEMS and the number of crucial aspects this word encompasses. I did understand that a microsensor is not only a microstructure which static and dynamic behaviors nicely agree with elegant analytical or finite-element models but also a dedicated and specific electronic set-up, a complex packaging-related set of issues as well as extensive FEM simulations trying to take into account temperature drift effects, parasitic vibrations, parasitic capacitances (they are anywhere!), ageing, fatigue and reliability.

For reasons that were already mentioned in the first chapter, I decided to come back to LAAS and I proposed a project dealing with the application of resonant MEMS arrays to the biology (and I was lucky because it did work). As the team I left after my PhD thesis continued to work in the microtechnologies for biochips applications area, needless to say that the soil I found when I came back was more than fertile for my project. Meanwhile, a new research group was founded (Nanobiotechnology group, now renamed as Nanobiosystems) and I had the opportunity to immediately join it.

If my first target was only the development of resonant MEMS for biological applications, the fact that our research group became (starting with 2004) a full partner in the FP6 Integrated Project "Emerging Nanopatterning Methods" (NaPa) made me somehow deviate from the predefined way as I was asked to take on my own the Bioplume development.

Starting with that moment, having a TEAM with me played a fundamental role. Indeed, dealing alone with ambitious projects such as Bioplume or resonant bioMEMS is impossible to conceive. Not only have I decided to manage both projects in the same time but also to couple them in a complementary way, i.e. developing Bioplume as a tool allowing to properly, differently and simultaneously functionalize arrays of MEMS so that biodetection at the microscale in parallel, within the same flow, of different species could become reality.

The present chapter will first describe Bioplume development in terms of design, fabrication and implementation of the system together with the main applications aiming at proving the functionality of this MEMS-based spotter. Second, piezoelectric micromembranes will be presented, from more fundamental studies (in terms of analytic models of the device) to their integration with dedicated electronic and fluidic set-up as well as the first step towards applications like DNA-hybridization and antigen-antibody interaction detection. The last part of the chapter will introduce the first application that directly benefits from the coupling between Bioplume and functional bioMEMS through the detection of herbicide 2,4-D using MIPs deposited onto the latter system using the former one.

BIOPLUME: a MEMS-based picoliter droplet dispenser for surface patterning

2.2.1 Previous work

In 2000, Christian Bergaud proposed to start the development of a silicon cantilever-based liquid dispensing tool as a direct patterning method inspired from stainless steel slit pins (currently used to fabricate biochips) relying on the deposition of liquid drops on substrate. Before going further, it has to be noted from the beginning that Christian thought up the idea and that was the important thing. The rest was just a matter of getting the technology and the applications done.

The original system was compact, simple and well-suited for basic experiments like generating low-scale biochips-like applications[244]. However, it rapidly exhibited several drawbacks that limited its potential capabilities. Lack of control of contact force and size of the printed droplets during deposition was one of the improvements that have been proposed in the Bioplume version of the former spotter. This issue has been addressed by both incorporating position sensors as well as active loading and deposition schemes to the depositing cantilevers. More than simply adding new functionalities to an existing system, the proposed solutions opened doors to new, until then unexploited applications like in-spot electrochemistry or polymers deposition, as it will be described in the followings.

2.2.2 Introduction

Unlike commercial stainless steel quills[134], the Bioplume tool consists of a silicon chip bearing pen-shaped microcantilevers. A simple PC-controlled automated motion stage is used to position the chip and execute the loading and deposition steps. Patterns are created from the superposition of deposited drops that act as liquid pixels. The manufacture of the cantilevers is based on conventional microfabrication techniques which enable to realize cantilevers with micrometer dimensions for picoliter droplet deposition and chips with several cantilevers for parallel patterning. The other advantage inherent to the cantilever fabrication is the ability to fabricate multiple chips on a single wafer, thus lowering the cost of a single chip. Each microcantilever incorporates a fluidic channel in its tip for liquid deposition. In order to avoid having a complicated fluidic system on the chip for liquid supply to the channel, the loading of the cantilever is carried out by external means. In addition, the cantilever can also bear a reservoir to increase the storage capacity and to allow depositing more spots without reloading. In order to facilitate the cantilever fabrication process and the possible cleaning of the fluidic system, the channel and the reservoir are open. This solves any clogging issue but raises evaporation problems that result in a decrease of liquid concentration with increasing number of prints. A high evaporation rate even prevents the deposition process to occur as no liquid remains in the channel by the time the chip is moved from the loading to the deposition point. Rather than working in a humid environment, a simple solution consists in adding high-boiling-point solvents to the deposited liquids.

To enhance the reliability and the performance of the Bioplume liquid deposition tool, there is an interest in monitoring the cantilever position regarding the surface to pattern and in controlling in situ the deposition process and the size of the printed drops. For this purpose, incorporation of position sensors, as well as active loading and deposition schemes to the cantilevers is proposed. Technical choices used to realize such detection and actuation methods are described in the following section. Then, the design and the fabrication of the Bioplume cantilevers are briefly presented in the next sections. After presenting the characterization results and the spotter implementation, this section ends with a review of experimental results aiming at proving the functionality of the Bioplume system.

2.2.3 Integration of sensors and actuators

[244] P. Belaubre *et al., Appl. Phys. Lett.* 82, 3122 (2003)

2.2.3.1 Force sensors

Since the cantilevers are used in contact mode for the printing process, measurement of their bending provides information on important parameters during deposition, such as the contact time and force. It is necessary to control such parameters because the contact time influences the size of the printed droplets and the force exerted can prevent the printing process (if too low), or can lead to surface scratching (if too high). Moreover, measuring the cantilever bending can also be used to estimate the position of the cantilevers regarding the surface to pattern or the loading area. Such a detection scheme is particularly important when working with an array of cantilevers because non-uniform depositions occur when the array is not perfectly parallel to the surface (i.e. when the cantilevers do not contact the surface evenly). The trim of the array in relation to the surface can simply be deduced and corrected by knowing the displacement of two cantilevers of the same array.

The rapid development of scanning probe techniques, such as atomic force microscopy (AFM), and the use of micromachined cantilevers as biosensors have led to the introduction of several displacement detection methods that allow measuring the bending of silicon microcantilevers with high sensitivity and resolution[245]. The most widespread method is the optical lever technique that relies on the reflection of a laser beam onto the cantilever[246]. The reflected beam hits a position sensitive photodetector and the bending of the cantilever is measured by the change of beam position on the detector. This method is highly accurate but necessitates the complex alignment of the optical devices and can not be integrated into the cantilever. It can be adapted to measure several cantilever displacements in parallel but requires precise knowledge and know-how because a beam and its optical setup are required for each cantilever.

The capacitive sensors that measure the bending as a change in capacitance of a plane capacitor can be integrated and provides absolute displacement[247]. However, it is not appropriate to measure large displacements, and the fabrication process used to realize such devices can be complicated.

Piezoelectricity can be used to sense the bending of a cantilever by integrating piezoelectric materials into the cantilever beam[248]. Under stress conditions, i.e. the bending of the cantilever, an electric field is created inside the material and measurement of the voltage difference in the layer provides the cantilever displacement. This approach is very interesting and efficient, but requires specific knowledge and fabrication tools in order to integrate good piezoelectric materials on the cantilever.

The variation of bulk resistivity with applied stress is known as the piezoresistive effect. A resistance made of piezoresistive material built onto a cantilever changes when the cantilever is stressed under displacement, providing a simple means to measure the bending[249]. The interesting advantage of this approach is that doped silicon exhibits a strong piezoresistive effect. Thus, the integration of a piezoresistor on the cantilever is simply achieved by adding a few fabrication steps. Moreover, measurement of the resistance change can be easily carried out with a Wheatstone bridge. Because piezoresistive elements are sensitive to light and temperature changes, stress measurement can be carried out by using a differential signal between a sensing cantilever and a reference one. Due to its numerous advantages and giving the fact that piezocantilevers have already been developed in our research group[250], the piezoresistive approach is the one selected for the Bioplume cantilevers.

---

[245] S. Raiteri *et al., Sens. Act. Chem. B*79, 115 (2001)
[246] S. Alexander *et al., J. Appl. Phys.* 65, 164 (1989)
[247] J. Brugger *et al., Sens. Act. Phys. A*43, 339 (1994)
[248] S. Watanabe and T. Fujii, *Rev. Sci. Instrum.* 67, 3898 (1996)
[249] M. Tortonese *et al., Proc. 1991 Int. Conf. Solid-State Sens. Act. (Transducers '91)* , 24-27 Jun., San Francisco, USA, 448 (1991)
[250] E. Cocheteau *et al., Proc. 11th Int. Conf. Solid-State Sens. Act. (Transducers '01)* , 10-14 Jun., Munich, Germany, 2, 1070 (2001)

2.2.3.2 Electro-assisted loading and deposition methods

Using a slit in the cantilever for liquid storage and deposition can lead to loading issues if the slit exhibits a square section and rough and hydrophobic walls. Indeed, the resulting capillary forces exerted on the liquid might be too weak to induce any rise of a liquid column in the channel. As a result, the loading of the device must be achieved by immersing the fluidic system of the cantilever in the liquid, requiring an important dead volume.

In order to reduce this dead volume, an active liquid loading method must be incorporated to the cantilevers such that only the tip extremity has to contact the liquid during the loading process. The implementation of such a scheme has another advantage: it allows loading the required volume of liquid to be deposited, thus reducing some possible wasted liquid remaining on the cantilever after the printing process. Those are pertinent improvements when using biological solutions that are expensive or are only obtained in very small quantities.

For its ease of implementation and use, since it does not require any mechanical moving parts, the electrowetting phenomenon is particularly appropriated for liquid actuation. Electrowetting consists in bringing electrostatic charges at a liquid/solid interface, resulting in a change of liquid contact angle thus modifying the spreading of the liquid[251]. This phenomenon is widely used on the microscale to move liquid droplets or columns on planar electrodes[252,253], and to induce the rise of liquid columns between a set of vertical electrodes[254]. In order to implement the electrowetting actuation scheme on the cantilevers, an electrode is incorporated in the channel so that liquid actuation occurs by applying a DC or low-frequency voltage between the electrode and the liquid, resulting in liquid motion inside the channel.

Liquid delivery by direct contact between the deposition tool and the substrate is a passive method governed by the spreading of the liquid onto the surface. Variation of contact time is usually used to adjust the amount of deposited material. However, this method strongly depends on the surface wettability and does not allow the three-dimensional control of the pattern. Electro-assisted methods can provide an efficient active method for the control of the deposition process. Indeed, the incorporation of an electrode in the fluidic channel of the cantilever enables redox reactions to occur in an electrolytic drop during deposition providing that the surface to pattern is conductive. Electrochemistry is a powerful way to deposit or etch various materials allowing a precise control of the reactions by monitoring the number of charges supplied to the cell[255]. Thus, the addition of an electrode patterned inside the channel of the cantilevers has two advantages: it enables the use of electrowetting for active loading and electrochemical deposition without complicating much the fabrication process of the cantilevers.

2.2.4 Design of the cantilevers

The geometry of the Bioplume cantilevers consists of a flexible beam ending with a sharp tip. The fluidic part of the cantilever comprises a slit that opens out into the extremity of the cantilever tip and a reservoir in the beam body. For force sensing purpose and electro-assisted filling and deposition, a piezoresistor is integrated into the cantilever and a metal electrode is incorporated in the channel. A schematic of the cantilever is displayed in Figure 2.1.

[251] C. Quillet and B. Berge, *Curr. Op. Coll. Int. Sci.* 6, 34 (2001)
[252,253] S. K. Cho *et al., J. of Microelectromech. Syst.* 12, 70 (2003); W. Satoh *et al., J. Appl. Phys.* 96, 835 (2004)
[254] T. B. Jones *et al., Langmuir* 20, 2813 (2004)
[255] F. Walsh, *A first course in Electrochemical Engineering* The Electrochemical Consultancy, Romsey (1993)

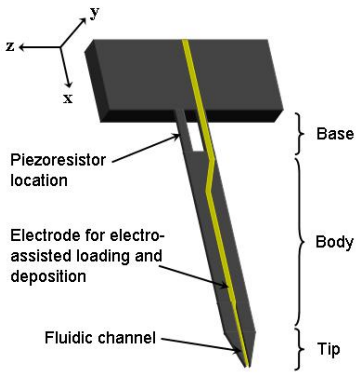

Figure 2.1: 3D schematic of the Bioplume cantilever showing the working coordinate system used in the following calculations.

The piezoresistor is located at the cantilever base, where the stress caused by the bending is maximum. The cantilever base exhibits a U-shape that permits the current to flow in one leg and out the other: this avoids possible shortage of the resistance and facilitates the overall fabrication process because the shape of the piezoresistor is defined during the cantilever fabrication without alignment issues. A metal electrode is patterned in the channel of the cantilever for electrowetting and electrochemistry implementations. The electrode must be located inside the channel so that the spreading of the liquid occurring onto the electrode allows filling the channel. This configuration also enables the electrode to contact the liquid drop during deposition, thus permitting electrochemical reactions to occur on the substrate. The working principle of these electro-assisted methods is based on the application of a potential difference between the cantilever and the substrate surface. Thus, shortage between the cantilever electrode and the contacting surface is to be avoided. For that purpose, the electrode is required to be shorter than the channel length. This ensures a constant distance between the electrode and the deposition surface.

The cantilever is solely made of silicon and electrical connections are realized with metal lines. Passivation layers are used to electrically insulate each part of the cantilever. The base of the cantilever is a critical part because it hosts the piezoresistor and provides electrical contact to the channel electrode. The choice of the cantilever dimensions is governed by the feasibility offered by the fabrication tools, the size of the drop to deposit, the resulting stiffness coefficient and the value and sensitivity of the piezoresistors.

The fabrication of the cantilever[88] is based on classical techniques used in the microelectronics industry and relies on photolithographic steps. The lateral dimensions of the cantilever are thus determined by the precision of the photolithography. With the classical photoresists and aligners used clean-room facilities, the reasonable minimum feature size is 2 µm. The thickness of the cantilever is set by the layer of silicon into which the cantilever is patterned. In order to precisely control this thickness, the starting substrate is a silicon-on-insulator (SOI) wafer with top silicon layer thickness that can range between several micrometers to tens of micrometers.

2.2.5 Fluidic requirements

The section of the channel and the sharpness of the tip dictate the range of deposited drop sizes. Because the tip is in the plane of the cantilever, deposition is carried out with the cantilever almost perpendicular to the surface (but not perfectly perpendicular to avoid the instantaneous buckling of the beam). This configuration allows achieving the smallest drop size. To deposit drops with diameters ranging from several micrometers to tens of micrometers, the channel must exhibit

micrometer dimensions. Besides, the slit must almost have a square cross-section for the formation of circular droplets.

The channel length and the size of the reservoir are chosen accordingly to the number of drops that are to be deposited without reloading (more than 50 droplets with sub-picoliter volumes). Giving those facts, the following dimensions are selected: the channel is 4 µm wide, 5 µm thick (specifying the thickness of the top silicon layer of the SOI wafer) and 200 µm long; the reservoir is 24 µm wide, 5 µm thick and 200 µm long. Because the thickness of the deposited layers (silicon dioxide and metal) constituting the patterned electrode is very thin (submicrometer), the volume of liquid loaded in the channel and the reservoir can be estimated from the dimensions given above. The approximated corresponding volumes are thus **4 pL and 24 pL**.

2.2.6 Mechanical considerations

The stiffness coefficient of the cantilever is an important parameter to take into account in the cantilever design. The spring constant correlates the force applied on the cantilever to the displacement of the tip. To avoid sticking of the cantilever on the deposition surface or in the loading droplet (i.e. the cantilever is not too compliant) while preventing the scratching of the surface (i.e. the cantilever is not too stiff), the stiffness coefficient should lie in between 0.03 N/m and 0.3 N/m[256]. Because there is no simple analytical expression of the axial stiffness coefficient k_x (describing the deposition configuration), the lateral coefficient (k_y, coupling the force and the displacement along the y axis) is used as an estimation of the cantilever behavior. Figure 2.2 shows a schematic of a simple U-shaped cantilever with a slit, and gives the geometrical dimensions used in the calculation of the stiffness coefficient.

Taking into account the electrical requirements specified hereafter, we chose the following dimensions for the cantilever: the total length of the beam is 1500 µm with a width of 120 µm, and each arm of the base is 200 µm long and 42 µm wide[88]. These dimensions lead to a stiffness coefficient of about 0.16 N/m (for E = 169 GPa).

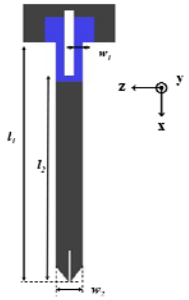

Figure 2.2: Illustration of the cantilever with annotated geometrical parameters.

2.2.7 Electrical considerations

The piezoresistor is integrated to the silicon cantilever by locally doping the initial substrate. The design of the piezoresistive element relies on the initial value of the piezoresistance and its expected sensitivity. When applying a lateral (y-directed) or an axial (x-directed) force at the cantilever tip, the cantilever bends up or down and the stress is maximum at the cantilever base. Along the piezoresistor path, this region corresponds to the two legs where the current flows in a direction parallel to the stress gradient. As a result, only the longitudinal component is taken into consideration in the calculation of the piezoresistor sensitivity. Moreover, the highest stress regions are localized at the surface of the cantilever. Thus, the piezoresistive element must be confined at the surface to exhibit a high sensitivity. The expression of the resistance value is:

[256] M. Zhang *et al., Nanotechnology* 13, 212 (2002)

$$R = \frac{\rho l_R}{A} \tag{2.1}$$

for the simple U-shaped cantilever, the resistor cross-section is:

$$A = w_1 \times t_R \tag{2.2}$$

where ρ is the resistivity of the fabricated piezoresistor, and l_R, w_1 and t_R are its length, width and thickness, respectively. Because the piezoresistor fabrication relies on a doped silicon layer, its thickness is equal to the doping junction depth, x_j. In a first and simple approximation, the resistance of the piezoresistor is estimated by the contribution of the two legs only, i.e. $l_R = 2 \times (l_1 - l_2)$. An initial value of several kΩ is required to meet the specifications of the electronics dedicated to the piezoresistance measurements. The expression of the relative change in resistance due to an applied lateral load, F_y, at the tip of the cantilever, is provided below[257]:

$$\frac{\Delta R}{R} = \frac{3\pi_L F_y (l_1 + l_2)}{2 w_1 t^2} \tag{2.3}$$

where π_L is the longitudinal piezoresistive coefficient. Equation (2.3) is obtained by considering only the contribution to the change in resistance given by the two legs and assuming a resistor perfectly confined at the cantilever surface. Knowing the stiffness coefficient from equation (2.1), we can express the theoretical lateral piezoresistor sensitivity (i.e. the fractional change in resistance for a unit displacement at the free end of the cantilever, u_y):

$$\left(\frac{\Delta R}{R}\right)\frac{1}{u_y} = \frac{3\pi_L k_y (l_1 + l_2)}{2 w_1 t^2} \tag{2.4}$$

The intrinsic properties of the piezoresistor (π_L and x_j) are dictated by the doped layer fabrication and the orientation of the cantilever toward specific crystal axes. The other design parameters, i.e. the dimensions of the cantilever and the piezoresistor, are chosen in order to obtain the required resistance value, to maximize the sensitivity, while resulting in a beam with a suitable stiffness.

2.2.8 Fabrication and packaging of the Bioplume chip

A schematic of the 5 mm x 5 mm Bioplume chip is shown in Figure 2.3. The chip is designed to incorporate 10 cantilevers for parallel liquid deposition (separated from each other by 320 µm). Two of these cantilevers incorporate a force gauge to measure and monitor the contact time and force during deposition. Two similar sensing force cantilevers are added on each side of the array for the trim control. These two cantilevers are placed forward on the chip, so that they touch the surface before the depositing cantilevers when moving the chip down to the surface.

This design allows correcting the array misalignment and detecting the deposition surface without proceeding to any deposition. An additional piezoresistive cantilever is integrated in the body of the chip for reference purpose: this cantilever undergoes the environmental changes (such as temperature, light, humidity) but is free from contact with a surface. Measuring the differential signal between any sensing cantilever and the reference one leads to the compensation of resistance change due to the environmental parameters. Finally, electric lines and bonding pads are designed to allow simple connections between the chip and its package.

[257] M. Tortonese, *Force Sensors for Scanning Probe Microscopy* PhD thesis, Stanford University (1993)

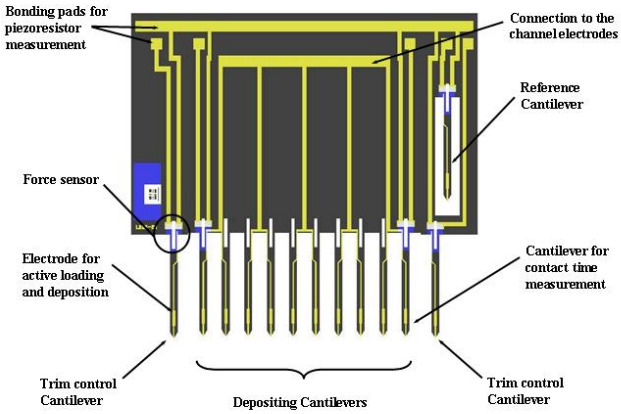

Figure 2.3: Schematic of the Bioplume array.

The fabrication of the Bioplume cantilever array (not detailed here) is based on standard micromachining techniques. The process includes 8 photolithographic steps[88]. The starting substrate is a 100 mm, (100), n-type SOI wafer, with a 1 µm thick buried oxide layer and a 5 µm thick top silicon layer (resistivity of 7 Ω.cm). Figure 2.4 shows a processed wafer before the final backside DRIE. Each wafer includes 192 Bioplume chips. Scanning electron microscope (SEM) pictures of a fabricated array, including a close-up view of the channel at the tip of a cantilever, are shown in Figure 2.5.

The Bioplume chips are then packaged to allow fixing it to the positioning apparatus and connecting it to the piezoresistor readout electronics. For that purpose, the chips are glued and bonded to a printed circuit board (PCB). Figure 2.6 shows a packaged device ready for testing.

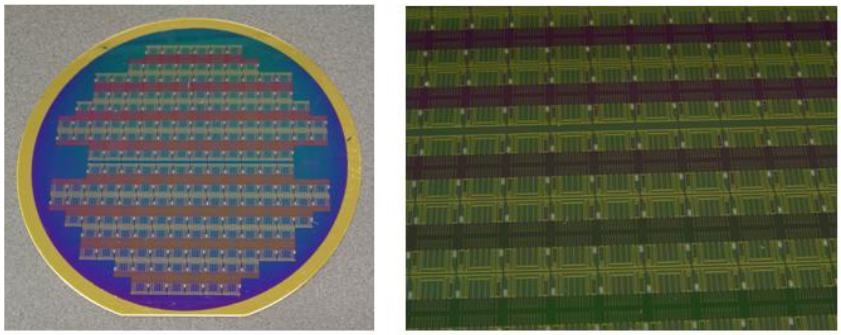

Figure 2.4: Photograph of a processed wafer (left) and close-up view (right).

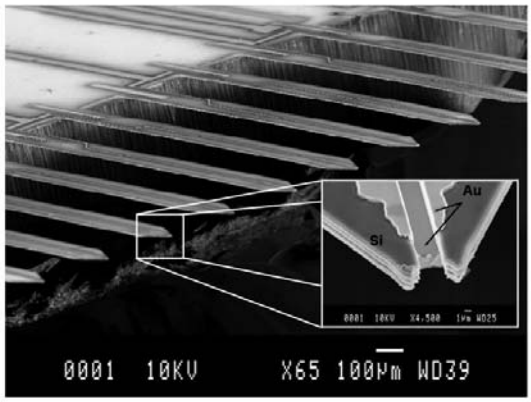

Figure 2.5: SEM picture of a cantilever array with SEM close-up view of the silicon tip showing the electrode inside the fluidic channel.

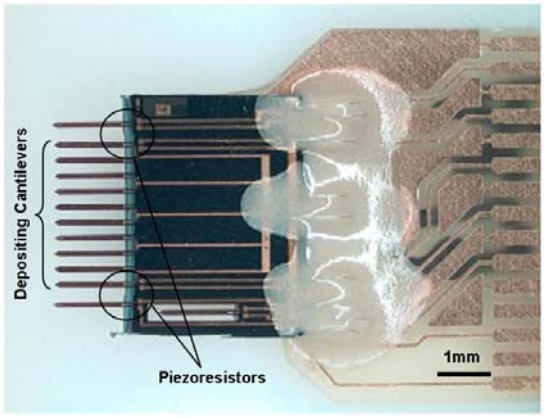

Figure 2.6: Optical photograph of the silicon cantilever array bonded onto a PCB support.

2.2.9 Piezoresistive cantilever measurement and characterizations

A conventional Wheatstone bridge is generally used to measure the static variation of a piezoresistor. However, a Wheatstone bridge does not lend itself to measurement optimizations. Indeed, this method is efficient under specific conditions (proper resistor dispersion ratio) that are not easily obtained when working with piezoresistors fabricated in laboratories. Thus, we use a method relying on a modified Wheatstone bridge[258], consisting in replacing the two static resistors of the bridge with controlled current generators. This solution (thoroughly detailed in Ref[88]) offers several advantages. Firstly, the current generators enable the compensation of the bridge by monitoring biasing voltages. Secondly, the transfer function of the system results in a twofold gain compared to the one of the Wheatstone bridge. The noise balance is equivalent in both methods, since the signal to noise ratios are equivalent.

To characterize the sensitivity of the fabricated cantilevers and the output of the electronic circuit, bending experiments were conducted. The Bioplume chip was attached to a positioning apparatus via the detection board: the chip was connected to the detection board, which was then used as a chip holder. For this purpose, the design of the detection board allowed directly mounting it onto a ceramic piezoactuator thanks to dedicated mechanical parts. The chip could be positioned in parallel or almost perpendicularly to the displacement axis and bending experiments were carried out by moving the cantilevers toward a fixed surface, as shown in Figure 2.7. The output voltage was recorded as the cantilevers bent on the surface.

[258] D. Saya *et al., Sens. Act. Phys. A*123-124, 23 (2005)

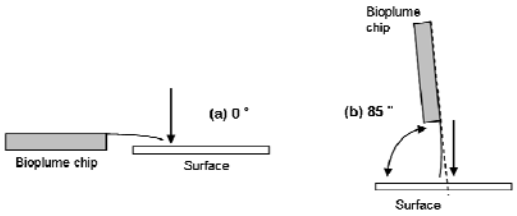

Figure 2.7: Lateral (a), and axial (b) bending conditions. The axial condition corresponds to the deposition configuration[88].

The injected power was approximately set to 500 μW in all the experiments. The estimated output noise was less than 30 mV (effective voltage), but significantly higher than the 10 mV theoretical noise of the electronics. This experimental noise was attributed to mechanical vibrations within the system and room lighting. After proper filtering, the noise value could be reduced to almost 10 mV.

Under lateral loads, the response of the piezoresistive cantilevers is linear in the range of the induced displacements since the cantilevers do not experience large bending (the maximum free end displacement stays under ten percent of the total length of the cantilever). The slope of the resulting line is the piezocantilever sensitivity in terms of output voltage per unit displacement. In this configuration, the cantilever bending can directly be obtained by reading the output voltage value.

The response of the cantilevers bending under axial loads is strongly non-linear and the resulting sensitivities are much higher than the ones observed for lateral displacements. This is consistent with the fact that higher stresses are induced in this configuration for a given tip displacement. This result is also very interesting because it means that the deflection precision is better in the deposition configuration. However, because the voltage output saturates around 11 V (due to the electronics design), no more than 10 to 20 μm of tip displacements can be detected with this technique.

In the depositing configuration, the output voltage varies non-linearly with the tip displacement. Thus, the piezoresistor sensitivity depends on the deflection in the tens of micrometer displacement range, before reaching the saturation of the electronics. The sensitivity can still be considered linear in the first micrometers of displacement, where it exhibits its maximum values, ranging from 1 V/μm to more than 3 V/μm. Considering an output noise of about 30 mV, the corresponding minimum tip displacement that can be detected lies in the range of tens of nanometers. This information is sufficient for surface detection applications.

2.2.10 Automated spotter in closed-loop configuration

The complete automated Bioplume spotter comprises the silicon chip associated to the electronic circuit, a four-degree-of-freedom automated displacement system and a PC. The electronics is dedicated to the measurement of the piezoresistor and the motion stage is used to position the cantilever array. The stage supporting the loading and deposition surfaces can be moved in the X, Y, and Z directions by means of step motors, whereas the vertical (X) displacement and the tilt (θ) of the array are respectively done by a piezoactuator for fine positioning and a step motor. Each axis is controlled by the PC thanks to specifically written LabWindows/CVI software. The output of the electronics is connected to the PC so that the microsystem is in a closed-loop configuration: the cantilever bending occurring when touching a solid surface or a liquid droplet leads to the determination of contact points thanks to a specific algorithm, which is then used to control the displacement of the array. Via a graphic user interface (GUI), the operator specifies the deposition parameters to carry out automated experiments. A schematic of the closed-loop automated spotter is shown in Figure 2.8.

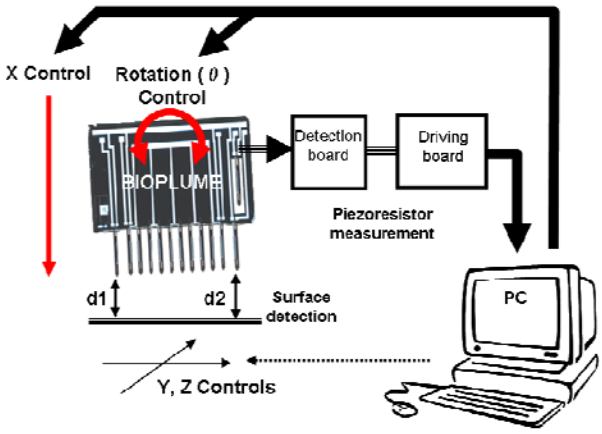

Figure 2.8: Diagram of the closed-loop Bioplume spotter[88].

Finally, a CCD camera connected to the PC is used to monitor the displacement of the chip regarding to the loading and deposition areas.

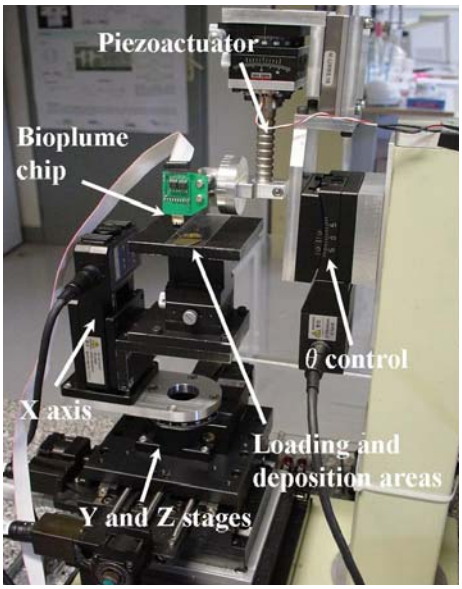

Figure 2.9: Picture of the four-degree-of-freedom depositing spotter including the cantilever array[88].

Experimentally, the Bioplume closed-loop configuration is used to detect the loading and deposition surfaces and to measure and correct the trim error before spotting. The angle error is estimated by comparing the two signals of the side cantilevers while approaching the deposition surface. Trim correction is carried out by adjusting the tilt until the signals are equal. The tilt adjustment is not carried out continuously but only when necessary, i.e. usually before the deposition process. The inside sensing cantilevers are then used to detect the loading and the deposition points, ensuring proper liquid transfers between the depositing cantilevers and the surfaces. Once these values are stored in the PC, matrices of spots are automatically printed at chosen locations with specific angles. Loading is previously achieved by dipping the cantilevers in a drop of the liquid to be spotted or in the reservoirs of a dedicated loading chip during a few seconds. During the deposition process the two depositing cantilevers bearing the piezoresistors are used to measure and control the contact time and force. The displacement of the chip can be adjusted; a speed of 10 mm/s ensures a fast and

secure operation. The time response of the overall system is estimated to be less than 1 ms, thus deposition times longer than 10 ms are usually used to ensure an accurate contact time.

2.2.11 Loading and deposition tests

2.2.11.1 Influence of deposition parameters on the printed features

The Bioplume spotting system was used to investigate the effect of the trim error on the uniformity of the printed drop matrices. The influence of the contact time and force on the size of the deposited droplets was also studied for different surface wettablities[259]. For this purpose, liquid drops were deposited onto surfaces exhibiting different wettabilities: gold, silicon and silicon dioxide. Experiments were performed with a water-glycerol mixture (75%-25% in volume) to avoid evaporation.

Deposition of matrices of drops was firstly carried out for different trim error angles during a single programmed run. The angle between the array and the surface was incremented from one row to another by 0.1° starting from a perfect alignment (Figure 2.10). As expected, the number of depositing cantilevers touching the surface lowered as the trim error increased. Therefore, droplets were missing and the printed matrix was non-uniform, thus demonstrating the importance of the tilt control.

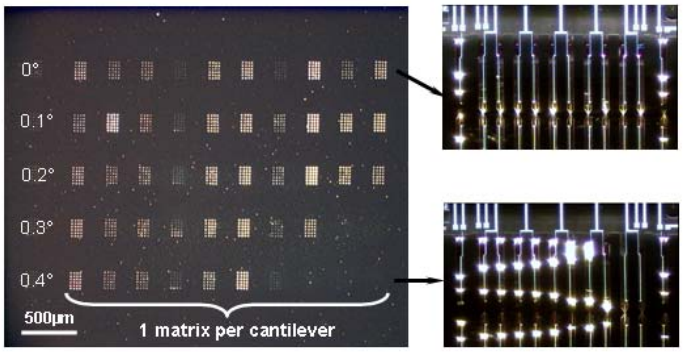

Figure 2.10: *Left*: Photograph of water-glycerol droplets' matrices realized by increasing the misalignment of the array. *Right*: Optical photographs of the array while depositing for 2 different tilt angles (Top: 0°. Bottom: 0.4°)[88]

In order to investigate the influence of the contact force used during deposition on the size of the printed spots, rows of droplets were realized by incrementing the displacement of the piezoactuator from 2 µm to 20 µm after the cantilevers touched the surface. As the piezoactuator moved the cantilever array down, the force exerted by the cantilevers onto the surface increased. An analogous experimental procedure was followed to study the influence of the time during which the cantilevers are in contact with the surface (thus allowing liquid transfer) on the size of the droplets. Rows of drops were deposited with contact times ranging from 20 ms to 20 s. Because of the actuation speed limitation of the spotter, shorter contact times were not included in the experiment.

The evolution of the droplet diameters was pretty steady for the three types of surfaces studied within the range of induced cantilever displacements. From this observation, we concluded that the size of the deposited droplets does not depend on the applied force (it is interesting to mention here that, according to some simulation results, the applied force does not vary linearly with the chip displacement). However, major differences in sizes existed between the droplets printed onto the silicon dioxide surface, and the gold and silicon surfaces. As expected, the more hydrophilic the surface is, the larger the droplets are. The contact time seemed to influence the size of the printed

[259] T. Leïchlé *et al., Proc. 1st IEEE Conf. on Nano/Micro Eng. and Mol. Syst. (IEEE-NEMS)*, 18-21 Jan., Zhuhai, China, 732 (2006)

droplets to a bigger extent. The same behavior was observed in the case of the three surfaces: the diameters increased rapidly within the first second. A plateau was then reached for the most hydrophobic substrate (silicon); the droplets exhibiting approximately a 10 µm diameter even with increasing contact time. We believe that this steady state occurred when the equilibrium between the Laplace pressure of the deposited drop and the pressure of the liquid contained in the cantilever fluidic channel was obtained. For gold and silicon dioxide, the diameter still augmented with time. However, this change was more pronounced for the more hydrophilic substrate (silicon dioxide). Thus it seems that the more hydrophilic the surface is, the more important the influence of time on the drop size is.

2.2.11.2 Deposition of biological solutions

To prove that the Bioplume system is suited for biological applications, deposition experiments were conducted with biomolecules[260]. The hybridization of two short synthetic oligonucleotides immobilized on aldehyde-dendrimer-coated-glass slides with the Bioplume spotter was studied.

We firstly showed that several solutions could be deposited successively with the same cantilevers without cross-contamination thanks to a simple cleaning procedure. The washing procedure was carried out by simply dipping the microcantilevers into water and gently agitating them. To evaluate the efficiency of this method, the following experiments were conducted using several cleaning times: fluorescent oligonucleotides were firstly deposited with Bioplume, then a washing step was performed and finally the subsequent deposition of clean buffer was done. We evaluated the immersion time necessary to remove any contaminants by measuring the residual fluorescence of the buffer spots and comparing it to the fluorescence of the firstly deposited oligonucleotide spots. A 15 minutes rinse was sufficient to eliminate 96% of the solution previously deposited and after a 60 minutes wash, the fluorescent signal was below detection. Unfortunately, these rinsing times are very long compared to the cleaning procedures used for commercial pins. This time should be lowered to a minute or less in order to be efficient and competitive. This cleaning procedure must be optimized and could be improved by using other chemical reagents for instance.

The biofunctionality of the oligonucleotides deposited with Bioplume was then checked by following a classic protocol used for microarrays and adapted to the size of the printed spots (20 µm diameter instead of the 200 µm achieved with commercial spotters). Bioplume was used to create arrays of 35-mer NH_2 oligonucleotide spots on a dendrislide. Then, buffer alone was spotted as a negative control. After completing the steps enabling DNA immobilization and covalent coupling, the spotted area was entirely covered with a solution containing the Cy5-labeled complementary oligonucleotides. After waiting for 30 min to allow hybridization reactions, the slide was washed to remove non-hybridized oligonucleotides. On the laser scanner image, fluorescent signal appeared where 35-mer NH_2 was spotted, but no fluorescence was detected at the location of the buffer spots or on the bare surface. This proves that hybridization occurred and was detected despite the scale reduction and the presence of 25% glycerol in the spotted solutions.

Spot-in-spot experiments were then conducted in order to demonstrate the successful hybridization between an oligonucleotide and its complementary, both locally deposited with Bioplume. Experimentally, a grid of 35-mer amino-oligonucleotide was addressed on an aldehyde dendrimer coated glass slide and immobilized via a covalent linkage. Treatment and washing were performed with a pipette on the fixed glass slide. Subsequently, the complementary 15-mer Cy5-labeled oligonucleotide was addressed, so that half of the spots were superposed. After 30 minutes of hybridization, the slide was rinsed. A specific signal was obtained only in the spots where both 35-mer NH_2 and 15-mer Cy5 oligonucleotides were deposited, thus demonstrating spot-in-spot hybridization. This method is of great interest because it permits reducing the volume of reagents used for revelation. Indeed, instead of entirely covering the slide surface with the complementary solution (classical procedure used for microarrays), only tiny droplets of the fluorescent complementary oligonucleotide were spotted on top of the immobilized spots.

[260] N. Berthet *et al., Proc. 10th Int. Conf. Min. Syst. Chem. Life Sci. (µTAS)*, 5-9 Nov., Tokyo, Japan 1217 (2006)

These results prove that protocols used with commercial apparatuses can be transposed to a smaller scale using Bioplume. Compared to protocols usually performed for microarray experiments, volumes of analytes and duration of experiment are considerably reduced. For example, 35-mer NH_2 covalent immobilization on the aldehyde dendrislide was reduced from 15 h to 30 min. The subsequent $NaBH_4$ treatment was also shortened from 3 h to 30 min. Moreover, contact printing with Bioplume allows successive superposed deposition of active biomolecules at micrometer-precise locations, possibly allowing the local functionalization of MEMS sensing devices. As deposition of biomolecules at computer-controlled positions is possible, potential use of the device can also be foreseen for molecular assembly.

2.2.11.3 Loading tests using electrowetting

In order to reduce the amount of dead volume required for the loading of the cantilevers, we have implemented a liquid actuation scheme based on electrowetting. Electrowetting occurs by applying a voltage between the electrode in the cantilever channel and the liquid to be loaded, resulting in the spreading of the liquid on the electrode. Experiments were conducted with the fabricated cantilevers to demonstrate the viability of the method[261]. The liquid to be loaded, either pure dimethyl sulfoxide (DMSO) or 50% DI water – 50% glycerol solution was placed in a metallic reservoir. Loading was achieved by dipping the tip of the cantilever in the liquid and applying a voltage between the cantilevers and the metallic reservoir. To ensure the proper loading of the cantilevers, matrices of spots were obtained by direct contact printing on silicon and gold surfaces.

The electrowetting phenomenon appeared when applying less than 4 V, resulting in a rise of liquid inside the channel only. The voltage was then slowly increased to keep the liquid moving forward in the channel. The channel and reservoir could be completely filled after setting the voltage to several tens of volts during a couple of seconds. As expected, because the electrodes were not properly passivated (probably due to the geometry of the cantilever tip), hydrolysis effects appeared when loading the water-glycerol solution, leading to power consumption and bubble production at the tip of the cantilevers. Deposition of more than 50 droplets per cantilever was then successfully performed onto silicon and gold surfaces (Figure 2.11).

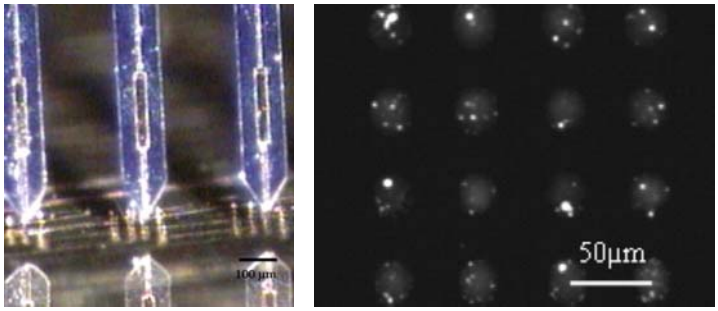

(a) (b)

[261] T. Leïchlé *et al., Sens. Act. Phys. A*132, 590 (2006)

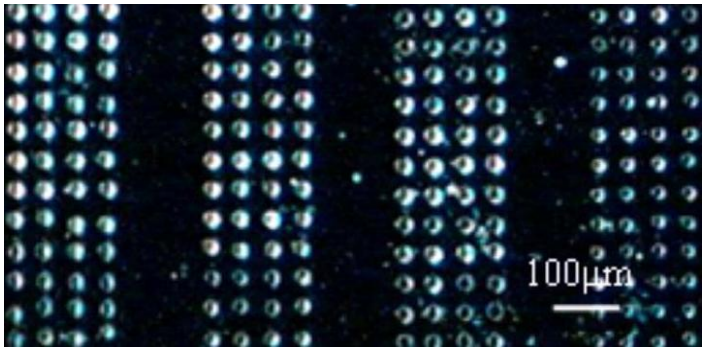

(c)

Figure 2.11: *(a)* Photograph of gold covered cantilevers while depositing; *(b)* Fluorescence image of DMSO-fluoresceine spots; *(c)* Picture of printed water-glycerol droplets matrices[88].

These results showed that electrowetting actuation is a promising solution for cantilever loading. However, the hydrolysis reactions occurring at the tip of the cantilever are to be avoided when using biological samples. Hence, a suitable insulating layer has to be selected to coat the metal electrodes. In this case, the actuation based on electrowetting on dielectric allows using conducting liquids with higher actuation voltages. Finally, a proper surface treatment has to be added to render the cantilevers surface hydrophobic with a low contact angle hysteresis. This is necessary to efficiently implement the electrowetting actuation scheme enabling the reversibility of the phenomenon[262]; and to keep the droplets size comparable to the depositing tip.

2.2.11.4 Local deposition of nanoparticles

Self-assembly is a very powerful way to create patterns onto a surface[88], but it needs to be associated with other techniques in order to precisely delimit the patterned areas. Bioplume is a tool perfectly suited for this purpose because it enables the local delivery of picoliter droplets. Particles or small entities dissolved in the spotted solution undergo self-organization during the drying of the drop, leaving a pattern within the deposition area. The use of self-assembly is of great interest for liquid-based patterning tools. Indeed, it provides means to nanostructure surfaces with micrometer size tips and to create patterns smaller than the minimum printed feature size. Moreover, the precise and reproducible size of the printed drops can be obtained by controlling the number of self-organized entities. In some cases, i.e. for solutions highly concentrated or deposited on hydrophobic surfaces, it is possible to create three-dimensional (3D) patterns. Finally, regarding the numerous entities used in self-assembly processes and their various physico-chemical properties, the capabilities of Bioplume are greatly enhanced in terms of the variety of materials and functions that can be deposited. In order to demonstrate the compatibility of Bioplume with self-assembly, we have carried out experiments focused solely on the deposition of nanoparticles.

Picoliter droplets of colloidal solution were deposited with Bioplume and studies of the particle self-assembly within the drops were carried out to provide methods for fabricating nanostructured well-defined spots with specific chemical functionalities. In a first attempt to demonstrate the possibility to print colloid spots, functionalized amorphous silica nanospheres were deposited on coated silicon surfaces[263]. The selection of SiO_2 beads was based on the possibility to saturate their surfaces with functional amino groups or antifouling polyethylene glycol derivatives. These aspects further support the idea of the use of nanoparticles as active parts of biomedical devices, such as biosensors and tissue engineering supports. Matrices of colloid spots ranging from 10 µm to 100 µm in diameter were successfully patterned. SEM characterizations of the nanoparticle geometry and spatial distribution within the spots revealed the colloid aggregation at the droplet rim and the selective

[262] H. J. J. Verheijen and M. W. J. Prins, *Langmuir* 15, 6616 (1999)
[263] T. Leïchlé *et al., Nanotechnology J.* 16, 525 (2005)

stability of the printed patterns. The polyethylene glycol SiO_2 nanoparticle-conjugates were used as masks during a selective reactive ion etching of the silicon substrate and silicon nanopillars were obtained.

Another set of experiments was then carried out to achieve the ordering, at a single particle level, of polystyrene nanobeads in hexagonal packing[264]. The surface wettability and the duration of the contact between the cantilevers and the substrate were used to control the printed area and thus the number of deposited particles. Well-defined nanobead microcrystals were successfully fabricated thanks to the adequate composition of the colloidal solution and the accurate control of the deposition parameters. Particularly, the self-assembly of perfect hexagonal features was obtained on polyallylamine surfaces (Figure 2.12).

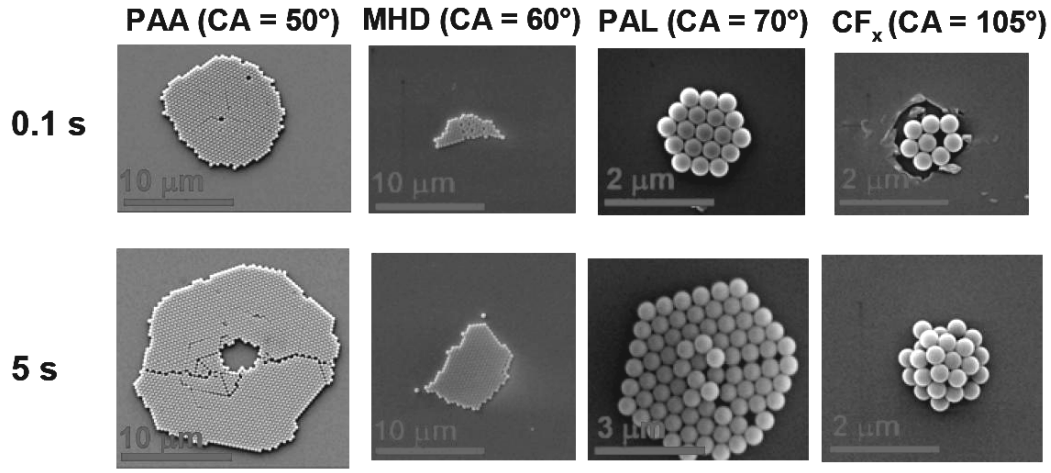

Figure 2.12: SEM pictures of the microspots of PS nanoparticles on the different substrates (polyacrylic acid (PAA), polyallylamine (PAL), fluorcarbon (CF_x) and mercaptohexadodecanoic acid (MHD)) for the minimum (0.1 s) and the maximum (5 s) contact time[88].

These structures can be of high interest in the field of photonics, since they are perfectly ordered structures with finite and tunable size. In general, this novel method of directly patterning particle during deposition opens a wide series of possible applications in the field of surface micro- and nanopatterning: printed nanobead crystals can be exploited as a mask for colloidal lithography processes with the possibility to create microarrays of nanostructured materials.

2.2.11.5 Electrospotting

Recently, we have demonstrated that Bioplume could be used as an electrospotting tool, combining spotting technology and electrical addressing via the physical localization of the electrodeposition process in a mobile electrochemical cell. To demonstrate the capability of the system, arrays of 20 µm diameter copper islands were firstly electrodeposited onto gold surfaces (Figure 2.13) using a commercial plating solution[265]. As predicted by Faraday's law, the copper bumps exhibited increasing heights as a result of longer deposition times. The electrochemistry implementation is thus an interesting added feature since it enables the fabrication of electroplated microstructures with controlled thicknesses. As a wide range of metals may be electrodeposited or etched using this technique (leading to metal bumps or holes, respectively) possible applications include the repair of microelectronic circuits, the fabrication of MEMSs, or the chemical and physical micropatterning of surfaces.

[264] A. Valsesia *et al., Small* 2, 1444 (2006)
[265] T. Leïchlé *et al., Appl. Phys. Lett.* 88, 254108 (2006)

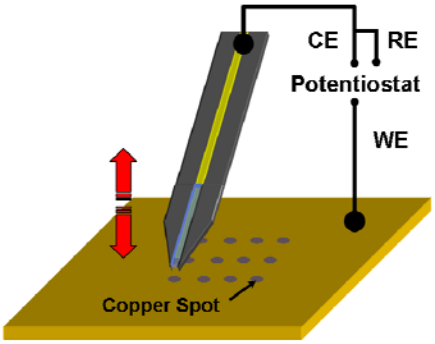

Figure 2.13: Schematic of the experimental setup[88].

The electrospotting principle was further used to structure surfaces with micrometer size ODN spots through electro-copolymerization of pyrrole and ODN bearing pyrrole monomers[266]. This method leads to the localized deposition of biologically active and mechanically stable polymer films and is very promising for the development of robust and uniform biochips. Fluorescence was observed after hybridizing fabricated spots with biotinylated complementary ODN, followed by a streptavidin-phycoerythrin revelation, thus proving the biological functionality of the polymer spots. Furthermore, in order to demonstrate the specificity of the coatings toward their DNA targets, we have designed a simple biochip with two different ODN probes. Specificity was demonstrated as no fluorescence signal was observed on the non specific spots. Finally, statistical operations were carried out on successively deposited droplets without any cantilever refill. The good reproducibility of the fluorescence signal provided by each spot highlights the reproducibility of the process and exemplifies the possibility to successively fabricate biochips without refilling the cantilevers. It is foreseen that electrospotting with Bioplume enables the rapid fabrication of biochips with a controlled probe density and ODN spots which conserve their specificity.

2.2.12 Conclusion

In this section the design, the fabrication and the characterizations of a liquid patterning tool, so-called Bioplume, have been presented; the tool is based on the use of an array of 12 silicon microcantilevers. Each cantilever enables the deposition of picoliter droplets thanks to a direct contact of the tip and the surface to pattern. The fabrication process of the cantilevers relies on conventional microfabrication techniques and silicon-on-insulator wafers. The cantilevers are 1.5 mm long, 120 µm wide and 5 µm thick. A fluidic channel is incorporated into each cantilever for liquid storage and delivery. The cantilever array is integrated into a closed-loop automated system enabling the control of the droplet homogeneity and the spatial positioning of the microarray. The automated system relies on the use of force sensors, i.e. piezoresistors, integrated into 4 of the 12 cantilevers of the array: 2 force sensing cantilevers placed on the side of the array are used for the adjustment of the trim, whereas 2 depositing cantilevers are used to control the deposition process. A dedicated electronics circuitry, based on a modified Wheatstone bridge, allows measuring the cantilever bending through the piezoresistance variations. The sensitivity of the piezoresistors is approximately 1 V/µm with an estimated noise value of less than 30 mV. These measurements result in a minimum detectable deflection of less than 30 nm. The depositing system comprises of the cantilever array silicon chip fixed on a four-degree-of-freedom automated spotter, the electronic circuit and a PC. The output of the electronics is connected to the PC so that the microsystem is in a closed-loop configuration: the

[266] E. Descamps *et al., Adv. Mat.* In press (2007)

bending of the cantilever occurring when touching a solid surface or a liquid droplet leads to the determination of contact points, which are then used to control the displacement of the array.

Preliminary experiments were conducted with this spotter to study the influence of the contact force and time during deposition on the size of the spots according to different surface wettabilities. We have observed that the drop size is not affected by the deposition force. However, as expected, the drop diameter increases with contact time, which can thus be used to control the size of printed features. When printing large areas of nonplanar samples, the misalignment and the contact height are expected to vary from one point to another. By using force sensing cantilevers in a closed-loop system, we ensure that the sample topography does not affect the consistency of the printed droplets. Furthermore, surface patterning that consists in a succession of liquid loading and deposition steps can be performed automatically by this system without the need of an external optical setup. Because it allows the precise control of the deposition parameters, the Bioplume system is particularly attractive for biological applications, i.e. biochip fabrication or biosensor functionalization. Indeed, the uniformity of the DNA or protein spots of biochip arrays is of importance to properly compare fluorescence signals from the different spots and thus to validate the results. Moreover, the functionalization of small and fragile MEMS-based sensors requires the precise delivery of droplets with a minimum force exerted on the surface. Experiments have thus been finally presented that demonstrate the ability of the Bioplume spotter to deposit functional biomolecules. These experiments proved that it is possible to address oligonucleotides with the same microcantilevers several times at the same location without contamination. Successful hybridization tests showed that biomolecules do not lose their biological properties after deposition. Compared to classical microarray protocols, volumes and time of assays were drastically reduced.

To further enhance the deposition potentials of the Bioplume system, in terms of the variety of deposited materials and 3D control of the printed patterns, mix and match approaches were then tested. We used the Bioplume direct liquid patterning system in combination with other deposition means: self-assembly and electro-assisted methods. The spotting system was employed to simply and directly create microspots of nanobeads without the need of a prepatterned surface. Picoliter droplets of colloidal solutions (functionalized silica and polystyrene nanobeads) were deposited onto surfaces exhibiting different wettabilities. The direct patterning of perfectly crystalline spots was achieved with polystyrene particles. By controlling the wettability of the surface to pattern and the contact time during deposition it was possible to tune the shape and the size of the spotted colloidal area. In a particular case it was possible to create microspots shaped like perfect hexagons.

Control of the deposition process using electro-assisted methods was also investigated by using the gold electrodes fabricated within the channel of each Bioplume cantilever. Drop size monitoring was achieved by using electrowetting during deposition. We demonstrated that droplets with a wide range of contact areas could be patterned onto highly hydrophobic surfaces by simply applying a voltage between the cantilever and the surface.

Finally, the Bioplume spotter was successfully used as an electrospotting tool, enabling electrochemical reactions to occur within the picoliter droplets. To prove the capability of the system, arrays of 20 μm diameter copper islands were firstly electrodeposited onto gold surfaces. As expected, the copper bumps exhibited increasing heights as a result of longer deposition times. The electrospotting principle was further used to structure surfaces with micrometer size ODN spots through electro-copolymerization of pyrrole and ODN bearing pyrrole monomers. The biological functionality of the polymer spots and the specificity of the films toward their DNA targets were successfully demonstrated.

In conclusion, the Bioplume patterning tool has reached an interesting maturity state in terms of versatility of printed materials and control over the deposition process. This patterning tool is foreseen to be of interest for fundamental research and applications in various technological fields because of its simplicity, ease-of-use and cost. The overall characteristics, provided in Table 2.1, can be used as comparison means regarding the more mature liquid-based patterning techniques, ink-jet and dip-pen.

Tool	Ink-jet	***Bioplume***	Dip-pen
Type	Non-contact	*Contact*	Contact
Environment	Atmospheric conditions	*Atmospheric conditions*	High humidity
Resolution - Range **Volume**	>20 µm → >100 µm 10 pL	*<10 µm → 100 µm* *<1 pL*	15 nm → 100 nm X
Deposited Area	Very large (>10 cm²)	*Large* *(>1 cm²)*	Very small (≈ mm^2)
Deposition rate	<1000 drops/s	*>10 drops/s*	Very low
Volume available	Very large (> 1 µL)	*30 pL on each cantilever* *≈ µL via the loading chip*	X
Materials	Biological solutions Polymers Particles Cells	*Biological solutions* *Polymers* *Metals* *Particles*	SAMs Biological entities Particles
Substrates	No restriction	*Flat surface*	Very flat surface
Controls	Volume ejected	*Force*	Force
In-situ characterization	X	*X*	AFM
Pros	- Mature technology - Available on the market - Parallel - Inexpensive - Simple	- *Parallel* - *Inexpensive* - *Simple* - *Disposable* - *Electrochemistry* - *Electrowetting*	- Mature technology - Available on the market - Parallel - Electrochemistry
Cons	- Accuracy - Difficult alignment - Limited viscosities	- *High-boiling point solvent required*	- Very slow

Table 2.1: Table providing the characteristics of the Bioplume system. The characteristics of the two mature technologies available on the market (ink-jet and dip-pen) and designed to pattern surfaces at different scales are given, as a comparison means[88].

2.3.1 Previous work

Silicon-based devices microfabrication and related micromechanics were the primary *raisons d'être* of my PhD thesis since the beginning, in 1997. Microcantilevers and microbridges fabricated in the LAAS' former cleanroom were the main "test vehicles" that allowed me to interestingly validate analytical mechanical models related to static and dynamic behaviour at the microscale[267-269].

Consequently, together with my PhD adviser, we both started to be interested in exploiting the dependence of the dynamic response of various microstructures on the surrounding medium characteristics. The microviscosimeter we developed[270] starting from the relation between the quality factor of a microcantilever in liquid and the physical properties (viscosity, density) of the latter, revealed the limits of the way we measured the oscillations of the devices at that time. We did it using the optical deflection method (previously explained in sub-section 2.2.3.1) which was convenient as far as the surrounding medium was transparent but became obsolete when dealing with opaque liquids or non-reflective surface state of the microcantilever. These limitations encouraged our quest for integrated detection schemes based on integration of materials exhibiting piezoelectric or piezoresistive properties.

A fruitful collaboration with a research team working on the elaboration of piezoelectric thin films (led by Prof. D Remiens) from University of Valenciennes, has been initiated in 1998 and the first PZT layers have been deposited and characterized onto freestanding silicon dioxide cantilevers one year later[271]. This was the starting point of an extraordinary (scientific and human) adventure that still continues today. Things have rapidly evolved with M. Guirardel's PhD thesis where successful integration of PZT films onto freestanding membranes with various geometries as well as static and dynamic actuation in air and liquid media (due to the converse piezoelectric effect) were demonstrated[272].

Based on Guirardel's early technological developments, I decided to continue exploring the piezoelectric-based MEMS area first by validating the piezoelectric effect onto silicon-based microfabricated membranes integrating PZT thin films, then by demonstrating multiplexed piezoelectric actuation and detection on chip and finally by moving forward with piezoMEMS for biological and chemical applications. Before giving a rapid survey of my research activity in the bioMEMS area following the previously indicated streamline, it has to be noted that working on piezoelectric membranes allowed me to come back from time to time to pure analytical models elaboration and their experimental validation, as introduced in the next subsection.

2.3.2 Motivation for continuing this work

As widely emphasized in the previous chapter, biological sensing systems represent nowadays a fast-growing field of research guided by continuously evolving issues as various as the wide range of applications they address, going from common pathologies diagnosis to environmental or biological warfare agents detection. Despite their different targets, the same basic principle is applied to any biosensor: a biorecognition molecule is immobilised over a signal transducer to give a reagentless analytical device. The biorecognition molecule, such as an enzyme, antibody, sequence of DNA, peptide or even a microorganism, provides the biosensor with its selectivity for the target analyte

---

[267-269] L. Nicu and C. Bergaud, *J. Appl. Phys.* 86, 5835 (1999); [268] L. Nicu *et al., J. Micromech. Microeng.* 9, 414 (1999) ; [269] C. Bergaud *et al., Jpn. J. Appl. Phys.* 38, 6521 (1999)
[270] C. Bergaud and L. Nicu, *Rev. Sci. Instrum.* 71, 2487 (2000)
[271] E. Cattan *et al., Sens. Act. Phys. A*74, 60 (1999)
[272] M. Guirardel, *PhD Thesis*, University Paul Sabatier, Toulouse, France (2003)

while the signal transducer determines the extent of the biorecognition event and converts it into an electronic signal, which can be outputted to the end user.

Among the common transducers developed up to now, the bioMEMS seem very promising to meet most of the critical requirements for such specific applications, like the high level of integration for portability purposes, rapid responses, high sensitivity, high signal-to-noise ratio etc. In this class of micro-transducers, silicon-based microcantilevers are the most widespread and proven micromachined biosensors allowing successful characterization of biomolecular systems in their natural aqueous environment[273-275]. When used in mass-sensing configuration, the adsorption of molecules on the surface of a cantilever changes the total mass and, consequently, the resonance frequency of the cantilever.

At this point, it is worth noting that the minimum detectable mass (meaning the smallest amount of target analyte to be detected) is directly dependent on the minimum detectable resonance frequency change, this latter parameter being linked to the quality factor Q of the resonator. In other words, the higher the Q-factor, the better the resolution of the biosensor. When considering that the Q-factor is a measure of the "sharpness" of the resonance peak (thus related to energy loss due to damping) it becomes evidence that getting high quality factors in liquid media (specific to biological applications) is one of the most important challenges in the cantilever-based biosensing field.

Until not long ago, Q-factors measured when operating microcantilevers in liquids rarely exceeded 10[270,276]. Several methods have been employed to "artificially" increase this parameter either by feeding back the output signal of the cantilever to the excitation scheme (a.k.a Q-control method)[277], by operating the cantilever on a higher harmonic[278] or by integrating the excitation in the cantilever's structure in order to achieve better actuation efficiency. Even if the first solution cited before allows an improvement of the Q-factor by up to three orders of magnitude, the major drawback is the addition of complementary electronics (phase shifters and gain controlled amplifiers) in the measurement chain. Using higher harmonics thus taking advantage of higher Q-factors is also an elegant method but unfortunately too much dependent on frequency instabilities and modal cross-talk.

It remains that the use of an integrated dual excitation-detection scheme (either capacitive or piezoelectric) could be the paved way to obtain higher Q-factors thus avoiding the disadvantages of the methods cited before. If the capacitive excitation is still challenging to adapt for actuation and detection in liquid media[279], the use of piezoelectric thin films (around 1-µm thick) integrated in the resonator's structure have shown promising capabilities in this field since the Itoh et al.[280] pioneering work (although the Q-factor in this latter case was not higher than 8…). More recently, arguing that the forces developed by piezoelectric thin-films are too small to overcome the high effective mass and viscous environment of the liquid, Park et al.[281] proposed the integration of $Pb(Zr_xTi_{1-x})O_3$ (PZT) thick-films (22-µm thick) in a Si-based cantilever structure thus demonstrating strong harmonic oscillations with Q-factors of about 23 in water.

Although not exhaustive, the aforementioned examples make evident that the cantilevered microscopic structure is **not intrinsically adapted** to dynamic high-resolution measurements in liquid media because too sensitive to the viscosity of the fluids in which it is immersed, let alone the brittleness of such a microstructure. This originated the need for alternative designs so as to come out with more adapted microstructures to the constraints specific to measurements in liquid media.

[273-275] J. K. Gimzewski *et al., Chem. Phys. Lett.* 217, 589 (1994) ; [274] R. Berger *et al., Microelectr. Eng.* 35, 373 (1997) ; [275] G. Abadal *et al., Nanotech. J.* 12, 100 (2001)
[276] S. Boskovic *et al., J. Rheol.* 46, 891 (2002)
[277] J. Tamayo *et al., Ultramicroscopy* 86, 167 (2001)
[278] M. K. Ghatkesar *et al., Proc. of the 3rd IEEE Conf. on Sens.* 24-27 Oct., Viena, Austria 1060 (2004)
[279] B. Legrand *et al., Appl. Phys. Lett.* 88, 034105 (2006)
[280] T. Itoh *et al., Proc. Of the Int. Conf. Solid-State Sens. Act. (Transducers '97)* 16-19 June, Chicago, USA 459 (1997)
[281] J. H. Park *et al., Adv. Funct. Mater.* 15, 2021 (2005)

Therefore, the aim of this part of my research work is to demonstrate that the use of micromachined circular piezoelectric membranes could be a potential alternative to the cantilevers for biological applications. Although it was extensively shown in the past that this design is well adapted to applications in liquid media (like the piezoelectric micromachined ultrasonic transducers, a.k.a. PMUTs[282]), only few examples make use of it as a potential biosensor[283,284]. However, as it will be shown further in this section, high quality factors (up to 200) of micromachined piezoelectric membranes resonating in various liquid mixtures (water/glycerol and water/ethanol) are easily achievable thus demonstrating that the variation of the liquid viscosity (if its absolute value remains lower than 10cP) has little, if no, effect on the dynamic behaviour of the devices. The latter result is of crucial importance for most of liquid biological samples with viscosity values rarely exceeding the value given above. For comparison purpose, blood viscosity at normal hematocrit (volume of blood occupied by red blood cells) rate of 40 is about 3 cP while plasma viscosity (blood from which red cells, white cells and platelets were retired) is about 1.5 cP[285].

Before gaining more insight into why using piezoelectric micromembranes in liquid media could be a suitable solution to biosensing at the microscale, several important results related to the micromechanics of such devices in air are worth to be previously discussed.

2.3.3 Introduction to multilayered piezoelectric micromembranes[286]

In most of cases, the membrane is a stack of several thin films (including the piezoelectric one) with corresponding functions (generally a silicon substrate for the elastic foundation of the device, dielectrics – quite often silicon dioxide, for isolating the metallic layers from the silicon substrate, metals – standing either as electrodes for electrical activation of the piezoelectric material or active layer for biological grafting etc.). It is well known that by stacking thin films on a membrane-like structure, if the resultant stress of the layers is compressive, one visible effect on the equilibrium position of the structure is a non-null out-of-plane initial static deflection (also known as buckling effect) that could dramatically affect the mechanical (and consequently, electrical) properties of the in-between piezoelectric film. It becomes thus of primary interest to theoretically and experimentally investigate the influence of the forced out-of-plane buckled equilibrium position of a membrane-like multilayer structure on the piezoelectric coefficients of an in-between piezoelectric layer.

For this to be done, an analytical model for bilayered circular membranes initially elaborated by Wang *et al.*[287] has been extrapolated to multilayered pre-stressed membranes. In this particular case, the input parameters were geometrical as well as material constants (Young's moduli, Poisson's ratios, in-plane stresses) and the expected output was the static profile of the membrane. Moreover, the so-adapted analytical model allowed, when taking into account an applied electric field across the piezoelectric layer, determining the piezoelectric coefficient d_{31} that represents the induced in-plane strain per unit electric field applied perpendicularly to the film plane using measured static profiles of membranes under different values of applied voltage. The main results were recently published[288], only the most important ones are considered hereafter.

As the fabrication process of the micromembranes is common to all following experiments in this chapter, it is worth to consider it at once. 4x4 matrices of piezoelectric micromembranes are

---

[282] P. Muralt *et al., IEEE Trans. Ultrason. Ferroelectr. Freq. Control* 52, 2276 (2005)
[283,284] M. Guirardel *et al., Jpn. J. Appl. Phys. Lett.*43, L111 (2004) ; Y. Xin *et al., Appl. Phys. Lett.* 89, 223508 (2006)
[285] A. C. Guyton and J. E. Hall, *Textbook of Medical Physiology, 10th ed.*, W. B. Saunders, Philadelphia, USA (2000)
[286] For the major part of results (some being still unpublished) presented from now and to the end of the second chapter I am indebted to my student, Cédric Ayela, who labored beyond the call of duty to make this happen.
[287] G. Wang *et al., Proc. ASME Int'l Mech. Eng. Congress and Expo. (IMECE'02), MEMS and Nanotechnology Symp.*, New Orleans, LA, Nov. (2002)
[288] C. Ayela, L. Nicu *et al., J. Appl. Phys.*100, 054908 (2006)

fabricated by standard micromachining techniques. Membranes are circular shaped with a total radius of 200 µm. Each micromembrane can be individually actuated through a $PbZr_xTi_{1-x}O_3$ (PZT) thin film. This active part is circular shaped with a radius of 75 µm.

The main steps of fabrication process are depicted in Figure 2.14.

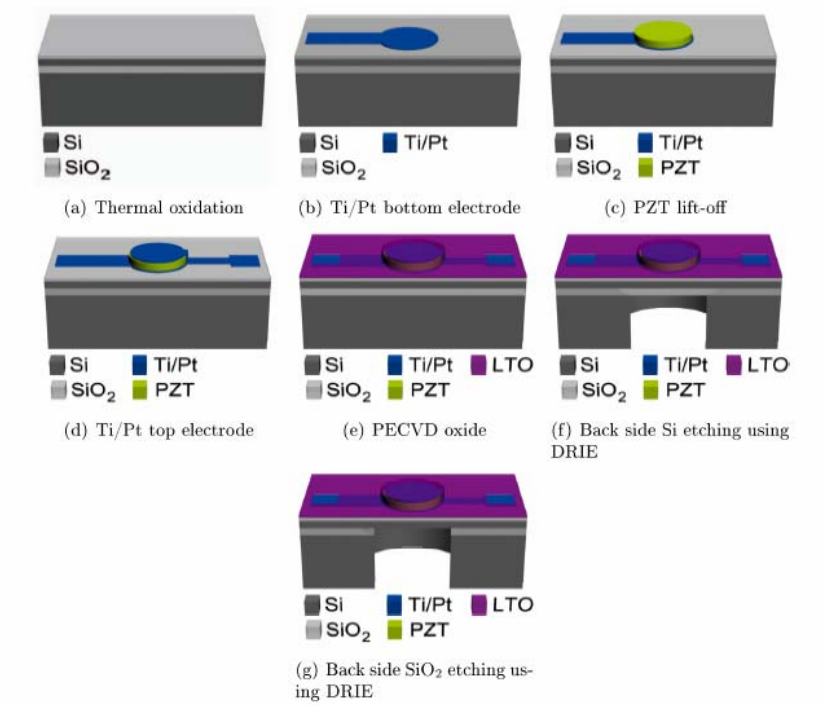

Figure 2.14: Fabrication steps of piezoelectric circular micromembranes

The starting substrate is a 100 mm, <100>, N-type Silicon-On-Insulator (SOI) wafer, with a 1 µm thick buried oxide and a 2 µm thick top silicon layer (resistivity of 7 Ω.cm). The first step consists of growing 50 nm thick thermal oxide on the entire SOI wafer before the sputtering of Pt/TiO_2 (150 nm/ 10 nm) for the bottom electrode. The film is lifted-off with a Shipley 1818 photoresist to define circular electrodes with a radius of 75 µm. The 950 nm thick 46/54 $PbZr_xTi_{1-x}O_3$ film is then deposited by RF magnetron sputtering. The 46/54 composition choice is due to its proximity with the morphotropic phase boundary composition (x=53), which has the largest piezoelectric and dielectric constants[289]. In most studies, PZT films are deposited at 650 °C. Instead, the PZT film is deposited here without intentional substrate heating to allow patterning by lift-off of the PZT film with the Shipley 1818 photoresist. This PZT layer is circular shaped with a radius 5 µm higher than electrode layers to avoid eventual shortcuts between the top and bottom metallic electrodes. Deposited films are therefore amorphous since temperature rise during deposition does not exceed 150 °C. After resist stripping, a 30 min crystallization annealing at 625 °C is performed. Then, another deposit followed by a lift-off is processed with Ti/Pt (10 nm/ 140 nm) for top circular electrodes with the same radius as bottom electrode. A passivation silicon oxide film (200 nm) is deposited by Plasma Enhanced Chemical Vapor Deposition (PECVD). Contact pads are then opened by a wet oxide etching using HF buffer. To finish, the circular membranes (with a total radius of 200 µm) are defined by vertical sidewalls etching on the backside of the SOI wafer using the Deep Reactive Ion etching technique. The 1 µm thick SiO_2 acts as an etch stop layer for the dry silicon etching. This layer is then removed using another Reactive Ion etching process.

Typical three-dimensional (3D) profile of such microdevices obtained using a Zoomsurf 3D© (Fogale Nanotech, Nîmes, France) dual-beam interferometer, is shown in Figure 2.15:

[289] J. Dolbow and M. Gosz, *Mech. Mater.* 23, 311 (1996)

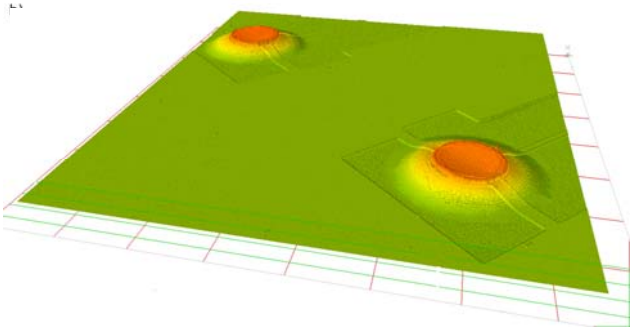

Figure 2.15: Typical 3D profile of micromembranes with R_1 = 75 µm and R_2= 200 µm obtained using a Fogale© interferometer

Measurements are made in static mode with the tungsten-halogen white source of the aforementioned interferometer because of the large deflection values of the devices. Displacement of the microstructure is directly measured by applying a static potential in range of -18 V to +18 V between top and bottom platinum electrodes. The induced electric field in the PZT thin film along the Z-axis changed deflection of the structure due to the reverse piezoelectric effect.

After poling the PZT thin film at 18 V for 15 minutes, DC voltage is changed from +18 V to -18 V in both ways with a step of 1 V. Measurements are made 1 min after changing the value of the DC bias. This time value is calibrated taking into account stabilization of structure for the new DC bias under influence of the remanant piezoelectricity. After measurement, microstructures are kept under DC value until equilibrium state is reached. Figure 2.16 shows an example of the deflection curve. It corresponds to the deflection at the center of the structure for R_1 = 75 µm and R_2 = 200 µm (where the thickness of top electrode, PZT and bottom electrode stack is subtracted) and shows a large displacement histeresys with two maximum peaks: -4 and +5V.

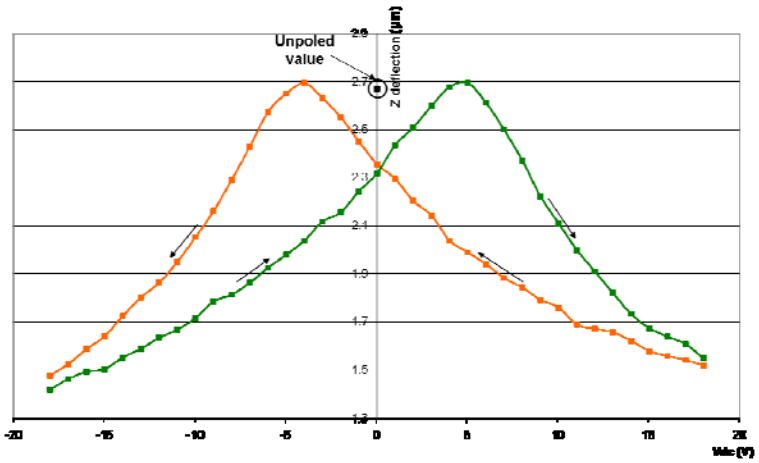

Figure 2.16: Influence of DC voltage on micromembranes' vertical deflection

These values are close to the coercive field[290] for PZT 54/46 thin films and deflection for these values is close to the deflection of unpoled membrane. The difference is due to initial internal polarization inducing a small variation of deflection of unpoled membrane. The close deflections indicate that after domains were well oriented in high potential values, changes in their orientation for lower values occur and induce strain relaxation of the PZT thin film until a maximum value of deflection that corresponds to the same behavior as the one for unpoled film, which is the zero piezoelectric strain point.

[290] E. Cattan *et al., J. Appl. Phys.* 86, 7017 (1999)

Coupling the analytical model previously introduced with measurements of vertical deflection of micromembranes allows determining the piezoelectric coefficient d_{31} values as a function of the voltage applied to the piezoelectric film (Figure 2.17).

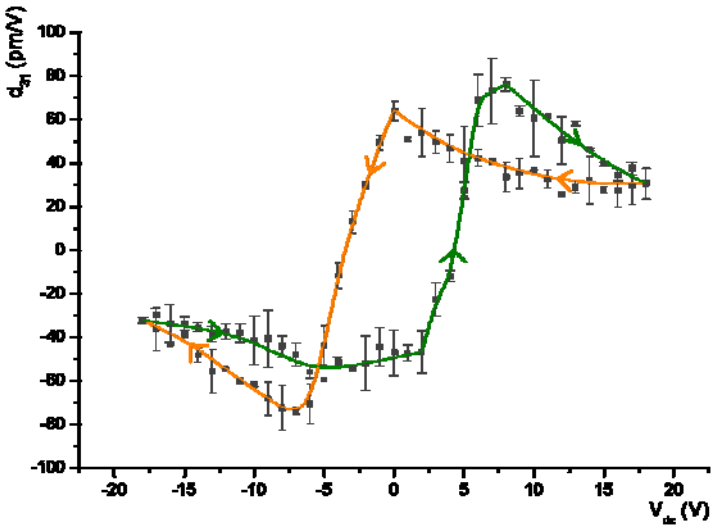

Figure 2.17: Influence of DC voltage on the piezoelectric constant d_{31} of PZT 54/46 thin film integrated onto microfabricated membranes

$|d_{31}|$ shows a strong dependence on applied voltage with large variations from 30 pm/V for ± 20V to 75 pm/V around ± 8V, depending on how the electrical potential is applied. So, large variations of d_{31} might be due to the off-axis motion of domains (such as reorientation of 90° domains) superimposed to the lattice motion. These results are in good agreement with literature[290,291]. It also should be noted that the d_{31} value is 0 pm/V when V_{dc} is close to ± 4V which corresponds to the coercive field value. These results are in good agreement with maximum of deflection that corresponds to the zero piezoelectric strain, as d_{31} represents the proportional constant of the piezoelectric strain generated by the transverse electric field.

Thorough understanding of piezoelectric micromembranes' mechanical and electrical behavior in air allowed undertaking similar investigations in liquid media; some key results are summarized in the next subsection.

2.3.4 Piezoelectric micromembranes in Newtonian liquid media

The dynamic behaviour of previously described piezoelectric micromembranes was studied in different liquid media (with viscosities ranging from 1cP to more than 150cP) aiming to demonstrate whether this microsensor configuration may be suited for biosensing application[200].

2.3.4.1 Experimental set-up

The experimental set-up consists of a flow-through cell, a peristaltic pump and a fluidic circuitry (capillary tubes, adaptive ports, etc.). The flow-through cell (shown in Figure 2.18) is made of two parts: a top one, made of transparent Plexiglas™ and a bottom one, in aluminium. The top part of the cell was drilled in a depth of 3mm so it fitted exactly on top of the TO8 package. Four plastic screws are holding together the two parts of the fluidic cell and the TO8 package that is placed in-between. The final volume of the cell is estimated at about 220µL. Two capillary tubes (255/510 µm, Capillary Peek Tubing, Upchurch Scivex) are connected through Nanoport® assemblies (Upchurch Scivex) to

[291] M.-A. Dubois and P. Muralt, *Sens. Act. A*77, 5810 (1999)

the flow-through cell inlet and outlet (1-mm diameter). This set-up allows to the liquid to continuously stream across the piezoelectric membranes with a constant velocity fixed by the peristaltic pump (Masterflex, 1 to 4 mL/h flow rate).

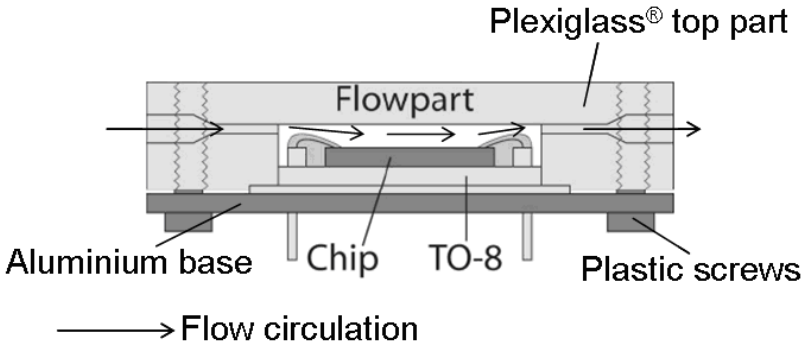

Figure 2.18: Schematics of the flow-through cell (not to scale). The top part is fabricated in Plexiglas™, the base in aluminium and the TO8 package of the piezoelectric membranes matrix is held together with the fluidic cell parts with four plastic screws.

Two resonant frequency measurement configurations in liquid are set up: first, liquid is continuously flown onto the membranes in the fluidic cell at a constant flow rate of 4mL/h (called "in-flow experiments") and the resonant frequency is continuously measured. Second, drops of 5µL (with a drop radius of 1.4mm for a measured contact angle of 80°) are deposited onto individual membranes using conventional volumetric pipette and the resonant frequency is measured while the membrane is oscillated into the liquid spot (called "in-spot experiments").

Two distinct families of newtonian fluids with known densities and viscosities are chosen for the experiments, i.e. water/ethanol and water/glycerol which variations of density and viscosity with respect to the proportion of water in the global mixture are radically different. In case of water/glycerol mixture the density and the viscosity values are increasing with the diminution of water proportion in the mixture (with an abrupt rise of the viscosity starting with 60% of glycerol solution). On the contrary, in case of water/ethanol mixture, the density is decreasing with the diminution of water proportion in the mixture while the viscosity is describing a bell-like curve with extrema values between 1cP and 2.5cP[200].

Resonant frequencies of the piezoelectric membranes are determined by performing admittance measurement using a HP4294A Impedance Analyzer from Agilent after poling the PZT film at E = -187 kV/cm (representing 2.5 times the PZT coercive field value) during 20 minutes and using an excitation AC signal of 100 mV in air and 500 mV in liquid. Before plugging the TO8 package to the testing board, an open circuit and short circuit compensations are done in order to avoid parasitic capacitances due to the connections and the testing set-up.

2.3.4.2 Lamb's model

It is a well known fact that as an elastic membrane vibrates in a fluid, the fluid immediately surrounding the vibrating structure is set into motion and thus imposes both added mass and damping forces on the membrane. The added mass lowers the natural frequency of the membrane compared to the one measured in air while the damping of the membrane is increased. H. Lamb proposed in 1920 a theoretical model[292] that allows to estimate the shift of the resonant frequency (from vacuum to water, the latter satisfying the assumption of an incompressible liquid) of a thin circular plate filling an aperture in a plane (and rigid) wall which is in contact on one side with an unlimited mass of water.

Starting with an assumed vibration shape of the membrane as follows:

[292] H. Lamb, *Proc. Roy. Soc. Lond. A*98, 205 (1920)

$$w(r,t) = C(t)\left(1-\frac{r^2}{R^2}\right)^2 \tag{2.5}$$

where *w(r,t)* is the normal displacement of the membrane at a distance *r* from the centre, *R* is the membrane radius and *C(t)* is a function of *t* only, H. Lamb calculated the kinetic and potential energies of the plate (in vacuum) as being:

$$\begin{aligned} T_{vac} &= \frac{\pi\rho_p hR^2}{10}\left(\frac{dC}{dt}\right)^2 \\ V_{vac} &= \frac{8\pi Eh^3}{9(1-\mu)R^2} \end{aligned} \tag{2.6}$$

where ρ_p is the plate density, *h* is the plate thickness, *E* is the value of Young's modulus for the plate material and μ Poisson's ratio.

In this model, the kinetic energy T_L of the liquid is then calculated and given by:

$$T_L = 0.21\cdot\rho_L\cdot R^3\cdot\left(\frac{dC}{dt}\right)^2 \tag{2.7}$$

where ρ_L is the liquid density.

Adding T_L to the kinetic energy of the vibrating membrane and applying the Rayleigh-Ritz method (that allows to calculate the resonant frequency of a multi degree of freedom system as a function of the ratio between the maximum values of the potential and the kinetic energies when assuming a known mode shape of vibration) provides an additional factor for the calculation of the resonant frequency in liquid:

$$f_L = \frac{f_{vac}}{\sqrt{1+\beta}} \tag{2.8},$$

where β, usually called added virtual mass incremental (AVMI) factor, is equal to:

$$\beta = 0.67\cdot\frac{\rho_L R}{\rho_M h} \tag{2.9},$$

with ρ_M and *h* respectively the density and the thickness of the membrane.

At this point, several fundamentals must be outlined: first, Lamb's model does not take into account the viscosity of the liquid medium. One of the main goals here is to prove that this hypothesis is verified if and only if the viscosity value does not exceed around 10cP. Second, as the piezoelectric membranes for experimental validation are multilayered structures (each film of the global stack being subject to internal mechanical stresses), the calculus of the resonant frequency in vacuum is somehow complex and beyond of the scope of this work. Moreover, consider that resonant frequencies in vacuum and in air are identical[293]. This is the reason why f_{vac} values are implemented in the model from resonant frequency measurements performed in the air. Lastly, Lamb's model also assumes that the membrane's structure is an isotropic monolayer (that is far from the structures tested in here).

2.3.4.3 Main results

Experiments focus both on measurement of resonant frequency and quality factor of different piezoelectric membranes while varying the viscosity and density of the liquids the devices are oscillating in. Comparison with Lamb's model predictions and interpretation of results allows

[293] R. D. Blevins, *Formulas for Natural Frequency and Mode Shape*, Van Nostrand Reinhold Company, New York, USA (1979)

unveiling high interest in using such a design of microfabricated structures for biosensing applications, as summarized below.

In case of resonant frequency, in-flow experiments are first performed in water/glycerol different mixtures obtained by progressively increasing the proportion of glycerol. Prior to this, solutions viscosities are measured using a commercial AR-G2 rheometer from TA Instruments. The same procedure is applied in case of water/ethanol studied mixtures. Resonant frequency shifts (from pure water to solutions of water/glycerol and water/ethanol, respectively) with respect to the solutions viscosities are represented in Figure 2.19.

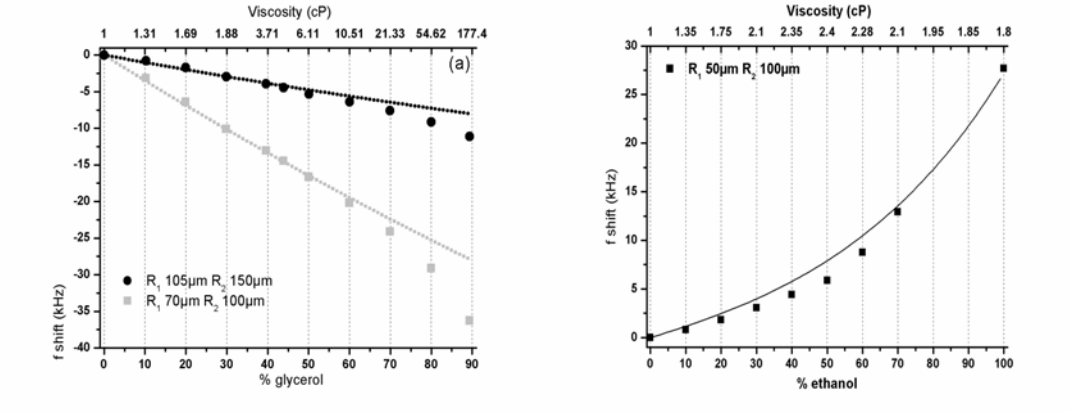

(a) (b)

Figure 2.19: (a) Resonant frequencies shift as a function of glycerol content for two piezoelectric membrane designs ; (b) Resonant frequency shift as a function of ethanol content for a piezoelectric membrane (R_2 = 100µm, R_1/R_2 = 0.5). Symbols stand for experimental values while line stands for theoretical data.

The experimental data are well fitting with Lamb's model (continuous line on the graph) until a certain limit that is established around 60% of glycerol in the water/glycerol solution (that is corresponding to a viscosity of 10cP[200]). It should also be pointed out that in the solution containing 80% of glycerol, the resonant frequency is difficult to detect meaning that for solutions with viscosity values higher than 175cP the piezoelectric membranes specifically designed in this work are reaching their detection limit. In addition, note that the resonant frequency is linearly decreasing with the increase of the glycerol proportion as the density of the solution is increasing (and so does the AVMI factor). This is mainly explained by the slight and linear variations of the AVMI factor with the quantity of glycerol yielded, after trivial variable change, by the Taylor expansion of eq 2.8. The first order of the development gives close values compared to the exact function, inducing a linear shift of the resonant frequency with the quantity of glycerol, as shown on Figure 2.19(a). In case of water/ethanol experiments (Figure 2.19(b)), these results are confirming those previously obtained using water/glycerol solutions in that sense that Lamb's model is rigorously verified in case of water/ethanol solutions which viscosities does not exceed 3 cP. In this case, the resonant frequency is varying increasingly with the amount of ethanol thus confirming the fact that the density of the liquid is decreasing at the same time.

Keeping in mind the damping effect investigation initial goal, Q-factor measurements simultaneously are performed either in water/ethanol of water/glycerol in-flow experiments[200] and values are higher than 50 (so far as the viscosity remain below reasonable value, about 10cP) that is one order of magnitude higher than the Q-factors of most of state-of-the art miromachined cantilevers used for applications in liquid media. Even more interesting, in-spot Q-factor measurements in water/glycerol exhibit values more than two-fold the ones corresponding to in-flow measurements for low viscosities. An eventual interpretation for the high Q-factor value in the in-spot configuration comes from the acoustics theory. When comparing the wavelength of the sound in the liquid to the

diameter of the piezoelectric membrane, it appears that in this regime the liquid is mostly reactive meaning that the virtual added mass effects are predominant (compared to the energy loss due to the viscous damping)[294]. Moreover, the compressibility of the interface liquid-air allows the piezoelectric membrane to "freely" oscillate in the liquid drop. On the contrary, in the case of the in-flow configuration, the Q-factor is initially limited (equal to 60) by liquid trapped between the silicon substrate and the rigid wall of the Plexiglass™ fluidic cell. For both configurations, the Q-factors values are decreasing towards the same low values (about 20) as the proportion of glycerol is progressively increased (starting with 60%) in the liquid solution meaning that for high viscosity values the in-spot configuration is no more sufficient to get a higher Q-factor.

To conclude, a last experiment is realized using the in-flow configuration: the experimental conditions are identical to the previous ones; the unique difference consisted in *intentionally trapping air bubbles in the fluidic cell* (by rapidly reversing the flowing direction of the liquid with the peristaltic pump) near the membranes chip. Q-factors measurements are performed and the results are plotted in Figure 2.20:

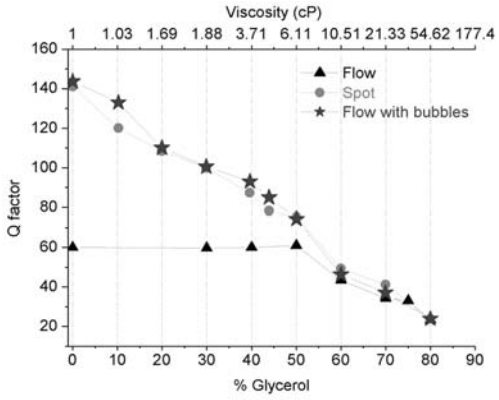

Figure 2.20: In-spot, in-flow and in-flow with air bubbles measured quality factors of a piezoelectric membrane (R_2 = 100µm, R_1/R_2 = 0.5) versus glycerol proportion in aqueous solutions.

Obviously, the Q-factors values of the in-flow configuration (with air bubbles trapped in the fluidic cell) are perfectly matching the in-spot data meaning that the high Q-factors values specific to the latter configuration could be recovered if air bubbles were trapped in a reproducible way in the fluidic cell (though far enough from the active device). This could represent an ideal configuration for biosensing applications where two major requirements have to be imperatively met: continuous flow of the analyte on the surface of the biosensor (in order to permanently refresh the target species and to avoid rebinding phenomena) and high-resolution measurements (realistic only if high Q-factors values are attainable in a liquid medium dynamic measurement configuration).

2.3.5 Completing the MEMS: associated electronics

One fundamental building block of the MEMS paradigm deals with associated electronics; though not enough emphasized so far in the present manuscript, it becomes hardly defendable to be part of the MEMS community without being concerned to same extent by the core microstructure AND the associated electronics. That is the reason why solving this issue (with the precious help of electronics engineers belonging to the LAAS' Instrumentation Service) represented, as in Bioplume's case, an important challenge on the way to the final achievement of the bioMEMS described inhere.

It is worth noting that the large-scale integration of microelectromechanical sensors is mainly depending on both the dimensions shrinking of the active mechanical elements and the integration of the excitation and the detection functions. If the first issue has been widely addressed by the technological evolutions in the past four decades, addressing MEMS matrices in parallel using

[294] D. T. Blackstock, *Fundamentals of Physical Acoustics,* Wiley Interscience Publications, USA (2000)

dedicated nearby electronic is still a great challenge. In this field, two schemes that allow addressing excitation and detection functions by the same physical phenomenon demonstrated superior potential with respect to the other ones: the capacitive and the piezoelectric effects, the work presented here dealing with the latter one. Since the pioneering Lee et al's works[295] on the atomic force microscope cantilevers integrating piezoelectric active layers, almost all the applications presented so far in this field used the same detection scheme: either a dummy cantilever (used as reference) close to the active one[295] or a passive components-based circuit used as reference branch[296]. Both schemes have the same role, i.e. cancelling of the current corresponding to the static capacitance of the piezoelectric layer, the main drawback of this method being the hopelessness to perfectly match the reference circuit with the active element.

2.3.5.1 The concept

Based on previous mechanoelectrical characterization, an innovative concept to perfectly compensate the static capacitance of piezoelectric micromembranes is proposed. Combining analogue and digital hardware elements with specific software treatment, this system enables the parallel excitation and detection of the resonant frequencies (and the quality factors) of piezoelectric silicon-based micromembranes integrated on the same chip. On the hardware level, two Digital Signal Synthesizers (DDS) generate the excitation of the membrane and the dynamic reference, and a third one completes the synchronous detection. A field-programmable gate array (FPGA) controls the electronic and the USB link to a PC. Specific developed software enables to characterize the intrinsic membranes electrical response and to automatically compute the compensation parameters in order to extract the resonant frequency and the quality factor by monitoring these values for up to eight membranes in parallel[297].

Figure 2.21(a) represents the frequency spectrum of one micromembrane measured without using the dynamic compensation. Concretely, the first automatic calibration step determines values of gain and phase (for each frequency around the resonant frequency) generating the function for the appropriate dynamic compensation of the static capacitance, as shown on Figure 2.21(b). It has to be noted that one limiting factor (due to fitting algorithm) makes the compensation being valid for a frequency bandwidth of 100 kHz around the resonant frequency which remains however sufficiently wider than the useful bandwidth for a complete spectrum (as shown on Figure 2.21(b)).

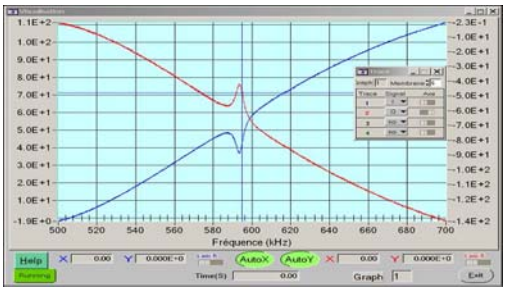

X.a)

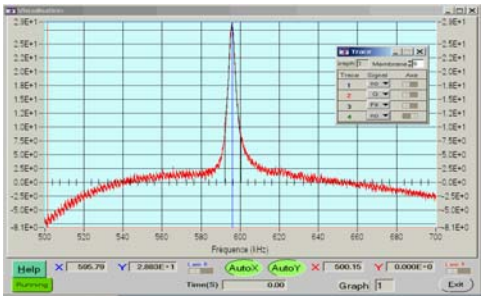

X.b)

Figure 2.21: Admittance curves of 100 microns diameter membrane at 0.1V AC voltage excitation level as measured by means of the proposed electronics *a)* without compensation, *b)* with dynamic compensation of the static capacitance.

[295] C. Lee *et al.*, *Sens. Act. A*72, 179 (1999)
[296] J. D. Adams *et al., Sens. Act. A*121, 262 (2005)
[297] D. Lagrange *et al., 2006 IEEE of Sensors Conference*, Daegu, South Korea, October, 22-26 (2006)

2.3.5.2 Mass sensitivity

Frequency spectra and the resulting calculations of the resonant frequency and quality factor yielded real-time monitoring for multiplexed use for up to eight membranes. Figure 2.22 shows the real-time monitoring of the resonant frequency shift and the quality factor on six membranes. The electronic design induced a frequency measurement stability of less than 1ppm allowing a precise monitoring. Signal variations in time are essentially due to thermal variations of the ambient air.

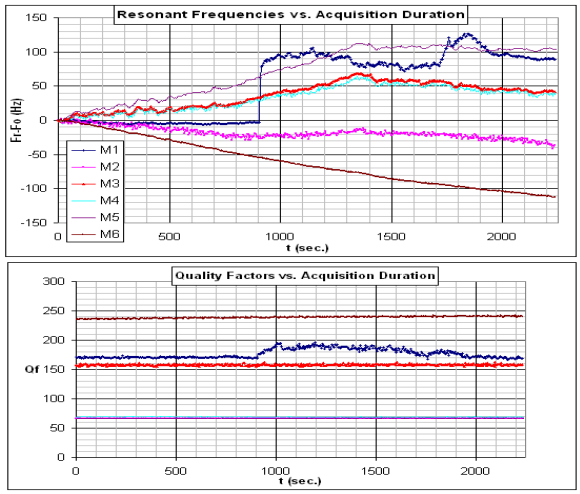

Figure 2.22: Resonant frequencies and corresponding quality factors stability of 6 piezoelectric membranes measured by means of the proposed electronics (except M3 and M4 that are identical, all the other devices have different piezoelectric patch diameters thus explaining the different behavior in time)

For an amount of mass uniformly deposited onto the micromachined membrane surface, the resonant frequency shift is proportional to the mass of the deposited layer:

$$\Delta f = function(\Delta m) \tag{2.10}$$

where Δf denotes the observed frequency shift and Δm stands for the amount of mass added on the device.

The sensitivity is defined as the ratio of the variation of the resonant frequency to that of the mass that induced the resonant frequency shift (for an invariant constant spring of the structure):

$$S_m = \frac{df}{dM} \tag{2.11}$$

The resonant of an oscillating membrane can be written as:

$$f_n = \frac{1}{2\pi}\sqrt{\frac{K_{eff,n}}{M_{eff,n}}} \tag{2.12}$$

where $K_{eff,n}$ and $M_{eff,n}$ respectively stand for the effective spring constant and mass of the membrane and the subscript n denotes the nth eigenmode.

By taking the derivative of Equation (2.12) for a constant $K_{eff,n}$ it is found that:

$$\frac{df_n}{dM_{eff,n}} = -\frac{1}{2}\frac{f_n}{M_{eff,n}} \tag{2.13}$$

Introducing (2.13) in (2.11) leads to:

$$S_m = -\frac{1}{2}\frac{f_n}{M_{eff,n}} \tag{2.14}$$

The modal mass of the membrane can be expressed as follows:

$$M_{eff,n} = \iint_{r,\theta} (\rho h)_{global}\, \phi_{ij}^2(r,\theta) r dr d\theta \tag{2.15}$$

where $(\rho h)_{global} = \int_z \rho_{layer\_i} dz$ (ρ_{layer_i} is the density of the *i*-th layer of the membrane) and

$$\phi_{ij}(r,\theta) = \cos(i\theta)\left[J_n(i,\lambda_{ij}\frac{r}{r_2}) - \frac{J_n(i,\lambda_{ij})}{I_n(i,\lambda_{ij})} I_n(i,\lambda_{ij}\frac{r}{r_2}) \right] \tag{2.16}$$

with J_n and I_n being respectively Bessel function and modified Bessel function of first kind, λ_{ij} is the dimensionless *ij*-mode eigenvalue and r_2 stands for the global radius of the membrane. For example, for (0,0) and (0,1) vibration modes of the membrane, λ_{ij} eigenvalues are equal to 3.197 and 4.611[293].

The physical parameters of the different structural layers of the composite membranes used for theoretical calculations are listed in Ref.[288] (the values of the Ti/Pt parameters have been intentionally disregarded in our calculi due to the insignificant thickness of those layers).

With this in mind, the theoretical sensitivity in air of the actual micromembranes is estimated to $15 pg/(mm^2 \cdot Hz)$. To fully evaluate the micromembranes performances in air (when used as mass sensors) calibrated microbeads (diameter 1,57 ± 0,06 µm, punctual mass of 4.42 pg, from Duke Scientific Corporation) are progressively deposited onto one oscillating membrane while monitoring the resonant frequency change in real time. The experimental set-up (developed at CEMES-CNRS, Toulouse, by Thierry Ondarçuhu) which allows delivering small amounts of solvent containing the microbeads is inspired from in-vitro fertilization set-ups and has been widely described elsewhere[298].

[298] C. Ayela *et al., IEEE of Sensors Journal*, in press (2007)

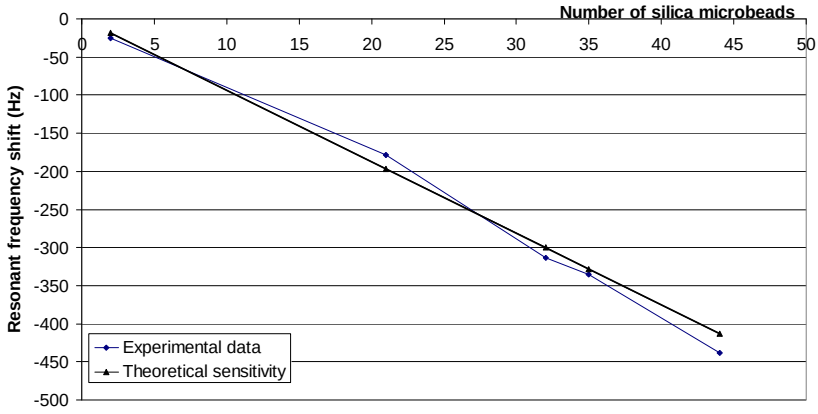

Figure 2.23: Measured and calculated resonant frequency shift after successive depositions of silica microbeads onto the surface of a piezoelectric membrane

In Figure 2.23, the resonant frequency shift monitored while adding microbeads is represented with respect to the estimated added mass after each deposition step (where basically the number of deposited microbeads is counted under an optical microscope). The comparison of the theoretical and the experimental curves shows excellent agreement which gives confidence in the calculated sensitivity.

2.3.5.3 Evaluation of the electronic scheme. Measurements in liquid media

Validation of the electronic set-up is continued by monitoring resonant frequency of three membranes for different water-glycerol mixtures. Changes in the density of the mixture with the quantity of glycerol induce variations of the resonant frequency (as demonstrated in the previous subsection). Figure 2.24 shows the experimental results for six different mixtures of water-glycerol (10, 20, 30, 40, 44 and 50% of glycerol diluted in water). As expected, dramatic frequency shifts are detected for each mixture. Frequency shift differences between the membranes are due to their own mass sensitivity defined by the geometrical parameters of the devices. This last result demonstrates the ability of the electronic set-up to precisely measure the resonant frequency of different membranes in liquid media with a lessened quality factor.

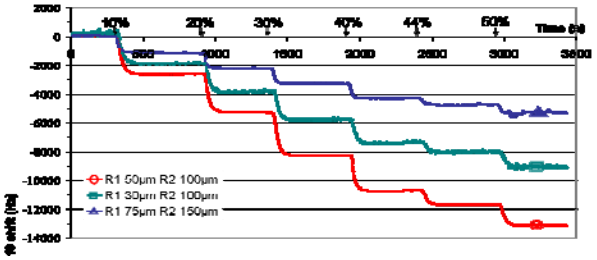

Figure 2.24: Real time measurement of resonant frequency evolution of three piezoelectric membranes for the injection of different water/Glycerol mixtures (0, 10, 20, 30, 40, 44 and 50% of glycerol diluted in water)

The so far encouraging evaluation of the piezoelectric micromembranes as mass sensors in air and liquid media foreshadows tremendous potential in the biosensing area; the first steps towards such applications are described in the next subsection.

2.3.6 Piezoelectric micromembranes for biological applications

For the detection of biomolecules in liquids several fluid handling configurations are possible, namely flow-through cells[299,300], static batch cells[301,302] and dip-and-dry techniques[303,304]. Flow-through systems are easy to automate and allow reproducible dosage of analytes but are comparatively expensive. The signal disturbances by addition of liquids are hard to handle in batch cells (which can be considered as a subcategory of the flow-through systems where the flow might be stopped), an advantage being their ease and chip set-up which makes them very attractive for automatic pipetting systems. Last of all, dip-and-dry techniques allow measurements of masses according to well-known models (such as Saurebrey's model[178] in quartz crystals' case) but repeated and complete drying cannot be performed reproducibly. In addition, the time for the analysis can be much longer.

Dip-and-dry and flow-through techniques are experimented integrating piezoelectric micromembranes in the set-up. Though the chronology is not respected regarding the associated electronics' development (presented in the previous subsection), both techniques will be successively presented in the next paragraphs for easiness of reading. In fact, dip-and-dry tests were performed using a former design of micromembranes associated to a basic electronic set-up[305] while the flow-through experiments were performed on the piezoelectric micromembranes described through this manuscript. This is the main reason why the sensors' sensitivities in both cases are rather different.

2.3.6.1 Detection of streptavidin-gold nanoparticles interaction with biotinylated DNA. Dip-and-dry technique.

Though the fabrication process of the piezoelectric micromembranes used in the next paragraphs remains identical to what was described in section 2.3.3, the geometry of both the upper electrode and the piezoelectric patch is different (ring-like, instead of a disc). The main reason of this difference is directly linked to the design trials made at the beginning of the "piezoelectric membranes" activity, in terms of actuation and sensing efficiency. Later, it appeared that one fundamental criterion to fulfil in order to get effective piezoelectric "actuation-sensing" was a disc-like shaped piezoelectric patch covering 0.5 of the entire surface of the freestanding membrane[287].

One single micromembrane is shown in Figure 2.25(a). This topography clearly shows the ring-like geometry of the PZT actuator and its electrodes. Figure 2.25(b) shows a 5×5 mm^2 die including a chip with 16 piezoelectric membranes that has been glued on a TO8 package with each membrane bonded to the TO8 pins. All membranes are connected with a common ground electrode. To protect the electrical signals from short circuiting through the fluid, each bonding wire is coated with a biocompatible silicon sealant (not shown on this photograph).

[299,300] I. Vikholm *et al., Thin Solid Films* 327-329, 643 (1997) ; C. Steinhem *et al., Biosens. Bioelectron.* 12, 787 (1997)
[301,302] C. Zheng *et al., Biosens. Bioelectron.* 12, 1219 (1997) ; L. Bao *et al., Anal. Chim. Acta* 369, 139 (1998)
[303,304] Y. Okahata *et al., Anal. Chem.* 70, 1288 (1998) ; K. Ito *et al., Anal. Chim. Acta* 327, 29 (1996)
[305] L. Nicu et al., *2004 IEEE International Ultrasonics, Ferroelectrics, and Frequency Control 50th Anniversary Joint Conference*, Montréal, Canada, 24-27 August, (2004)

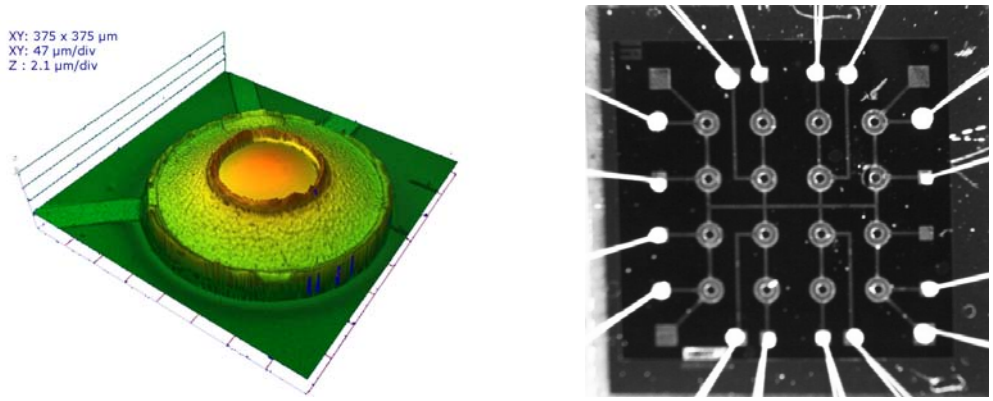

(a) (b)

Figure 2.25: a) 3D static profile (obtained by optical interferometry) of a single piezoelectric membrane; **b)** Optical microscope photograph of 5x5 mm² chip of 4x4 membranes matrix with wire connections

Two different protocols are carried out on the surfaces of the piezoelectric micromachined membranes to emphasize their biosensing potential. These protocols are described below.

a) Gold colloids adsorption protocol

The procedure for gold colloids detection experiment is as follows: to clean the piezoelectric membranes surfaces, the chip is rinsed with ultrapure ethanol and deionized water. A drying step using nitrogen is then performed. The membranes are then coated with an amino-silane layer by dispensing an amino-propyltrimethoxysilane (APTS, Aldrich) solution, followed by a bake step at 140 °C for 10 min. Suspensions containing 40-nm gold colloids (Tebu-Bio) with a concentration of $9 \cdot 10^{12}$ particles/mL at different pH (in a sodium acetate buffer) are prepared. As described eslewhere[283], negatively charge gold colloids (synthesized by citrate reduction of HAuCl4 solutions and having a negative surface charge as a consequence of bond citrate required for colloidal surface saturation) adsorb on the previously functionalized surface by the amino-silane layer. Indeed, under acidic conditions, the amino group is protonated and the resulting positively charged monolayer shows strong affinity with the negatively charged gold colloids.

1-mL of gold colloids suspension (pH equal to 3.7) is thus injected into the sample loop of the flow-through system previously described in 2.3.4.1 (flow velocity equal to 1mL/h) so as to be spread onto the surface of the chip embedded in the chamber reaction. First, a buffer solution (sodium acetate 0.03M at pH 3.7) is injected into the reaction chamber until the resonant frequency of the piezoelectric membrane is stabilized. For the experiment discussed here, the piezoelectric membrane is excited on its (0,1) resonant mode (at 341.7 kHz), since the amplitude of the oscillation at the (0,1) resonant frequency is higher than that at the (0,0) resonant frequency. The stabilization step takes around 90 min. Then, the colloidal solution is injected into the reaction chamber and the resonant frequency value starts to gradually decrease (as shown in Figure 2.26). The decrease of the resonant frequency is continuous during 120 min before flattening out at 339.4 kHz.

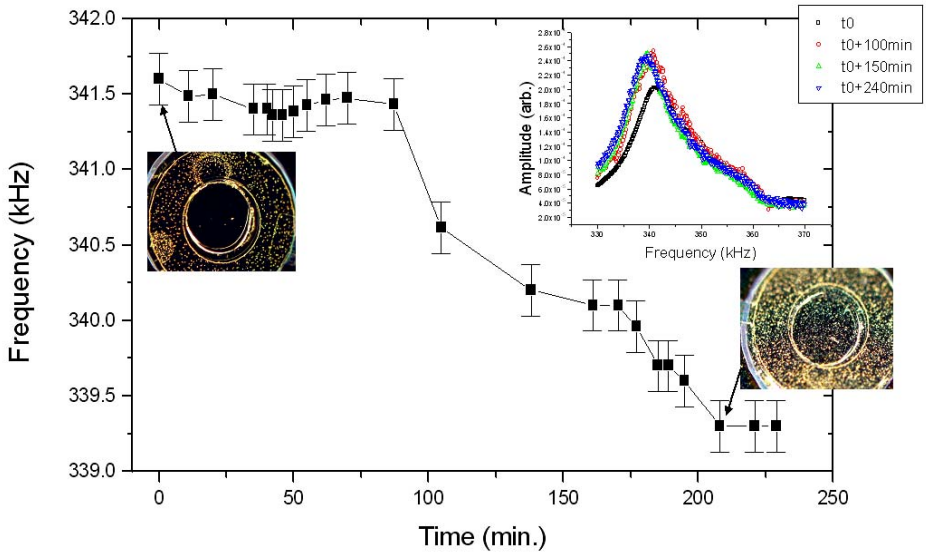

Figure 2.26: Evolution of the (0,1) resonant frequency of the piezoelectric membrane *vs.* time during the injection of a colloidal solution (at pH 5.3) into the reaction chamber of the flow-through system. The two optical microscope photographs show the piezoelectric membrane before and after adsorption of gold colloids on its surface. Error bars represent the standard deviation of the measured resonant frequency during 5 experiments.

This resonant frequency shift can be directly related to the number of gold colloids adsorbed at the surface of the piezoelectric membrane by calculating the mass sensitivity of the sensor as indicated in Eq. (2.14). Replacing f_n by the (0,1) experimental resonant frequency of the membrane yields a mass sensitivity S_m equal to -3.6 Hz/pg. After dividing this value by the resonant frequency of the device and taking into account its active area, mass sensitivity becomes -7.4(Hz/MHz)(ng/cm2)-1 which is two decades higher than state-of-art values for piezoelectric mass-sensing devices187. The ratio between the resonant frequency shift and the mass sensitivity value allows calculating the amount of mass added on the surface of the piezoelectric membrane that can be directly converted into a density (number of particles/µm2) of gold colloids adsorbed onto the active area of the device. Thus, the 2.4 kHz resonant frequency shift yields a density of gold colloids adsorbed onto the surface of the device that equals 130 nanoparticles/µm2. This is two times lower than the density of nanoparticles adsorbed on the surface of a SiO2 control sample (260 nanoparticles/µm2) incubated during 120 min. into a colloidal suspension at the same pH (3.7)[306].

This discrepancy could be accounted for by the fact that both experiments are conducted under different conditions: whereas the adsorption experiment onto control samples is realized under static conditions, the real test using a piezoelectric device is performed under a continuous stream of gold colloids suspension that could dramatically affect the yield of adsorption of gold colloids on the active area of the sensor. Moreover, the dimensions of the reaction chamber and the velocity of the flow of the colloidal suspension injected in are not really optimized. Further optimization could reduce the thickness of the Nernst diffusion layer[307] thus accelerating the diffusion process of the gold nanoparticles towards the active area of the device and consequently increasing the yield of the number of nanoparticles adsorbed per µm^2 of amino-silanized surface.

[306] L. Nicu *et al., Sens. Act. Chem. B*110, 125 (2005)
[307] K. Cammann, *Phys. Chem. Chem. Phys.* 5, 5159 (2003)

b) Biotinylated DNA hybridization and biomolecular recognition by streptavidin-conjugated gold nanoparticles

Cleaning of membranes' surfaces and self -assembly of the amino-silane monolayer onto the are carried out in the same way as in the gold colloids adsorption experiment. Phosphorus dendrimers with CHO end groups, generation 4 (G4), are synthesized according to a method published earlier[307]. Dendrimers are used to avoid interactions of DNA with the surface and to facilitate hybridization. The devices are incubated in a solution containing phosphorous dendrimers (0.1%, w/v) in tetrahydrofuran (THF) for 7 hr at room temperature under gentle agitation. Then, several rinsing steps were performed with THF, 95% ethanol and finally, absolute ethanol. Drying has been done under a nitrogen stream.

Aminated oligonucleotide (NH2-5'-AAG ATT ACT CCG ATA CCA TT-3') is diluted to the appropriate concentration in 300 mM sodium phosphate buffer (Na2HPO4, pH 9.0) and deposited onto the samples. After incubation overnight, samples are incubated for 1 hr with a sodium borohydride solution (3.5 mg mL-1 in deionized water). They are rinsed three times with deionized water and finally dried under nitrogen stream. Hybridizations are carried out by adding a solution containing the complementary target biotinylated oligonucleotide (3'-TTC TAA TGA GGC TAT GGT AAT TTT T-biotin) in saline-sodium-phosphate-EDTA (SSPE: 20 mM NaH2PO4, 0.3 M NaCl, 2 mM EDTA) buffer, containing sodium dodecyl sulfate (SDS, 0.1%, w/v), pH 7.4, for 30 min. at room temperature. The 5 additional thymines (italicized in the previous target sequence) allow taking away the biotin from the hybrids. The samples were then washed twice for 10 min with the washing buffer (20 mM NaH2PO4, 0.3 M NaCl, 2 mM EDTA, 0.1% SDS), then with diluted buffer (2 mM NaH2PO4, 0.03 M NaCl, 0.2 mM EDTA). After hybridization and washing, 20 mL of gold colloids functionalized with streptavidin (Streptomyces Avidinii S0677, Sigma Aldrich) are deposited onto the devices. The streptavidin-conjugated gold nanoparticles are to be used as "nano-weights" during the "dip-and-dry" test performed with the piezoelectric membrane. Indeed, the biotin group of immobilized oligonucleotides fixed on the samples can create a strong complex with streptavidin. The conjugates streptavidin-gold colloids are home-made following a specific protocol described in Ref[306].

After completing the above described protocol, the resonant spectrum of one piezoelectric membrane is traced by using the optical beam deflection technique. The resonant frequency corresponding to the fundamental resonant mode (0,0) is measured at 476 kHz. Then, 20 mL of gold colloids functionalized with streptavidin are deposited on the membranes chip. After 15 min of incubation time followed by immersion in washing buffer (SSPE: 20 mM NaH2PO4, 0.3 M NaCl, 2 mM EDTA, 0.1% SDS) and by several rinsing steps under deionized water and pure ethanol, the chip is dried under nitrogen stream. The resonant spectrum is traced and the resonant frequency corresponding to the fundamental resonant mode (0,0) is again measured, its value being equal to 472.1 kHz. As shown in Figure 2.27, a resonant frequency shift equal to 3.9 kHz is recorded, indicating that the streptavidin-conjugated gold colloids are fixed by the biotinylated DNA oligonucleotides initially grafted on the surface of the piezoelectric membrane.

[307] N. Launay *et al., Angew. Chem. Int. Ed. Engl.* 33, 1589 (1994)

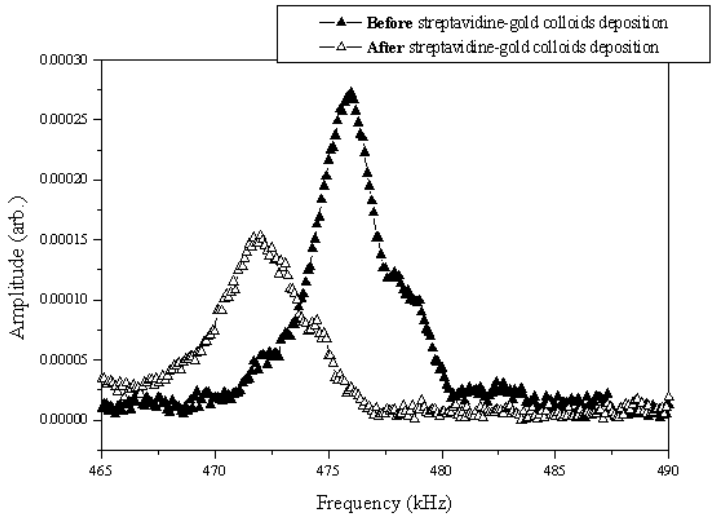

Figure 2.27: (0,0) resonant frequencies measured before and after the deposition of streptavidin-conjugated gold colloids on the surface of a piezoelectric membrane where biotinylated DNA oligonucleotides were previously hybridized with complementary oligonucleotides sequences

Though these preliminary biological experiments onto piezoelectric micromembranes may seem today so "unrefined" (and so they are in the eyes of the forewarned beholder who may rise relevant questions related to the use of nanoparticles, the specificity of the biological recognition emphasized here or the system's limits in terms of minimal detectable concentration), they had the merit, three years ago, to reveal basic aspects related to the use of MEMS as biosensors such as, for instance, packaging issues or output signals drifts due to ambient temperature variations. As an example, photographs of the membranes chip after completion of the entire protocol showed that the biocompatible silicon sealant (that protects each bonding wire) was severely damaged by the succession of biochemical baths. Consequently, sustained work had to be performed either on the protection of the bonding wires issue[308] or on the thermoregulation of the fluidic cell.

Inasmuch as experience has been acquired at the frontier between MEMS and biology, new applications related to immunological field were targeted making use of piezoelectric micromembranes as sensing elements for antigen-antibody specific recognition. The next subsection provides only a glance of that, the details are about to be published in the forthcoming Ref[308].

2.3.6.2 Real-time monitoring of antigen-antibody reactions. Flow-through experiments

Labeling molecules for the quantitative measurement of biological interactions (like, for instance, the use of gold nanoparticles in the previous subsection) might influence the binding efficiency because of change of the ligand-analyte interaction kinetic parameters induced by conformation changes or steric hindrance due to the labeling marker. That is why no-labeling techniques such as Surface Plasmon Resonance (SPR) or Quartz Crystal Microbalance (QCM) for the measurement of biological interactions recently showed tremendous potential, as widely discussed in the first chapter. For reminder's sake, while SPR techniques use refraction index changes for the quantification of the biological interactions, QCM measurements are based on mass changes due to the affinity between the two partners.

Starting with the same measurement principle, matrices of piezoelectric micromembranes working in dynamic mode (resonant frequency variation vs sensor's mass change) are employed for

[308] C. Ayela, *PhD Thesis* being prepared (2008)

the real-time quantification of biological interactions. Each micromembrane integrates a $PbZr_xTi_{1-x}O_3$ piezoelectric patch (PZT) used for the internal actuation and read-out.

4×4 matrices of membranes have been fabricated by standard silicon micromachining techniques starting with Silicon-On-Insulator wafer. Several dimensions were designed either in terms of global radius R_2 of the membrane (100 µm or 150 µm) or radius R_1 of the PZT patch (R_1/R_2 equal to 0.3, 0.5 or 0.7). The chips were wire-bounded on TO8 supports and a specific sealant (EPOTEK H70E-2 from Epotecny) was used for wire coating in order to prevent short-cuts during operation in liquid media. The packaged chips were plugged to the dedicated home-made electronic set-up described in the previous section 2.3.5, developed to obtain a multiplexed tracking of the resonant frequency and quality factor of the fabricated micromembranes (Figure 2.28). This system allowed acquiring several resonant frequencies (and quality factors) in parallel with a frequency measurement stability of less than 1ppm (1-2 Hz), a switching capability of 4 membranes/second and a measurement bandwidth of 1.5 MHz[297].

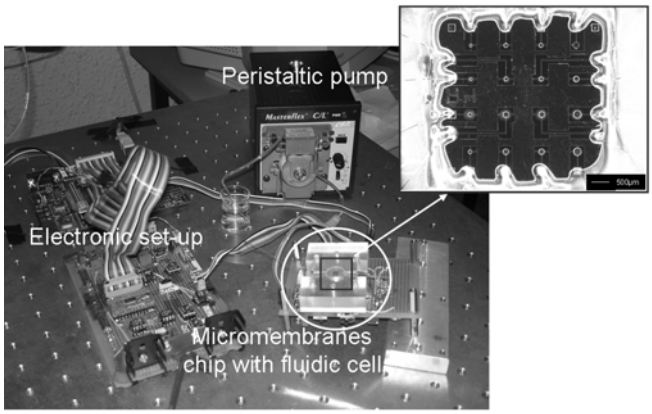

Figure 2.28: Photograph of the global system with the electronic set-up, the liquid injection pump and the fluidic cell including the membranes chip. The inset shows a top view of a chip with the fabricated micromembranes, the wire-bondings and the silicon sealant.

To demonstrate the surface-based detection of proteins, the binding of anti-fluorescein isothiocyanate (anti-FITC) to FITC (immobilized onto the micromembranes surface via polymer chemistry as previously described in 1.5.1.3) is measured.

In a first step of the established protocol, poly-L-Lysine polymer with Poly(ethylene-glycol) chains was used to bind FITC molecules onto the surface of the micromembranes. It is now well acknowledged that the PLL backbone offers an easy-to-use polymer for self-assembling on silicon dioxide surface while the grafted PEG chains act as a barrier for non-specific adsorption[309]. In addition, their functionalization capability with bio-molecules allows their use for an analyte immobilization on SiO_2 surfaces, as depicted on Figure 2.29.

[309] N. P. Huang *et al., Langmuir* 17, 489 (2001)

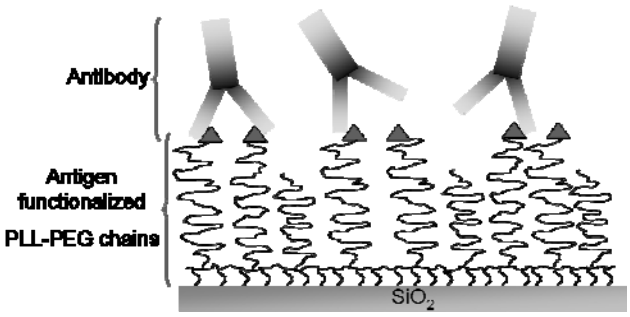

Figure 2.29: Image of the chosen format for the interaction study. Antigen is immobilized thanks to PLL-PEG polymer and antibody is injected on the immobilized antigen.

One kind of functionalized PLL-PEG polymer (supplied by Surface Solutions, Switzerland[310]) is used here, the PLL(20)-g[3.5]-PEG(2)/ FITC, *i.e.* PLL(20 KDa) grafted with PEG(2 KDa) having g (Lys units /PEG chains) = 3.5 with FITC attached to PLL backbone. Figure 2.30 shows the electrostatic adsorption of PLL-PEG-FITC (1mg/ml) on a fabricated micromembrane with a global radius of 100µm and a R_1/R_2 ratio of 0.5. The resonant frequency decrease results from mass increasing on the surface caused by the polymer adsorption.

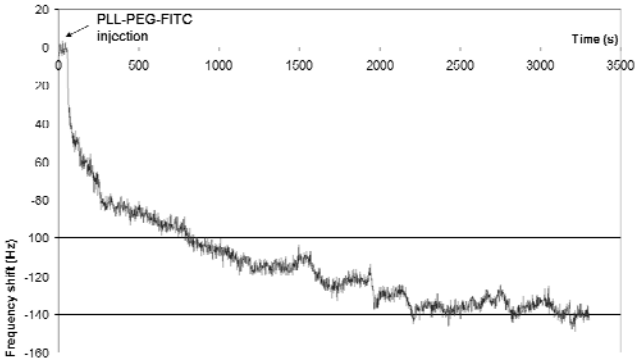

Figure 2.30: Real-time monitoring of the resonant frequency during the injection PLL-PEG-FITC (1 mg/ml) on a membrane with a global radius of 100µm and a R_1/R_2 ratio of 0.5.

Anti-FITC antibodies (supplied by Sigma Aldrich, France) are consequently used to study their specificity with FITC in an antigen-antibody format. The aim consists in the real-time monitoring of the resonant frequency to quantitatively measure the ligand-analyte affinity, meaning the specific and no-specific interactions. Figure 2.31 shows the real-time binding of anti-FITC injected at a concentration of 330nM on 4 micromembranes functionalized with PLL-PEG-FITC.

[310] http://www.susos.com/home.php

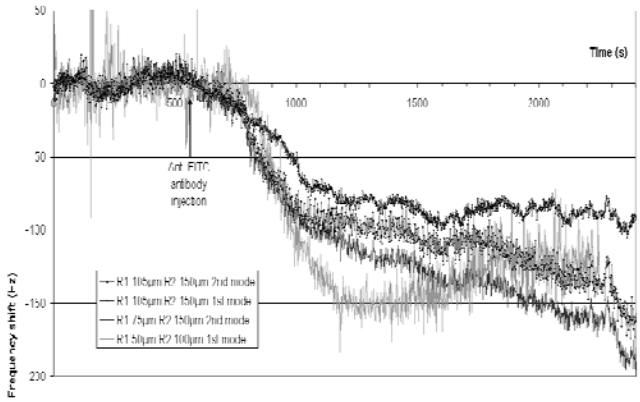

Figure 2.31: Real-time monitoring of the resonant frequency during the anti-FITC (330nM) / FITC interaction on 4 micromembranes.

The decrease of the resonant frequency is significant of the increased mass caused by anti-FITC/FITC interaction and the different levels are due to the intrinsic mass sensitivity of the membranes, as their geometrical properties were significantly different. However, the estimated intrinsic mass sensitivity is in the range of 40 pg/(Hz.mm²) and corresponds to roughly 10 times the sensitivity of commercial QCM machines.

Work is currently ongoing to study the non-specific interactions, to better evaluate the sensitivity and the resolution of the sensors as well as to achieve individual functionalization of membranes with different bio-molecules (using Bioplume system) for the fabrication of a diagnostic chip[308]. Nonetheless, the potential of Bioplume to individually functionalize micromembranes has been already addressed in another assay format, using molecularly imprinted polymers, as described in the next section.

Completing the puzzle: Bioplume as a tool for bioMEMS functionalization

Remember that the initial aim of my research work (dealing with two *double-stranded projects*, Bioplume and bioMEMS) was to develop Bioplume as a tool allowing to properly, differently and simultaneously functionalize arrays of MEMS so that biodetection at the microscale in parallel, within the same flow, of different species could be possible. Though encouraging results related to spot-in-spot biological interactions were obtained (see subsection 2.2.11.2), tests of localized biological interactions onto piezoelectric membranes using Bioplume have not yet been preformed. Instead, the initial foreseen way of convergence of both tools was somehow deviated by the collaboration (started in 2004) between Prof. Karsten Haupt's team and mine regarding the local structuring of molecularly imprinted polymers using Bioplume.

More than uniquely validating the successful deposition of MIP microdots on various surfaces (gold, silica, silicon)[311], a common effort was further concentrated on monitoring the real-time polymerisation as well as cycles of washing/re-incubation of MIPs using piezoelectric micromembranes. A selection of representative results obtained due to enthusiastic work of both teams (especially preformed by F. Vandevelde and C. Ayela, our respective PhD students) is given below.

As stated in the first chapter, MIPs represent a novel type of bioinspired materials that mimic the behaviour of natural antibodies, while exhibiting far greater stability than their natural counterparts. Even though their usefulness has no more to be demonstrated for biological applications such as immunoassays or biosensors, the difficulty for commercial development of MIP may be due to a

[311] F. Vandevelde *et al., Langmuir* 23, 6490 (2007)

sometimes lacking compatibility with standard immunoassay formats. This is all the more obvious when considering the necessity of labelling the template molecules for biodetection purposes (using fluorescent or radioactive labels), thus decreasing the experiments' ease. Coupling silicon-based microfabricated structures with MIPs used as sensitive layer could overcome their main drawbacks by combining them with a high-sensitivity and high-resolution transduction mechanism eliminating the need of labelling.

In this study, a 4-vinylpyridine-based MIP label-free immunoassay for the herbicide 2,4-dichlorophenoxyacetic acid (2,4-D) is validated using piezoelectric circular micro-membranes working in dynamic mode. The membranes are circular shaped with a total radius R2 equal to 100 µm. Each membrane can be individually actuated by a piezoelectric $PbZr_xTi_{1-x}O_3$ (PZT) thin film with its two platinum electrodes. This active part is circular shaped with a radius R1 designed so that the ratio R1/R2 is equal to 0.5. The piezoelectric layer allows simultaneous actuation and detection of the resonant frequency (and corresponding quality factor) of the membranes using the electronic set-up described in section 2.3.5.

First, after the assembly step (Figure 1.6 in the previous chapter), a MIP precursor solution containing the template molecule 2,4-D and a corresponding non-imprinted polymer (NIP) precursor solution without 2,4-D as a control are deposited on the membranes using the specific cantilever array-based microspotting tool Bioplume. The deposition protocol starts with loading the cantilevers. The cantilever tips are dipped for a few seconds into a reservoir containing the mixture of polymers, the channel being filled by capillary forces. The cantilever array is then moved above the activated glass slide using the Bioplumes's *XYZ* motion control system. Droplet deposition occurs by a direct contact of the cantilever tip with the surface to pattern, allowing the liquid to be transferred onto the membrane. The polymer drop is spreading from the center of the membrane to the periphery, the covered area depending both of the hydrophilic state of the micromembrane's surface and the contact time between the cantilever and the surface. Typically, contact times of about 5s allow depositing 0.1nL of polymer solution onto the micromembrane's surface which in turn may cover the entire upper electrode area (Figure 2.32).

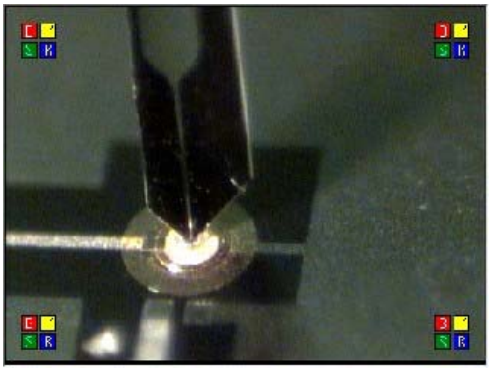

Figure 2.32: Photograph of one Bioplume cantilever depositing onto a piezoelectric micromembrane

The second step consists in the polymerization of the MIP and NIP, respectively, under UV light (365 nm) and nitrogen stream. For the first time to our knowledge, real time MIP polymerization is monitored by following the membrane's resonant frequency shift and quality factor variations thus determining a minimum time for a complete polymerization and allowing the study of viscoelastic properties of the MIP during this phase (Figure 2.33).

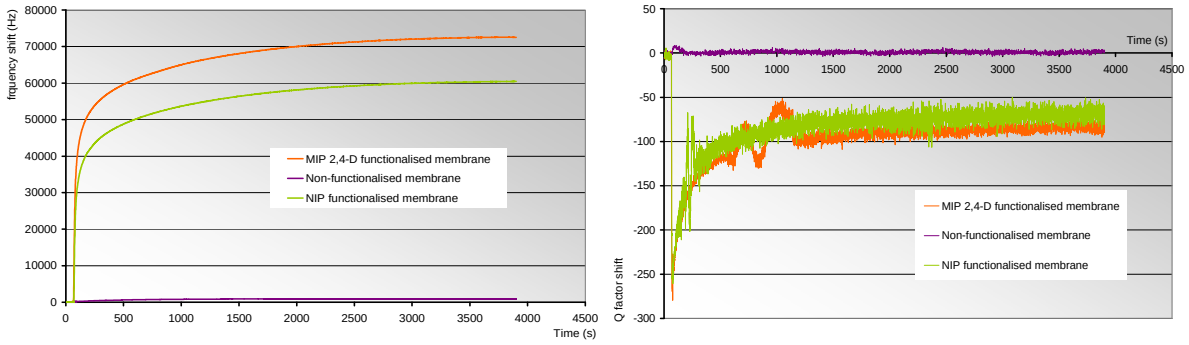

(a) (b)

Figure 2.33: Real-time *(a)* resonant frequency and *(b)* quality factor variations during the polymerization phase of the MIP and NIP, respectively, compared to the output signal of a non-functionnalized membrane

It is worth noting that both the resonant frequency increase and the Q-factor sudden drop followed by progressive increase qualitatively correspond to the reticulation of the MIP and subsequent cross-linking on the membranes' surfaces under the UV light.

Following to the polymerization, dip-and-dry experiments are performed in order to validate the MIP's functionality. A first washing step of the template results in a high increase of the resonant frequency for the micromembrane bearing the MIP (hereafter called the "MIP device") while no significant effect is noted on the micromembrane bearing the NIP (hereafter called "the NIP device"). In contrast, after the incubation step, the resonant frequency decreases for the MIP device whereas still no significant variation is observed for the NIP device. Normally, one should expect the resonant frequency after the first incubation step return to the value before washing that is obviously not the case. One possible explanation could concern amounts of poly(vinyl acetate), used as co-porogen agent, that are removed together with the template during the first washing step.

The washing and incubation steps are therefore alternated and the reproducibility of the resonant frequency levels at the end of each cycle is significant, with a standard deviation of about 1.7 kHz that represents less than 4% of the resonant frequency value after ending the MIP polymerization.

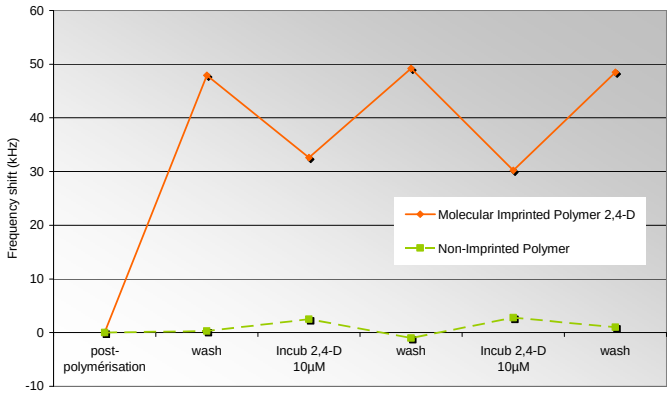

Figure 2.34: Dip-and-dry resonant frequency shifts measured on micromembranes bearing MIP and NIP, respectively, after completion of successive template washing and incubation steps

Attempts have been made to determine the minimum detectable concentration of 2,4-D template. For this to be achieved, the MIP and NIP devices were successively incubated in template solutions with concentrations ranging from 2.5 to 100µM. The behavior naturally expected is an increase of the

resonant frequency shift with the increase of the template concentration until a plateau (meaning the MIP's saturation) is reached[312]. Surprisingly, in the present case, the resonant frequency of the "MIP device" significantly drops (- 16 kHz) as soon as the polymer is incubated at template concentrations higher than 10µM (no matter the value) whereas no significant variation is obtained for template solutions concentrated at less than 10 µM (Figure 2.35).

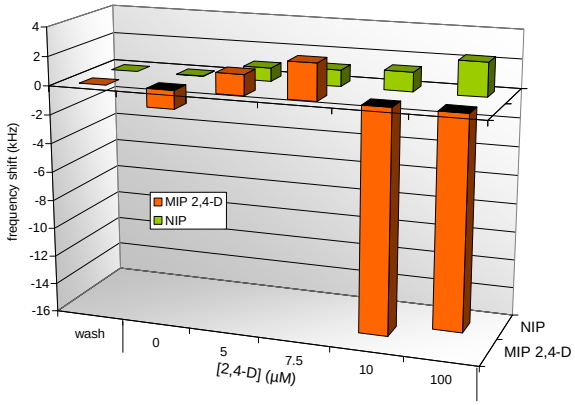

Figure 2.35: Resonant frequency shifts of piezoelectric micromembranes bearing MIP and NIP, respectively, relative to the template concentration

Though the MIP deposited onto the piezoelectric micromembrane seems to have more an "all-or-nothing" than a "linear" response, it is worth noting that the "NIP device" behaves in the same manner, no matter the template concentration value (that is quite encouraging). A first explanation relates to the minimum detectable mass of the piezoelectric membranes which might be too important to allow detecting the template in poorly concentrated solutions. Moreover, given the fact the template incubation is made in aqueous environment[313], it might be possible that π–π stacking effects[314] (which impart hydrophobic properties to the imprinted cavities of the subsequently formed polymer) are responsible for the "all-or-nothing" behaviour. Subsequent work in collaboration with Prof. K. Haupt hopefully remains to be carried out so as to gain further insight into the specific behaviour of the MIP when coupled to vibrating MEMS.

To conclude, because of the proven ability to deposit dots of functional MIPs at precise and desired location onto piezoelectric micromembranes along with the demonstrated potential of the latter when used as mass sensors in this specific configuration, it is foreseeable that this technique is highly promising for the fabrication of integrated biomimetic microchips as well as other types of integrated biosensors.

Conclusion

In this section, a complete set-up including silicon-based micromembranes with piezoelectric integrated actuation and read-out capabilities, associated electronics and fluidics has been designed, modellized and characterized so as to address the biosensing issue using of microelectromechanical systems.

After completing the fabrication of the devices, preliminary studies consisted in the determination of the piezoelectric transverse coefficient d_{31} of $PbZr_xTi_{1-x}O_3$ (PZT) thin films integrated

[312] K. Haupt *et al., Anal. Chem.* 70, 628 (1998)
[313] This choice was driven by constraints related to the chemical resistance of the bonding wires sealant that is relatively uncertain in acetonitrile-based solvents which are more convenient for dissolving 2,4-D.
[314] J. O'Mahony *et al., Biosens. Bioelectron.* 20, 1884 (2005)

in multilayer silicon-based micromembranes. An analytical model specific to this configuration was first built and used for the calculation of d_{31} starting with the static profiles of the microfabricated devices determined by means of a double-beam interferometer. Influence of DC voltage and buckling effects on the d_{31} piezoelectric coefficient at the microscale were investigated and high values were obtained, from 30 pm/V to 75 pm/V, within a hysteresys-like cycle. These results demonstrated the good electrical behavior of PZT thin films at the microscale with a low influence of buckling effects and determined optimal operation conditions for high values of d_{31}.

Subsequent work dealt with the study of the dynamic behavior in different liquid media of 4x4 matrices of piezoelectric membranes previously fabricated. Two kinds of resonant frequency measurements have been performed: first, liquid was continuously flown onto the membranes in the fluidic cell at a constant flow rate ("in-flow experiments") and the resonant frequency was continuously measured. Second, drops of 5µl were deposited onto individual membranes and the resonant frequency was measured while the membrane was oscillated into the liquid spot ("in-spot experiments"). The dynamic behavior of the membranes was experimentally investigated on a range of two distinct families of newtonian fluids (water/glycerol and water/ethanol) with known densities and viscosities. Experimental resonant frequency data were in good agreement with theoretical values calculated using the Lamb's model showing that the liquid viscosity effect can be neglected for values lower than 10 cP. Moreover, the piezoelectric membranes exhibited high Q-factors (up to 150) in the aforementioned liquid solutions with values measured in case of the in-spot configuration more than twofold the ones corresponding to in-flow measurements. This last finding suggests that intentionally trapping air bubbles in a fluidic cell containing micromachined membranes for dynamic liquid media measurements could represent an interesting way to improve the measurement capabilities of the sensing devices.

The development of an associated electronics specific to the former piezoelectric membranes was another crucial issue to tackle on the way towards biosensing applications. The developed electronic set-up allowed an appropriate compensation of the static capacitance due to the piezoelectric film thus allowing precise fitting of resonance spectra and subsequent determination of the resonant frequency and quality factor values. The real-time multiplexed tracking of the resonant frequency and quality factor on eight membranes was performed in different liquid media, showing the high capability of measurement on dramatically attenuated signals. Prior to these measurements, calibration in air has been done making use of silica microbeads successive depositions onto piezoelectric membranes' surface. The mass sensitivity in air has thus been estimated at $15 pg/(mm^2 \cdot Hz)$, in excellent agreement with the calculated value. Combining the model used in air with the Lamb's theory allowed estimating a mass sensitivity in liquid equal to $42 pg/(mm^2 \cdot Hz)$ (in case of a piezoelectric membrane with R1/R2 ratio equal to 0.5).

For first biological experiments to be performed, a suitable flow-through cell-based system allowing real-time reaction kinetics track has been developed. In a first attempt, the mass sensing functionality of the piezoelectric micromembranes has been validated in two ways: on the one hand, the piezoelectric membranes have been used to measure the real-time kinetics of gold colloid adsorption, the whole matrix being integrated into the FIA system. On the other hand, the dip-and-dry technique has been used to measure mass loading induced by the binding of streptavidin-conjugated gold nanoparticles to biotinylated target cDNA fixed onto the surface of the piezoelectric membranes. Measurements of resonant frequency of one piezoelectric membrane have been carried before and after adsorption of the streptavidin-gold colloids conjugates and a shift of the resonant frequency has been recorded meaning that the streptavidin-gold colloids are fixed by the biotinylated DNA oligonucleotides initially grafted on the surface of the piezoelectric membrane.

These preliminary results were quite encouraging for us to keep on going further with the biosensing applications and thus to perform the first antigen-antibody interactions onto piezoelectric micromembranes. After immobilizing PLL-PEG-FITC polymer onto the surface of a chip bearing 4×4

active devices, real-time monitoring of the resonant frequency during the anti-FITC (330nM)/FITC interaction on 4 micromembranes has been successfully carried out.

Though a lot of work remains to be done to thoroughly evaluate other specifications like resolution or stability in time as well as to achieve the ultimate goal of the individual functionalization of membranes with different biomolecules (using Bioplume system), the convergence between Bioplume and piezoelectric MEMS has been achieved through the printing of MIPs and the study of their functionality using micromembranes. In this most recent work, the effort was concentrated on monitoring the real-time polymerization of 4-vinylpyridine-based MIP (and correspondent NIP) as well as cycles of washing/incubation of its specific template (herbicide 2,4-D), using piezoelectric micromembranes. Promising results have been obtained due to the Bioplume's ability to perform the assembly of either the MIP or NIP onto micromembranes. Dip-and-dry successive washing and incubation measurements of the resonant frequency of different devices showed remarkable reproducibility of the MIP and NIP behaviors thus foreshadowing tremendous potential of the established technique for the fabrication of biomimetic microsensors.

The overall characteristics of piezoelectric membranes, provided in Table 2.2, are compared regarding the more known mechanical system-based biosensing techniques, quartz crystal microbalance and microcantilevers (in liquid media).

Tool		QCM-D*	***piezoMEMBRANE***	Microcantilevers (*Ref.*[193.a])
Type		Quartz crystal	*Silicon-based circular membrane integrating piezoelectric actuation and read-out*	Silicon-based microcantilevers with external piezo excitation and optical read-out
Sensitivity	***In air***	*5 pg/(mm^2·Hz)*	*15 pg/(mm^2·Hz)*	N.D.
	In water	*18 pg/(mm^2·Hz)*	*42 pg/(mm^2·Hz)*	10^4 pg/(mm^2·Hz)
Fluidic cell volume		200 µL	*220 µL*	5 µL
Response time		1 min	*1 min*	30 min
Portability		Complex (18 kg)	*Straightforward (<3kg)*	Impossible
Multiplexed measurements		Yes (4 sensors)	*Yes (16 sensors)*	No
Pros		- Mature technology - Available on the market - Parallel - Simple - Accuracy	- *Parallel* - *Potentially inexpensive* - *Disposable sensors* - *Portable*	- Simple technology - Low analyte volumes - Well-known techniques of actuation and read-out
Cons		- Expensive - Limited parallelization	- *Immature technology* - *Complex technology*	- Very slow - Low sensitivity - Portability hard to be achieved

Table 2.2: Main specifications of piezoelectric micromembrane-based sensors related to commercial quartz crystal microbalance and microcantilever techniques

* *from QCM-D E4 Datasheet System by Q-Sense*

3. PROSPECTIVE OUTLOOK

Preliminary considerations

I have started writing this manuscript by making reference to Thomas Kuhn's "The Structure of Scientific Revolutions" book[315] and I decided to finish it by doing the same. Before entering into the details of how I see the prospective of my research work at least six years from now, I will try to take a critical look to what I have done until now and what is finally the main goal of my work, so far and so forth, from Kuhn's theory of science point of view.

Blending science and philosophy was quite a new but crucial exercise at this point of my carrier. It first certainly allowed me to realistically consider my past research work. It is now obvious (it was certainly before reading Kuhn's book but the science vision within put words on some of my intimate convictions) that no scientific revolution but just "doing normal science" is stemming from my previous work. What I now take for granted is that I am part of a scientific community (the *MEMS*' one) that consists of men that share a paradigm, i.e. a specific scientific practice including law, theory, application, and instrumentation together. Though laws and theories specific to *MEMS*' paradigm are taking roots in old "Newtonian dynamics" (yet "quantum mechanics" recently begun to provide new areas to explore for Nano-ElectroMechanical Systems or *NEMS*), applications and subsequent instrumentations for *MEMS* are quite contemporary (that will rapidly lead to the "progress goal" notion, discussed in the next paragraphs).

What was my first motivation to be part of this community and how am I addressing some of its specific issues? To answer at the first part of this question, I again found help in Kuhn's explanation of why a man may be attracted to science. Four main reasons are invoked: "the desire to be useful, the excitement of exploring new territory, the hope of finding order and the drive to test established knowledge". It may seem at a first sight as a sort of "taking oath" of science membership; however, I acknowledged at least the excitement of exploring new territory and the hope of finding order as being among my very first motivations, the desire to be useful arriving later than the others with the "*MEMS applied to biology*" part of my work.

Obviously, the way I addressed some of the *MEMS*' paradigm issues was by "solving puzzles" which is again, upon Kuhn's theory of scientific work, the way "doing normal science" is. The "scientific puzzle" has to be considered as a problem of science that can serve to test ingenuity or skill in *solution which assured existence is always taken for granted*. On the contrary, as underscored by T. Kuhn, there are really pressing problems, e.g. the cure for a kind of cancer or the design of a lasting peace, that are often not puzzles at all, largely because they may not have solutions[316]. Reporting this fact to my own experience allows identifying such "solving puzzles" activity in my past research either, e.g. in the case of the application of the Lamb's model to the microscale or, even more significant, in putting together Bioplume and piezoelectric membranes for MIP-based sensing applications.

It is clear that no scientific revolution will be originated from such "solving puzzles" activity (at least, hopefully, so far!), though, fortunately, this performance criterion is not systematically expected from "common" researchers or people performing "normal science". It surely may create frustration but when intimately linked to each ones ego, I think.

What about the future? To answer the question, one needs to define the goal of any scientific enterprise. It is indeed fixing a point under the horizon that always allows advancing towards future

[315] T. S. Kuhn, *The Structure of Scientific Revolutions,3rd edition* The University of Chicago Press, Ltd., London (1996)
[316] p.36-37 in Ref.[315]

(and eventually, unexplored) lands. Let us take a last look at the "goal in science" definition upon T. Kuhn. The author ends his book by a series of questions addressing "some goal set by nature in advance" within any scientific activity[317]. These are: "*Need there be any such goal? Can we not account for both science's existence and its success in terms of evolution from the community's state of knowledge at any given time? Does it really help to imagine that there is some one full, objective, true account of nature and that the proper measure of scientific achievement is the extent to which it brings us closer to that ultimate goal?"* The author leaves these questions unanswered, though some of them are pure rhetoric. In the absence of such a clear objective, the intrinsic goal of science might be sort of perpetual evolution from "*what-we-do-know towards what-we-wish-to-know*". As this remains quite abstract mainly because opened to subjective analysis, I would prefer the "*progress*" formula to characterize the scientific enterprise, i.e. solving new and exciting scientific problems to generate progress.

Before leaving the epistemological considerations area, a last personal feeling about all those things makes me note that T. Kuhn's work represented sort of lighthouse in the middle of an ocean of questions and the so found answers allow me continuing in a more lucid way.

In the six years to come, three main objectives will be targeted:

- completing the work dealing with piezoelectric micromembranes in terms of overall characterization of their potential as biosensors (*until 2009*);
- investigating the electrokinetic effects on biological species in order to achieve effective concentration of analytes on biosensors surfaces, the goal being to decrease the time of response for applications like e.g. detection of pathogen agents (*until 2009 and beyond, if relevant*);
- integrating transduction method for NEMS systems based on piezoelectric materials, the aim of this (European) project being focussed on understanding the downscaling effects of piezoelectrics in order to optimise their integration into new functional nanodevices, developing innovative technologies for piezoelectric material structuring and characterization at the mesoscale and developing simulations methods required to model the behaviour of piezoelectric NEMS (*until, at least, 2013*).

These research objectives are detailed in the next paragraphs.

Continuing the miniaturization – towards electrical-assisted bioconcentration

Bioplume project is now about to be completed. From a scientific and technological point of view, though one could merely conclude that new challenges related to Bioplume are hard to be found, the range of applications the tool may now address becomes wider and wider every day. Yet setting-up the whole system is ending up, the next step will be to make it available for the whole community in order to perform either passive or active (electrically assisted) printing alternative applications using polymers, nanoparticles, electrolytes or biological solutions.

One cannot similarly conclude regarding to the piezoelectric micromembranes applied to the biology. Even though preliminary antigen-antibody interactions measurements seem encouraging, a lot of work is still to be done to better quantify orders of magnitude of minimum detectable mass, minimum concentration of analyte to be sensed by the micromembranes, time of response, etc. These specifications are of primary importance when addressing issues like e.g. early stage of disease diagnosis or biodetection of potentially threatening agents.

[317] p. 171 in Ref.[315]

What if finally all these specifications will unveil disappointing performance potential of piezoelectric micromembranes for biological applications, despite the theoretical models seem to predict? One possible solution would be to continue the miniaturization of the membranes towards the ultimate submicron scale; indeed, until recently, scaling down sensors seemed to systematically bring an answer to any improve of performance need.

However this is no more the case, at least for biosensors, since the recent works of P. E. Sheehan and L. J. Whitman[235], P. R. Nair and M. A. Alam[318], and J. J. Gooding[319], respectively. They separately pointed out that while most of researchers of nanoscale phenomena have continuously emphasized the fact that miniaturizing a sensor often increases its signal-to-noise ratio, nobody had considered the effect of nanoscale miniaturization on the overall sensitivity. Using simple models inspired from Berg's theory[320] of diffusion-driven accumulation of species onto differently shaped surfaces, these authors examined the mass-transport effects on biosensing at the nanoscale and concluded that previously reported femtomolar detection limits[229] for bioassays are likely an analyte transport limitation (towards nanoscale surfaces) rather than signal transduction limitation (Figure 3.1 from Ref[235] is given below to better illustrate this point).

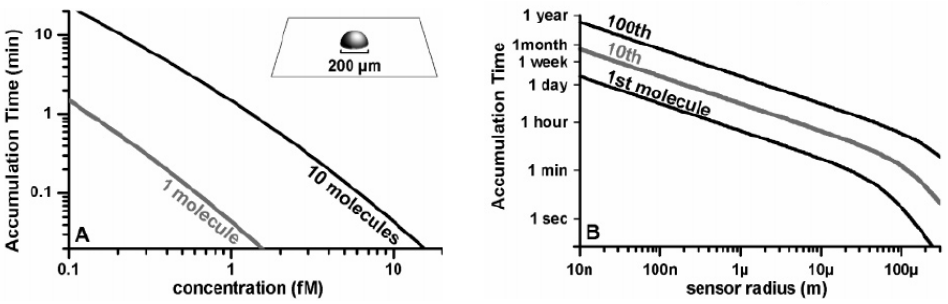

Figure 3.1: (A) Time required to accumulate one or 10 analyte molecules via static diffusion onto a 200 μm-diameter hemisphere for a diffusion constant of 150 $\mu m^2\ s^{-1}$, characteristic of single stranded DNA approximately 20 bases long. After one minute, a few molecules can be expected on the sensor for a sample concentration of 1 fM. The inset shows the sensor geometry. (B) Time required for this sensor to accumulate 1, 10, and 100 molecules when submerged in a semi-infinite 1 fM solution. For radii smaller than 10 μm the required time varies linearly with the radius[235] (*courtesy of Nano Letters editorial board*)

The conclusion of these works is that, without methods to *actively direct biomolecules to a sensor surface*, individual nanoscale sensors will be subject to picomolar-order detection limits for practical time scales (few minutes). Among the available methods of actively directing (thus artificially and very locally concentrating) biomolecules to a sensor surface, electrokinetic effects (namely, *electroosmotic flows*) may efficiently serve this cause.

Starting from these considerations, I decided to initiate a new (for my lab) axis of research dealing with the modelization and the subsequent experimentation of AC-electroosmostic flows for concentration of particles on biosensors. The subject was entrusted to Laurent Tanguy, PhD student since 2005 within my team.

Without entering into details of Laurent's work, it is worth noting that examples of effective concentration can be found in the literature using AC-electroosmosis[321]. This way of particles concentration can be used on microscale sensors to improve the time of response. The phenomenon relies on the apparition of electrical double layers (EDL) at the surface of electrically charged

[318] P. R. Nair and M. A. Alam, *Appl. Phys. Lett.* 88, 233120 (2006)
[319] J. J. Gooding, *Small* 2, 313 (2006)
[320] H.C. Berg, *Random Walks in Biology* Princeton University Press, Princeton, NJ (1993)
[321] P. K. Wong *et al.*, *Anal. Chem.* 76, 6908 (2004)

electrodes. These layers can be displaced by applied transverse electric field. Their characteristic dimensions are so thin compared to the other dimensions that the displacement of the layers acts like a slip velocity at the surface of the electrodes. These fluid displacements create then bulk fluid movements. In our case, the charged electrodes create both the EDL and the electric field necessary to move the layers. Particles in suspension follow the bulk flow and are transported through the fluid. Other forces like dielectrophoresis (DEP) or electrophoresis can attract the particles on the electrodes forcing them to artificially concentrate.

The main objective of this work is to study the AC-electroosmosis for different potential sensors geometries (circular, linear) and to set-up a generic model allowing predicting specifications like duration for efficient concentration, efficiency of the phenomenon, etc. depending on physical parameters like nature and size of the electrodes, applied voltage and frequency, conductivity of the liquid. The established technique could be applicable both for microscale sensors (like piezoelectric micromembranes) and nano-electromechanical sensors. The latter represents a completely new area of investigation to me that I intend to tackle within the next six years not alone but within a European Consortium that I have already initiated and that is briefly summarized in the next section.

Smart NEMS – the ultimate challenge

In contrast to MicroElectroMechanical Systems (MEMS) that after 30 years of development have made major contributions to every-day life in automotive, domestic, health care and information technology applications, NanoElectroMechanical Systems (NEMS) devices are still at the stage of more fundamental R&D pursued by laboratories using very exigent processing tools. Besides the initial challenges of fabricating ultrasmall mechanical devices, a current barrier to their practical development and widespread use is the difficulty of achieving sensitive motion transduction at the nanoscale. Successful realization of parallel NEMS requires that they are self-sensing and self-actuating, thus addressing the doubly hard challenge of realizing very high frequency motion sensing while attaining extreme sub-micrometre resolution. To achieve both targets simultaneously at the nanoscale represents a true breakthrough within this field.

Many displacement-sensing techniques for nanomechanical devices have already been proposed and demonstrated (see Table 3.1). However none of them has until now simultaneously fulfilled the requirements of *integration, sensitivity, signal-to-noise ratio, resolution as well as adaptability to the macroscopic realm, at the level required for building fully integrated NEMS for real life applications.* Piezoelectric materials are the candidate of choice in view of integrated NEMS. It is clearly foreseeable that downscaling piezoelectric materials without altering their mechano-electrical transduction properties could fulfil the above-mentioned criteria, thus becoming the fundamental prerequisite for attaining the ultimate capability from nanoelectromechanical systems: reading out the NEMS motional response induced by an applied stimulus.

Biology	Energy harvesting	Pattern recognition using NEMS-based neural networks
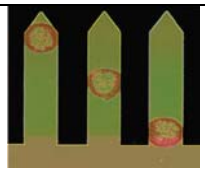 *Bacteria at different positions on a nano-cantilever* ***H. Craighead, Nature Nanotech.18, 2 (2007)***	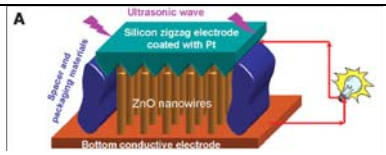 *Direct-Current Nanogenerator Driven by Ultrasonic Waves* ***Xudong Wang et al., Science 102, 316 (2007)***	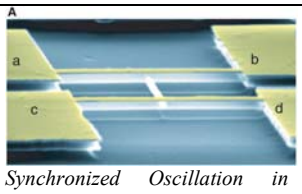 *Synchronized Oscillation in Coupled Nanomechanical Oscillators* ***Seung-Bo Shim et al., Science 95, 316 (2007)***
NEMS-based cantilevers for sensing, scanning probe and VHF applications	Radio-frequency mechanical amplifier	Concept of qubit storage and entanglement using piezo-NEMS resonator
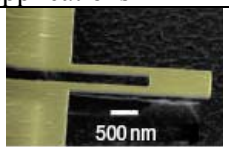 *Piezoresistively detected resonant response from a family of SiC nanocantilevers to a 1 nN a.c. drive signal versus frequency, at room temperature in vacuum* ***M. Li et al., Nature Nanotech117, 2 (2007)***	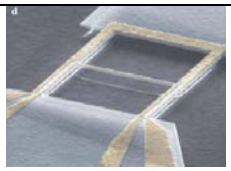 *A parametric radio-frequency mechanical amplifier that provides a thousand fold boost of signal displacements at 17 MHz* ***K. Schwab and M. Roukes, Phys. Today 36, 7 (2005)***	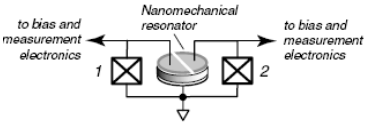 *Two phase qubits coupled to a piezoelectric resonator* ***A. Cleland and M. Geller, PRL 070501, 93 (2004)***

Table 3.1: Sample state-of-the-art application area of NEMS

At the European level, the increase in the understanding of all phenomena in piezoelectric materials and structures, and the direct application of this knowledge to the design of new and improved devices such as sensors, transducers, actuators and motors for applications ranging from medical diagnostics and therapy to industrial measurements are already, for instance, the objectives of the NoE ***MIND***[322] funded within the FP6 framework (2005-2009).

MIND's vision is completely in phase with guidelines delivered by the Institute of Materials, Minerals and Mining Task Force members in their 'Materials Foresight. Functional Materials and future directions' report, in 2003[323]; according to that document it is expected a *'...great potential in micro-system sensors and actuators if they (piezoelectric materials, in text) can be made in thin (<1 μm) or thick (1-100 μm) film forms'.*

Despite its known and generally recognized importance, downscaling piezoelectric materials to the nanoscale while integrating them onto functional nanoelectromechanical systems still remains an emerging research area, which to the best of our knowledge, has not yet been addressed systematically as such. Although piezoelectric–based MEMS are a key enabling technology for mobile communications, automotive, aerospace and medical applications, a roadblock still exists at the nanoscale integration capabilities of piezoelectric materials, with as of yet, no clear path to follow.

Overcoming these current limits is precisely at the core of the future research work I intend to tackle together with European colleagues within a common project, named NEMSPIEZO. The consortium is formed by CNM Barcelona, CSEM Neuchâtel, EPFL Lausanne, CNRS/IEMN Lille, UT-IMS Twente, Tyndall Cork Syntagma Conseil Toulouse and LAAS, as Coordinator. Our common commitment will address the front lines of understanding the effects of (micro-to-nano) downscaling

[322] The acronym MIND stands for "Multifunctional Integrated Devices" - **Action Line:** NMP-2003-3.4.2.1-1 Understanding materials phenomena - cf. www.mind-noe.org
[323] cf. www.iop.org/activity/policy/Publications/file_6428.pdf

of piezoelectrics and of their optimum integration onto functional nanodevices.

To do so, the main objective of the project is to develop innovative methods and technologies for material structuring, characterization, benchmarking and system integration within the field of NEMS. In particular, the material structuring plays a key role. As an example, surface contaminations of nanostructures induced by photoresist-based lithography alter their physical-electronic performances. This is particularly important in the case of junction devices, where the interface purity determines the device characteristics. Structuring materials in a clean way without using organic resist is possible with stencil lithography, an in-vacuum shadow-mask method scalable down to sub-100 nm. In the previous 6FP EU funded IP NaPa, we have already demonstrated that all-oxide ferroelectric junctions show superior switching properties compared to devices made by conventional lithography and etching techniques. It is proposed in NEMSPIEZO to use stencil lithography to micro and nanostructure piezomaterials in order to compare to conventionally fabricated devices integrated into systems. NEMSPIEZO will thus contribute to the development of new functional NEMS integrating high added value actuation and read-out piezoelectric-related schemes.

The detailed objectives are to:

- **Address novel applications related to piezo-NEMS**, focussing on ultrasensitive detection of mass (*less than 10^{-21} g*), fabrication of Scanning Force Microscopy probes arrays (*of more than 10^3 self-actuated, self-sensed cantilevers*) for liquid media and development of the quantum bus concept based on high-Q (*~10^5*), high-frequency (*between 100 MHz and 1 GHz*) mechanical resonators.
- **Explore piezomaterials properties deposited as thin films (several nanometers thick)** by sputtering and pulsed laser deposition (PLD);
- **Investigate both conventional** (lithography + etching) **and non-conventional methods** (FIB[324] as rapid prototyping and stencil lithography) **for creating piezoelectric micro and nanostrutures** (*sub-100 nm lateral size*);
- **Perform characterization of the as-deposited piezoelectric films at two levels**: **on the substrate level or on the free-standing micro/nanostructures**. While the first approach relies on standard physical characterization techniques of piezoelectric films both at the microscale (XRD[325], SEM[326]) and at the nanoscale (AFM[327], TEM[328]), the characterization of free-standing micro/nanostructures integrating the piezoelectric film will be performed by means of optical profilometer and holographic experiments, for instance;
- **Benchmark nanoscale devices fabricated by complementary silicon processing techniques and integrating piezoelectric films deposited beforehand** in order to select the appropriate configurations for effective actuation (*submicron range*) and sensing levels (*subnanometer, subpiconewton[329] range*);
- **Establish the theoretical and modeling support for the fabrication and experimental work in designing reliable high performance devices with optimal sensing and actuation capabilities**. These models, currently missing, will also focus on the verification of the applicability of conventional continuum models to nanoscale electromechanical devices. This will be done either by adapting them or by developing complementary models to be combined with existing ones for accurate simulation of piezoelectric effects at the nanoscale;

[324] Focus Ion Beam
[325] X-Ray Diffraction
[326] Scanning Electron Microscopy
[327] Atomic Force Microscopy
[328] Transmission Electron Microscopy
[329] Range of interactions between biological species like antigen-antibody recognition in their aqueous, native media

Moreover, NEMSPIEZO will explore such questions as whether downscaling a piezoelectric material with a specific shape, or under specific material processing conditions, can have consequences on the transduction effects in terms of actuation, sensing or energy storing.

In that sense, NEMSPIEZO will address the above-mentioned targeted objectives following two strands stemming from a common point:

- the **first strand** will be based on processing of *known* materials (Lead Zirconate Titanate – PZT, zinc oxide – ZnO, aluminum nitride – AlN), integrated onto *known* mechanical structures (cantilevers, bridges or membranes) using *known* deposition techniques (sputtering, for instance). The technical challenge within this strand is situated within the downscaling to sub-micrometer dimension, while the techniques being used will be readily "application-oriented". Foreseen risks: does the piezoeffect scale with the reducing in size? Can piezoeffects be enhanced by downscaling? Are process-induced surface and interface damages relevant and to which extent?

- the **second strand,** which is higher risk, will be the "move forward" approach, testing alternative material (like Barium-modified bismuth sodium titanate – BNBT, which is lead-free), mechanical structures and deposition techniques, again with the goal of achieving downscaling challenges within these systems. "New designs" means not necessary new geometrical forms but also different electrode shapes and/or different ways of managing the clamping zone of freestanding elements in, for instance, tuning fork-like structures. Risks are foreseen in the extreme downscaling for these material systems, as structural and process related properties remain largely unexplored.

Thus the project will develop new and alternative approaches to fabrication and integration of piezoelectric NEMS, starting with the current technologies and then rapidly progress beyond the state-of-the-art by a systematic approach designed to achieve significant breakthroughs.

As direct outcome of the NEMSPIEZO project, high force sensitivity, wide bandwidth and very fast response nanodevices development will become possible, these being crucial attributes for applications such as fast scanning SPM technologies, subpiconewton force sensing and VHF force detection.

The NEMSPIEZO consortium also anticipates that the type of self-actuating/self-sensing NEMS aimed for within the project will prove to be of central importance for a number of other fields; they will readily engender scale-up to large-array sensor technologies, simplified "systems" realizations for portable sensing, and realization of multi-sensors elements enabling correlated or stochastic detection. Furthermore, the use of on-chip electronic actuation and read-out will prove especially advantageous for detection in liquid environments of low or arbitrarily varying optical transparency, as well as for operation at cryogenic temperatures, where maintenance of precise optical component alignment becomes problematic.

By gathering together academic and research institutes partners with proven track records on the field of MEMS and NEMS, I strongly believe that the NEMSPIEZO project will ensure, through piezomaterials modelling, structuring, integration and characterization, considerable progress towards self-actuating/self-sensing piezoelectric-based nano-electromechanical devices thus contributing to the convergence towards the ultimate quantum limits[330] of force, mass and displacement detection.

[330] The quantum limit for a continuous measurement of displacement using a NEMS resonator of mass m and resonant frequency ω is equal to $\Delta x_{QL} = \left(\frac{\hbar}{\ln 3 \cdot m\omega} \right)^{1/2}$ which in case of a silicon nano-cantilever 1µm-thick, 500 nm-wide and 3 µm-long is equal to $2.7 \cdot 10^{-5}$ nm.